Stock assessment of albacore tuna in the Indian Ocean using Stock Synthesis for 2019.

Adam Langley, 1 July 2019

1 Introduction

Commercial fisheries for albacore tunas have operated in the Indian Ocean since the early 1950s. The earliest known exploitation was by the Japanese longline fishery in the 1950s, followed by the Korean and Taiwanese longline fisheries in the mid and late 1950s (Kim *et al.* 2010; Chen 2009). Drift nets were employed in the albacore fishery from the early-1980s until 1992 when an international ban on drift net fishing came into force. Taiwanese and Indonesian longline catch has recently accounted for around 70% of the total catch. Between 2008 and 2011, following the onset of piracy in waters off Somalia, part of the longline fleets that had traditionally targeted tropical tunas or swordfish in those waters moved towards albacore fishing grounds in the southern Eastern Indian Ocean.

Like albacore fisheries in other oceans, the Indian Ocean fishery is characterised by smaller fish at higher latitudes. Unlike other oceans however, there is no significant troll or pole and line fishery for albacore, and since the ban on the drift net fishery there has been no large-scale targeting of small fish.

Stock assessments of the Indian Ocean albacore stock have been conducted in the past using several different methods, including the non-equilibrium production model ASPIC (Chang *et al.* 2012, Matsumoto *et al.* 2012, Matsumoto *et al.* 2014, Matsumoto 2016), the age-structured production model ASPM (Nishida *et al.* 2012< Nishida et al. 2016), a Bayesian biomass dynamic model (Guan et al. 2016), and Stock Synthesis (SS) (Kitakado *et al.* 2012, Hoyle *et al*. 2014, Langley & Hoyle 2016).

The most recent (2016) assessment using Stock Synthesis incorporated data to 2014 (Langley & Hoyle 2016). The assessment incorporated longline CPUE indices for albacore from a collaborative project between Japan, Taiwan, Korea, and the IOTC (Hoyle *et al.* 2015, Hoyle *et al.* 2016). The standardised CPUE indices were derived from operational-level longline data from the three fleets, incorporating cluster analyses to address the effects of target change and standardization models including vessel effects and spatial effects. The project built on a study applying similar methods to Indian Ocean bigeye and yellowfin tuna (Hoyle *et al.* 2015).

The 2016 assessment investigated the interactions between the key data sets (CPUE indices and length compositions) and the uncertainty associated with the key biological parameters (natural mortality and SRR steepness). The WPTmT6 adopted a subset of the SS model scenarios for the determination of the stock status of Indian Ocean albacore and the formulation of management advice for 2016. The estimates of stock status were also relatively consistent with the results of complimentary assessment modelling conducted using a range of other approaches. WPTmT6 concluded that "*stock status in relation to the Commission's B_{MSY} and F_{MSY} target reference points indicates that the stock is not overfished and not subject to overfishing, although considerable uncertainty remains in the SS3 assessment, particularly due to the lack of biological information on Indian Ocean albacore tuna stocks, indicating that a precautionary approach to the management of albacore should be applied by capping total catch levels to MSY levels (approximately 40,000 t)"* (IOTC 2016).

In advance of the current assessment, a preparatory meeting was held in January 2019 to compile the data sets for the assessment (IOTC 2019). The meeting reviewed the updated CPUE indices derived from operational data from the Indian Ocean longline fleets (Hoyle *et al.* 2019), recent biological studies and updated catch data. The meeting also specified the details of the assessment modelling to be conducted for WPTmT7 (see Table 2 in IOTC 2019). This report presents the preliminary results of the 2019 stock assessment modelling of Indian Ocean albacore tuna using Stock Synthesis (Version 3.30.12). The assessment results will be finalised at the WPTmT7 meeting.

2 Data compilation

The data used in the albacore tuna assessment consist of fishery specific catch and length composition data and standardised longline CPUE indices. The details of the configuration of the fishery specific data sets is described below.

2.1 Spatial stratification

The 2016 assessment partitioned the Indian Ocean into four quadrants demarcated at 25°S latitude and 75°E longitude (Langley & Hoyle 2016). The spatial stratification was primarily adopted to partition the longline fisheries by the size of fish caught; the longline fisheries in the southern area tend to catch albacore that are considerably smaller than the fisheries in the northern area (Chen *et al*. 2004, Geehan & Hoyle 2013, Nikolic et al 2013). Higher longline CPUE for albacore has been associated with the North Subtropical Front in the southern Indian Ocean (30–35°S latitude) where SST was 15–19°C (Lan et al 2011).

There is no indication of a longitudinal trend in the size of albacore caught by the longline fisheries (Geehan & Hoyle 2013) and the overall distribution of the southern longline fishery is continuous throughout the southern region (Figure 1). However, during the history of the fishery there were periods when there was an appreciable separation between the operation of the longline fishery in the southwestern and south-eastern quadrants of the Indian Ocean, most notably during the 1960s and 1970s (Figure 2). To account for potential longitudinal variation in the key fishery data sets, the northern and southern areas of the Indian Ocean were partitioned at 75°E longitude.

An investigation of the stock structure of Indian Ocean albacore by morphometric and DNA sequence methods categorised samples into two major groups partitioned by 90°E longitude suggesting that there may be two albacore stocks in the Indian Ocean (Yeh *et al*. 1995). Thus, the spatial stratification of the assessment data sets can be applied to approximate the more complex stock structure within the Indian Ocean.

The four regions of the Indian Ocean were used to define the spatial domain of the model fisheries and define the region specific longline data sets for the CPUE analysis (Hoyle *et al* 2016 and 2019). There are apparent differences in the trends in albacore CPUE indices between the two southern areas over the last decade.

2.2 Temporal stratification

The time period covered by the assessment is 1950–2017 representing the period for which catch data are available from the commercial fishing fleets. The model was further stratified by quarter of the calendar year (Jan–Mar, Apr–Jun, Jul–Sep, Oct–Dec) and the various data sets were compiled accordingly.

2.3 Definition of fisheries

The spatial stratification was applied to define model fisheries based on region and fishing gear. These "fisheries" are considered to represent relatively homogeneous fishing units, with similar selectivity and catchability characteristics.

A total of eleven fisheries were defined, including a single aggregate longline fishery in each region (Table 2).

Longline northwest (LL1). The composite longline fishery in the north-western region was initially developed by the Japanese fleet in the mid 1950s. Data for the Taiwanese fleet are available from the late 1960s and the fleet has operated continuously since then. Japanese fishing effort declined in the early 1970s and remained relatively low until the mid 1990s. Fishing effort by the Japanese fleet recovered to a moderate level during the late 1990s and 2000s but was at a relatively low level from 2010. The composite longline fishery included effort by the Korean longline fleet during the late 1970s and 1980s. Limited albacore catches have been taken by other fleets, most notably the Chinese longline fleet operating during the last decade.

Longline northeast (LL2). The composite longline fishery in the north-eastern region has a similar composition to the LL1 fishery. The Japanese fleet was the dominant component of the fishery during 1953–1970 and continued to operate at a lower level over the subsequent years. Data for the Taiwanese fleet's operations in the area are available from the late 1960s, while the Korean fleet primarily operated in the fishery during 1976–1987.

Longline southwest (LL3) . The composite longline fishery in the south-western region was dominated by the Japanese fleet from the inception of the fishery in the late 1950s until the introduction of the Taiwanese fleet in the mid-1960s. Since the early 1970s, most of the catch was taken by the Taiwanese fleet. There was a short period of higher Japanese catch during 2004–2008.

Longline southeast (LL4) . The composite longline fishery in the south-eastern region was dominated by the Japanese fleet from the inception of the fishery in the late 1950s until the introduction of the Taiwanese fleet in the early 1970s. During 1974–2006, most of the catch was taken by the Taiwanese fleet. Japanese longline catches increased from 2006 and in recent years considerable catches have also been taken by China and Korea.

Drift net fisheries. Drift net fisheries were defined for the south-western (DN3) and south-eastern (DN4) regions. These fisheries were comprised exclusively of drift net vessels flagged to Taiwan,China, which operated in the southern waters of the Indian Ocean from 1982 until 1992 when the UN adopted a worldwide ban on drift nets.

Purse seine. A single purse seine fishery (PS1) was defined as virtually all purse seine catch was taken within the north-western region. The purse seine fishery is made up of various fleets although the majority of the catches of albacore are reported by purse seiners flagged to the European Union and other fleets under EU ownership, including the Seychelles (86% of the total catches of albacore over the time series). The purse seine catches of Iran, Japan, Mauritius, Thailand, and the Republic of Korea are also included in the fishery.

Other. A miscellaneous ("Other") fishery was defined for each of the regions. The "Other" fisheries include various coastal longline, gillnet, trolling, hand lines and other minor artisanal gears, which are used in coastal countries of the Indian Ocean. Collectively, the "Other" fisheries account for a small proportion of the Indian Ocean albacore catch (2% of the entire catch). Most of the catch was reported by Indonesia with the remainder of the catches reported by Mauritius, Reunion and Mayotte (EU), Comoros, Australia, South Africa, and East Timor.

2.4 Catch data

Catch data were compiled by IOTC secretariat based on the fishery definitions (IOTC-2019-WPTmT07-DATA12 - SA.xlsx). All catches were expressed in metric tonnes (mt). There were minor changes in the gear specific catch histories from the previous assessment (Langley & Hoyle 2016). The most notable change was a redistribution of the annual longline catches amongst the model regions due to a revison of the spatial catches from the longline fleet.

The longline fisheries for albacore developed from the mid 1950s and total annual catches averaged about 17,000 t during 1960–1980 (Figure 3). Catches increased during the period of drift net fishing in the late 1980s and early 1990s and continued to increase with the expansion of the longline fishery in the late 1990s to reach a peak in catch of 40–45,000 t in 1998–2001. Total catches declined to about 30,000 t in 2003–2006 and have since fluctuated between 33–43,000 t per annum (Figure 3). During the last decade, the longline fisheries have accounted for 95% of the total albacore catch apportioned amongst the regions as follows: northwest 23%, northeast 13%, southwest 34% and southeast 30%. Most of the catch from the southern longline fisheries occurs during the 2nd and 3rd quarter of the year, while catches from the north-western longline fishery are predominantly taken in the 4th quarter.

Longline northwest (LL1). The longline catch was relatively low from the north-western region during the late 1980s and early 1990s immediately following the reduction in fishing by the Korean fleet and during a period of low catch by the Japanese fleet. The high catches in 2000 and 2001 were predominantly attributable to higher catches by the Taiwanese fleet in those years (Figure 4). Annual catches averaged about 8,000 t per annum over the last decade (2008–2017).

Longline northeast (LL2). The higher catches from the fishery in the late 2000s (2007 and 2008) are primarily attributable to higher catches by the Taiwanese fleet in 2007 and 2008 and the Indonesian longline fleet during 2009 and 2010. Catches have declined over the last 10 years and were about 1500 t in 2016 and 2017.

Longline southwest (LL3) The high catches from the fishery during 1996–2002 are primarily attributable to a considerable increase in catch by the Taiwanese fleet during that period (Figure 4). Annual catches dropped markedly in 2003 and the catch from the Taiwanese fleet remained relatively low during 2003–2005. Annual catches increased steadily from 2006 to 2017, recovering to the previous highest level of catch of about 18,000 t in 2017.

Longline southeast (LL4) . Longline catches from the south-eastern region reached an historically high level of about 14,000 t in 2010. The higher level of catch around this time was primarily attributable to an increase in catch by the Japanese fleet since 2006. Annual catches have declined in more recent years and were about 9,000 t in 2016 and 2017.

Drift net fisheries. The drift net fleet of Taiwan,China operated in Southern waters of the Indian Ocean between 1982 and 1992, reporting catches of juvenile albacore of up to 26,000 mt in 1990 (Figure 3). Most of the drift net catch was taken in the south-eastern region of the Indian Ocean (Figure 4). Most of the catch of albacore by drift nets occurred during the 1st and 4th quarter of each year, with minor catches also recorded during the 2nd quarter. No catches at all were recorded during the 3rd quarter.

Purse seine. Industrial purse seiners have caught adult albacore in the western central Indian Ocean and Mozambique Channel, as a bycatch, since the early 1980s (2% of the total catches of albacore). Purse seine catches of albacore have never been high, with peak catches recorded in 1992 (3,300 mt) and declined over the following decade. Catches averaged 850 t per annum during the 2000s and 500 t per annum during 2013–2017.

Albacore is caught over the entire year, mainly between the 2nd and 3rd quarter as a bycatch of purse seine fishing on free-schools, during the 1st and 2nd quarters in waters South of Seychelles, and off-North Madagascar, and, to a lesser extent, during the 1st and 4th quarters in waters to the East of the Seychelles. A very minor amount of albacore was taken by purse seiners in waters south of 20°S.

Other. Collectively, the "Other" fisheries account for a small proportion of the Indian Ocean albacore catch (2% of the entire catch) (Figure 3). Most of the catch was reported by Indonesia in the north-eastern region (Other2 fishery) with the remainder of the catches reported by Mauritius, Reunion and Mayotte (EU), Comoros, Australia, South Africa, and East Timor.

The catch data do not include allowances for discarded catches of albacore. Estimates of discards are available for the Indian Ocean Taiwanese longline fleet from an analysis of observer data from 2004–2007 (Huang & Liu 2010). The discarded catch of albacore was estimated to represent a very small proportion (0.80%) of the total albacore catch. Estimates of discards are not available for other fleets.

2.5 CPUE indices

For each of the four regions, standardised CPUE indices for albacore tuna were derived using generalized linear models (GLM) from operational longline catch and effort data provided by Japan, Korea, Taiwan,China and Seychelles (Hoyle *et al* 2019). Cluster analyses of species composition data by vessel-month for each fleet were used to separate datasets into fisheries understood to target different species. Selected clusters were then combined and standardized using generalized linear models. In addition to the year-quarter, models included covariates for vessel identity, 5 square location, hooks, and cluster. The analysis is a refinement of the approach used to derive the CPUE indices included in the 2016 albacore stock assessment (Hoyle *et al* 2016) with the inclusion of the data from the Seychelles longline fleet.

Four sets of CPUE indices were derived based on different treatment of the fishing vessel variable in the CPUE modelling (Hoyle *et al* 2019). Models were run for the period 1952-1979 without vessel identity (*novess_5279*), for the later period 1979-2017 with vessel identity (*vessid_79nd*), and for the whole period 1952-2017 both with and without vessel identity.

Initially, the assessment data sets incorporated two separate sets of CPUE indices for each region: the CPUE indices from the early period of the fishery (*novess_5279*) and the more recent CPUE series that incorporates the vessel identity (*vessid_79nd*). The continuous sets of CPUE indices were not included as previous assessments have highlighted that the large decline in the CPUE indices during the early period (1960-1970) was not consistent with the relatively low catches taken from each of these regions during the period (Langley & Hoyle 2016). The LL1–3 CPUE indices are each characterised by a large decline in the indices prior to 1970 (Figure 5). The large decline in CPUE indices during the early period is not apparent in the LL4 fishery (Figure 5). Prior to 1970, the fishery in that region primarily caught southern bluefin tuna and a difference in target species may account for the lower CPUE indices for albacore compared to the other regions.

Further evaluation of the CPUE indices from the 1970s highlighted concerns regarding the utility of these indices also. For this period, the CPUE indices were derived from a small number of logsheet records, due to the decline in the scale of the operation of the Japanese fleet and a shift in the targeting activity of the Japanese fleet from albacore to other species (yellowfin, bigeye and southern bluefin tuna) and a lack of logsheet data from the Taiwanese fleet. Consequently, LL1 and LL2 CPUE indices were sparse through the 1970s. There is also concern that the decline in the LL3 CPUE indices during the 1970s may have been primarily attributable to a shift in targeting behaviour (Figure 5).

During preliminary model development, both sets of regional CPUE indices were incorporated in the modelling frame work. The results of the preliminary modelling reaffirmed the previous conclusions that the initial decline in the CPUE indices was not consistent with the magnitude of the catch from the fishery. This supports the previous conclusions of the WPTmT that the longline CPUE indices during the development phase of these fisheries are not indicative of trends in stock abundance.

For the final model options, the CPUE indices were limited to the regional indices from 1979–2017 (*vessid_79nd*) (Figure 6). The CPUE indices from this period were generally considered to provide a more reliable index of stock abundance especially for the southern regions (LL3 & LL4) as there was a more consistent target fishery for albacore operating throughout the period (primarily the Taiwanese fleet). The CPUE modelling also incorporated the individual vessel effects during that period, enabling the CPUE indices to potentially account for changes in the efficiency of the longline fleet over time (Hoyle *et al* 2019).

In the assessment modelling, a common catchability coefficient was estimated for the four sets of CPUE indices, thereby, linking the respective CPUE indices among regions. This significantly increases the power of the model to estimate the relative (and absolute) level of biomass amongst regions. However, as CPUE indices are essentially density estimates it is necessary to scale the CPUE indices to represent the relative abundance of albacore in each region. This was implemented by determining regional scaling factors that incorporated both the size of the region and the relative catch rate of albacore tuna to determine the relative level of exploitable longline biomass among regions (Hoyle 2019). A number of approaches were used to derive the scaling factors based on different data time periods and model configurations. A preferred option was selected (1979–1994 Method 8) that assigned regional scaling factors of 0.392, 0.546, 1.000, 0.693 to the NW, NE, SW and SE regions, respectively (Hoyle 2019). These regional scaling factors were applied to mediate the magnitude of the four sets of CPUE indices (Figure 7).

A number of important trends are evident in the *vessid_79nd* CPUE indices from the four regions (Figure 6 and Figure 7).

- The relative scale of the CPUE indices for each region reflects the regional scaling factors applied to each series. The CPUE indices are generally highest for the LL3 fishery and progressively lower for the LL4, LL2 and LL1 fisheries.
- There are strong seasonal trends in the CPUE indices from each region, although the relative strength of the seasonal trends differs over time for each of the fisheries. This may relate to the operation of different components of the fleet and/or changes in targeting over the time period.
- CPUE indices from the north-western region (LL1) tend to decline during the 1980s, increased in the early 1990s. CPUE indices from quarter 1 (Q1) and quarter 4 (Q4) declined over the subsequent period, whereas, the CPUE indices from Q2 and Q3 remained more stable through the period.
- The LL2 CPUE indices increased for a short period in the late 1980s. The CPUE indices have fluctuated without trend from the early 1990s.
- The LL3 CPUE indices declined considerably during the late 1980s, recovering slightly in the early 1990s. As with the LL1 CPUE indices, the Q1 and Q4 indices generally declined during the last two decades, whereas the Q2 and Q3 CPUE indices remained at the higher level.
- LL4 CPUE indices fluctuate without trend during the 1980s and 1990s. From the late 2000s, there was a strong increase in CPUE indices from Q1, while the indices from Q1 and Q4 tended to decline. For the most recent years (2014–2017), LL4 CPUE indices are only available from Q2 and Q3.
- Overall, the general trends in the CPUE indices differ amongst the four regions (Figure 7). Correlation coefficients were determined amongst the set of CPUE indices with different time lags (to account for differences in the length composition between the southern and northern regions). There were no strong correlations amongst the set of CPUE indices; the highest correlations were between LL 1 and LL 3 (corr. coef. 0.347) and between LL 3 and LL 4 (corr. coef. 0.331) and a weak negative correlation between LL1 and LL2 (corr. coef. -0.216).
- Trends in the CPUE indices from each region do not appear to be strongly influenced by the magnitude of catch from the region; i.e., a period of large catch in a region does not appear to be followed by a decline in the CPUE indices from the region (Figure 8).
- The differences in the trends in the CPUE indices amongst regions may be attributable to the influence of the prevailing oceanographic conditions. The Indian Ocean Dipole (IOD) Index provides a general index of the oceanographic conditions throughout the Indian Ocean (Saji & Yamagata 2003). Correlation coefficients were derived between the IOD index, with lags of between 0 to 5 years, and the sets of

CPUE indices. There are weak positive correlations between the IOD index (no lag) and LL1 (0.251), LL3 (0.306) and LL4 (0.268) CPUE indices and a weak negative correlation between the IOD index (no lag) and LL2 CPUE indices (-0.244). However, there is no indication of a consistent relationship between the IOD index and the CPUE indices throughout the period (Figure 9).

There is a strong seasonal trend in the southern longline CPUE indices with higher indices during the 2nd and 3rd quarters compared to the 1st and 4th quarters. Preliminary modelling investigated the sensitivity of incorporating seasonal variation in the fitting of the two sets of CPUE indices from the southern regions (by fitting each set of quarterly indices as separate series). The model results were insensitive to the seasonal treatment of the CPUE indices and, to reduce model complexity, seasonal variation was not incorporated in the final model options.

A short time series of annual Taiwanese drift net CPUE indices is available from 1985–1992 (Chang & Liu 1995) (Figure 10). The indices exhibit a high degree of interannual variability with high CPUE indices for 1987 and 1990. The reliability of the indices as an index of albacore abundance is unknown, although the high variability may provide some indication of variation in year class strength during the period given that the drift net fisheries typically catch a relatively narrow length range of albacore (corresponding to fish of about 1–2 years old). The annual indices were assumed to represent the relative abundance in the first quarter of the year (corresponding to the peak season of DN catch).

2.6 Length-frequency data

Longline fishery

Size frequency data are available for the Japan longline fishery from 1965. Length and weight data were collected from sampling aboard Japanese commercial, research and training vessels. Weight frequency data collected from the fleet (as live weight) have been converted to length frequency data via a weight-length key. Levels of sampling aboard the Japanese composite longline fleet over time were uneven in terms of both the sampling platform (commercial and non-commercial vessels) and sampling source (fishermen, scientists, observers). While in recent years the majority of the samples available have come from scientific observers on commercial vessels, in the past samples came from training and research vessels (scientists), and commercial vessels (fishermen). Length frequency data from the Taiwanese longline fleet are also available from 1980. In recent years, length data are also available from other fleets and periods (e.g. Indonesia fresh-tuna longline, Seychelles, etc.).

Prior to the mid-2000s the length frequency data set is dominated by sampling from the Taiwanese deep-freezing longline fleet. Length samples from this component come from commercial vessels and include lengths recorded by fishermen and, to a lesser extent, lengths measured by scientific observers on some of those vessels, in recent years. A review of the Taiwanese length frequency data identified major differences in the length frequencies of albacore recorded before and after 2003, with the majority of the smaller albacore missing from the length distributions since that year (Geehan and Hoyle 2013). It is unknown whether the temporal trends in the length composition of samples represent changes in the underlying length structure of the population or are attributable to changes in sample collection over the study period. Nonetheless, the large increase in fish length in the early 2000s corresponded to a large increase in the reported level of length sampling from the Taiwanese fleet, indicating a change in sampling approaches. At the same time the average fish weight from the Taiwanese catch (total weight of catch/total number of fish) revealed no corresponding increase in any species. Furthermore, the limited length data available from the Japanese composite longline fishery revealed no strong trend in the size of albacore caught during the period. On that basis, it appears more likely that the observed trends in length composition of the Taiwanese longline fisheries are due to changes in the sampling of the fishery and may indicate unrepresentative sampling of the catch from the Taiwanese longline fleet (biased towards the sampling of larger fish).

Due to concerns regarding the reliability of these data, all length samples collected from the Taiwanese longline fleet via logbooks from 2003–2017 were excluded from the length composition data sets. There is also concern regarding the reliability of all earlier (pre 2003) length data collected from the Taiwanese longline fleet via logbooks. It was recommended that these data were not included in the current assessment. However, excluding these data substantially reduces the temporal coverage of the length composition data sets for the longline fisheries. Instead, two sets of length composition data either including or excluding the earlier (pre 2003) Taiwanese logbook data. The influence of the data was then evaluated by comparative model scenarios.

For each quadrant of the Indian Ocean, the core area of the albacore fishery was defined to derive length compositions of albacore that were consistent with the main component of the catch. The core areas for each region were defined as follows.

LL1 Latitude range 25–15° S

LL2 Latitude range 25–20° S

LL3 Latitude range 35–30° S

LL4 Latitude range 35–30° S

The main effect of applying the core area criteria was to exclude the Japanese length samples collected from the LL2 fishery. These samples were generally comprised of larger fish than sampled by Taiwanese fishery operating primarily in the core area (see Appendix 1 Langley & Hoyle 2016). As in LL2, the core area length compositions from LL1 and LL4 were dominated by length composition data from the Taiwanese fleet, while the LL3 length composition dataset retained length samples from the Japanese fishery.

A comparison of the length samples from the Japanese and Taiwanese longline fleets from the core area of the LL1 fishery did not reveal any systematic difference between the length samples, although there is limited temporal overlap between the two data sets (Figure 12). For LL3, the fish sampled from the Taiwanese fleet were generally smaller than from the Japanese fleet (Figure 13) and this pattern persisted across the main fishing seasons. For LL4, there is limited temporal overlap to enable a direct comparison between the size of fish sampled by between the two fleets (Figure 14).

For inclusion in the assessment model, the length-frequency data for each fishery were aggregated into 55 2-cm size classes (30–32 cm to 138–140 cm) by year/quarter. Length data are available from the four fisheries from about 1979 onwards with more sporadic sampling from the fisheries in the earlier years (Figure 11).

Overall, the length compositions from the two northern longline fisheries are dominated by larger fish (90–100 cm) than the length compositions from the southern longline fisheries (65–85 cm) (Figure 15).

For the longline fisheries, there are strong temporal trends in the length composition, especially for the LL1 and LL2 fisheries (Figure 16). For LL1, considerably larger fish were sampled during the late 1980s–early 1990s and late 2000s. A similar general trend was evident in the LL2 length composition data.

Albacore sampled from the LL3 fishery do not reveal a strong trend over the study period, although there is considerable variation amongst the individual quarterly samples. In addition, the fish sampled from the early 2000s are slightly larger than the fish sampled in the preceding years. The length composition data from LL4 reveals more systematic variation over time than the data from the LL3 fishery (Figure 16).

For the four LL fisheries, there is no indication of a correlation between the trends in the length composition and the corresponding CPUE indices from the fishery (Figure 16 and Figure 17). Such a relationship may indicate that changes in fish size are directly related to changes in fish abundance via variation in recruitment and/or differential rates of exploitation.

In the assessment modelling, the individual longline length frequency observations were assigned a relative weighting based on the number of fish measured, up to a maximum of 2000 fish (nfish). The Effective Sample Size (ESS) was determined from the number of fish divided by 400 (nfish/400) giving a maximum ESS of 5. The samples were assigned the relatively low ESS due to concerns regarding the reliability of the length samples from some key data sets.

Purse seine fishery

Purse seine fisheries catch adult albacore, as a by catch (90–120cm), in the western central Indian Ocean (Figure 15 and Figure 18). Albacore lengths are measured in port, by enumerators, during the unloading of purse seiners flagged in the EU and Seychelles. Length samples are available from the fishery from 1990–2017 (Figure 11). The ESS of the individual samples was determined in the same manner as described for the longline fisheries.

Drift net fishery

Drift nets catch juvenile or sub-adult albacore (62–75 cm) (Figure 15). The 2019 assessment is the first time length composition data have been available from the Indian Ocean fishery. The data are from sampling of

the Taiwanese drift net catch during 1985–1991 (Figure 11). These data were recently provided to IOTC by T. Nishida (IOTC 2019).

Other fisheries

No reliable length data are available from the four "Other" fisheries.

3 Model structure and assumptions

The 2019 assessment models were implemented using Stock Synthesis version 3.30. (Methot 2015, Methot & Wetzel 2013).

3.1 Population dynamics

The model population was structured by sex and age with age classes of 0–13 years and an aggregate age class of 14+ fish. The model commences in 1950 at the start of the available catch history. The initial population age structure was assumed to be in an unexploited, equilibrium state. The terminal year of the model estimation period is 2017. Model years are partitioned into four quarterly seasons.

A range of spatial structures for the Indian Ocean albacore stock were investigated in the preliminary modelling phase: a single region encompassing the entire Indian Ocean (spatially aggregated), a two region structure partitioning the western and eastern Indian Ocean, and a four region structure partitioning the Indian Ocean into four quadrants (Figure 1).

3.1.1 Sex ratio

The patterns of sex ratio at recruitment and at older ages and larger sizes are likely to be caused by features of albacore biology that are consistent across all oceans. A large amount of data on sex ratio at length is available for the south Pacific, and there is strong trend towards male bias above the length of female maturity (Hoyle 2008). Similar trends have been observed in the Atlantic and Mediterranean (Karakulak *et al.* 2011). Such a trend could be explained by differential growth and/or differential mortality. Differential growth is well supported, since males have been shown to grow considerably larger than females in the north Pacific (Chen *et al.* 2012), south Pacific (Williams *et al.* 2012), north Atlantic (Santiago and Arrizabalaga 2005), and Mediterranean (Megalofonou 2000).

Differential mortality is a possibility, although age sampling in the north and south Pacific has not been sufficiently randomized or intensive to draw conclusions about the relative numbers at age of males and females. Maximum observed ages are higher for males in both the north and south Pacific, suggesting that males may on average experience lower natural mortality than females. However, these observations may have been biased by non-random sampling, or sampling of more males than females.

There is no evidence for unbalanced sex ratio at the age of recruitment. Sex ratio at recruitment was assumed to be equivalent (1:1).

3.1.2 Growth and maturation

Previous estimates of growth for Indian Ocean albacore tuna have been based on ageing using scale patterns (Huang *et al.* 1991) and vertebrae (Lee and Liu 1992), and on size frequency data (Chang *et al.* 1993). While ageing using otoliths has been validated for a variety of tuna species including albacore, across a range of ages (Farley *et al.* 2013), ageing methods using dorsal spines, vertebrae, and scales have not been validated to the same degree. Due to the potential bias in the growth estimates, growth curves based on direct ageing of otoliths were preferred. For the recent (2014 and 2016) Indian Ocean albacore stock assessments, growth was parameterised using a sex specific growth curve derived for north Pacific albacore from the otolith ageing (Chen *et al.* 2012).

A study to determine the age and growth of Indian Ocean albacore using otoliths was recently completed (Farley *et al.* 2019) using the ageing protocols developed for the South Pacific. The study sampled albacore from the western Indian Ocean, primarily from the longline fishery with smaller fish also sampled from pole-an-line and purse seine fisheries. The sampled fish ranged in length from 74 to 108 cm FL for females and 67 to 115 cm FL for males (Farley *et al.* 2019). The age estimates were used to determine von Bertalanffy and Richards growth functions for male and female albacore. The two growth models yielded virtually identical growth functions. Growth differed between the sexes, with males growing faster than females

after ~85 cm FL and reaching larger mean asymptotic length. The von Bertalanffy growth models were adopted as the primary growth curves included in the current stock assessment.

The new study estimated slightly higher initial growth for male and female albacore compared to the South Pacific (Williams *et al.* 2012) and North Pacific (Chen *et al.* 2012). There is some concern that the initial growth may be over-estimated due to the limited number of smaller fish (< 75 cm F.L.) included in the sample (Farley *et al.* 2019, Nishida & Dhurmeea 2019). Estimates of Linfinity from the new study are 103.8 cm and 110.6 cm for females and males, respectively, compared to 114 cm for both sexes from the Chen *et al.* (2012).

The individual ageing observations from Farley *et al.* (2019) were examined to determine the magnitude of variation in the mean length-at-age for male and female albacore. For male and female albacore, the coefficient of variation of length-at-age was higher for the younger (2-5 years) age classes and decreased with age; the coefficient of variation of length-at-age for the older age classes is very low (Figure 22). For the assessment model, variation in length-at-age was parameterised as a function of age with a coefficient of variation of 0.06 for the younger age classes and decreasing to 0.025 for the older age classes. The sensitivity of the model results to this assumption were investigated.

Longitudinal spatial variation in albacore length at age has been found within the south Pacific (Williams *et al.* 2012) and may also occur in the north Pacific (Xu *et al.* 2014). Such variation may result from spatially varying growth, selectivity, or size-dependent movement. In the south Pacific the magnitude of spatial variation was smaller than the difference between sexes, but sufficient to affect management advice from the stock assessment (Hoyle *et al.* 2012). Insufficient data are available from the Indian Ocean to investigate spatial variation in growth.

In previous assessments, the relationship between albacore length and fish weight has been parameterised based on a study of South Atlantic albacore tuna (Penny 1994). Length-weight relationships from studies of Indian Ocean albacore tuna have generally been considered less reliable due to the relatively limited length range of fish sampled (Nishida & Dhurmeea 2019). However, a recent study has derived the allometric curve for albacore from a broad length range of fish sampled from a wide area of the Indian Ocean (Kitakado et al. 2019). This new study estimated an allometric curve that predicts lower overall fish weights (by 10-15%) compared to Penny (1994). For the current assessment, the length-weight relationship of Penny (1994) was retained, although a sensitivity analysis was conducted using the new relationship from Kitakado et al. (2019).

Reproductive potential of female albacore was assumed to be equivalent to south Pacific albacore maturity-at-length (Farley *et al.* 2014) (Figure 23). This ogive takes into account sex ratio, sexual maturity, spawning fraction, and fecundity and so represents female reproductive output at length. The ogive has fish attaining sexual maturity at about 85 cm and 50% reproductive potential is reached at about 92 cm (Figure 23). When converted to age using the new Indian Ocean albacore growth curve (Farley *et al.* 2019), sexual maturity is attained at about age 4 years and 50% reproductive potential is reached at about 5 years. As an alternative, the maturity ogive derived for western Indian Ocean albacore (Dhurmeea *et al.* 2016) was also considered, although the ogive is considered less reliable due to the limited number of fish sampled from the smaller length classes (below L50).

3.1.3 Natural mortality

Natural mortality was assumed to be 0.3 for both sexes, based on the value applied in the north Pacific and the north Atlantic albacore stock assessments. A lower value of 0.2207 was applied as sensitivity; the alternative level of natural mortality corresponds to a maximum age of about 20 years compared to a maximum age of 15 years observed from the South Pacific. The recent Indian Ocean ageing study recorded a maximum age of 16 years for females and 14 years for males (from an exploited population) (Farley *et al.* 2019).

Age specific natural mortality at age was investigated in a sensitivity analysis (Figure 24).

3.1.4 Recruitment

Recruitment in the model occurs in the fourth quarter of each year, reflecting the summer spawning season (and the ageing protocol that assumed a birthday of 1 December Farley *et al.* 2019). Recruitment was based on a BH stock recruitment relationship (SRR) and annual deviates were estimated for the "data rich" period of the model (1975−2015). Deviates were given a small penalty, so that recruitment estimates in periods with less data were estimated closer to the mean. The applied penalty was based on the assumption that the true standard deviation of recruitment deviates (σ_R) is 0.3, reflecting the upper range of the magnitude in the

variation of recruitment deviates estimated during preliminary modelling. Imperfections in models and lack of full information in the data cause models to underestimate recruitment variability, and recruitment variability tends to change across the time series, as information availability changes.

Since recruitment variability is assumed to be lognormally distributed, mean recruitment is higher than median recruitment. Equilibrium recruitment is meant to represent the average recruitment through time, so the median value in the recruitment function must be bias-corrected upwards. Given this lognormal bias, underestimation of recruitment variability also implies the need for bias correction so that mean recruitment over a period is accurate. The degree of bias correction depends on how much the variability is underestimated. Following Methot and Taylor (2011), the bias correction was adjusted across the time series according to the relationship between the assumed and estimated recruitment variability.

In the final set of models recruitment deviates were estimated for 1975−2015. Preliminary modelling revealed that the length composition data were influential in estimation of the recruitment deviates in the earlier period (1950−1974) in the absence of any abundance (CPUE) indices for the period. The length composition data from the longline fishery are not considered to provide reliable information regarding annual recruitment, particularly in isolation of indicators of stock abundance. No information is available in the model to reliably estimate recruitment in 2016 and 2017 as these age classes had not recruited to the fishery in the terminal year of the model (2017).

For the spatially stratified models (two and four region models), the overall proportional distribution of recruitment amongst regions was estimated. Annual deviates of the regional distribution of recruitment were also estimated for 1980−2015.

The final model options included three (fixed) values of steepness of the BH SRR (h 0.7, 0.8 and 0.9). These values are considered to encompass the plausible range of steepness values for tuna species such as albacore tuna and are routinely adopted in tuna assessments conducted by other tuna RFMOs.

3.1.5 Movement

For the spatially stratified models, movements were estimated between adjacent regions (Figure 25). Movement was assumed to be age specific and occurred annually, at the start of the year (Season 1). Movement rates were estimated separately for younger (ages1−3) fish and older (6+ year) fish, with a linear interpolation for the intermediate age class. The two age classes partition immature and mature fish. The movement dynamics are intended to represent the overall transition in the spatial distribution of fish as observed in the length compositions of the longline fisheries.

3.2 Fishery dynamics

Modelled fishery selectivity was assumed to be a function of fish length. For all fisheries, selectivity was parameterised using a double-normal function (Methot 2015). For the single region models, the two southern longline fisheries (LL3 & LL4) shared a common selectivity as the length composition of the sampled catches from the two regional fisheries were comparable. The length of fish sampled tends to be considerably smaller than from the northern longline fisheries. Thus, the parameterisation of the selectivity function for the southern longline fisheries was given considerable flexibility to estimate a lower selectivity for the larger length classes (declining right hand limb).

The length composition data from the two northern longline fisheries (LL1 & LL2) indicate that these fisheries catch very similar sizes of fish and a common selectivity was estimated for these two fisheries. Initial modelling results indicated that it was necessary to constrain the selectivity function to maintain full selectivity of the largest length classes; i.e. approximating a logistic selectivity function.

A double normal selectivity was estimated for the purse seine fishery (PS1). The availability of length composition data from the drift net fishery enabled the estimation of a selectivity function for this method. The selectivity was parameterised as a double normal function and assumed to be equivalent for the two fisheries (DN3 & DN4).

No reliable length frequency data are available for the four “Other” fisheries. The selectivity of the “Other” fisheries was assumed to be equivalent to the selectivity of the drift net fishery. Initial modelling indicated that the model results were not sensitive to the selectivity assumed for the four Other fisheries due to the small magnitude of the catch associated with each of these fisheries.

Fishing mortality was modelled using the hybrid method that the harvest rate using the Pope's approximation then converts it to an approximation of the corresponding *F* (Methot & Wetzel 2013).

3.3 Observation models for the data

The total likelihood is composed of three main components: the fit to the abundance indices (CPUE), fishery length frequency data and catch data. There are also contributions to the total likelihood from the recruitment deviates and priors on the individual model parameters. The model is configured to fit the catch almost exactly so the catch component of the likelihood is very small. Details of the formulation of the individual components of the likelihood are provided in Methot & Wetzel (2013).

For the current assessment, the weighting of the CPUE indices followed the general approach of Francis (2011). An initial (four region) model was implemented that down weighted all the length composition data. The RMSE of the resulting fit to each set of CPUE indices was determined as a measure of the magnitude of the variation of each set of indices CPUE indices. The resulting RMSEs were comparable for the four longline fisheries (RMSE 0.21-0.28) while the drift net CPUE indices had a higher level of deviance (0.31). On that basis, a CV of 0.20 was assigned to each set of longline CPUE indices and the drift net CPUE indices were assigned a CV of 0.30. The final preferred model option incorporates a single set of longline CPUE indices (from the south-western fishery).

The reliability of the length composition data is likely to be variable amongst fisheries and over time periods. For that reason, it was considered that the length composition data should not be allowed to dominate the model likelihood and directly influence the trends in stock abundance. The relative weighting of the length data sets was investigated during the preliminary modelling phase by examining the influence of the length composition data on the overall magnitude of the stock size. The results indicated that a maximum ESS of 5 (all fisheries, all time periods) ensured that the length composition data were sufficiently informative to provide reasonable estimates of fishery selectivity and, hence, reasonable fits to the length composition data but were not strongly influencing overall stock size or the stock trajectory.

The Hessian matrix computed at the mode of the posterior distribution was used to obtain estimates of the covariance matrix, which was used in combination with the Delta method to compute approximate confidence intervals for parameters of interest.

4 Preliminary modelling

The 2016 stock assessment investigated a wide range of structural assumptions and those results informed to structure of the final (2016) assessment. For the current assessmetn, there are no additional data to enable any further investigation of some of the main structural assumptions related to fishery selectivities, initial conditions and recruitment estimation. Instead, the preliminary modelling conducted for the current assessment focussed on the development of the spatial structure of the model, primarily to accommodate the differences in the length composition and CPUE trends amongst the four regional longline fisheries. The results of the preliminary modelling are summarised in Appendix 1.

Initially, a four region model was implemented based on the spatial definitions applied to derive the four sets of longline CPUE indices and the configuration of the catches and length composition data (Figure 25). The model shared longline selectivities and catchability coefficients amongst regions and estimated the overall regional distribution of recruitments. Movements were estimated amongst regions allowing the model to predict the general movement of larger fish from the southern regions to the northern regions. However, the resulting fits to the main data sets were very poor, as the model could not accommodate the different trends in the longline CPUE indices from the four regions.

The four region model was refined to estimate variability in the distribution of the annual recruitments amongst the four regions. Overall, the model provided a reasonable fit to the four sets of CPUE indices (Figure 27 and Figure 28) which are accommodated by considerable differences in the estimated recruitment trends for the four regions (Appendix 1, Figure A5). However, there are strong seasonal patterns evident in the residuals of the fits to the CPUE indices. The seasonal variation in the CPUE indices was investigated by restructuring the regional CPUE indices by quarter (i.e. four quarterly sets of CPUE indices in each region) and sharing the quarterly catchability coefficients amongst regions. This inclusion of seasonal CPUE indices did not result in an appreciable change in the estimated stock dynamics. However, it highlighted temporal trends in the fit to the seasonal CPUE indices in some regions, most notably in LL 1 (Figure 29). For LL 1, there is an apparent

conflict between the CPUE indices from quarters 1 & 4 and quarters 2 & 3. The latter set of CPUE indices are over-estimated in the earlier period of the time-series (1980s and early 1990s) and under-estimated in the latter period (2005-2015). Less pronounced patterns in the residuals of the fit to the seasonal CPUE indices are also evident in the other regions (Figure 29). This indicates trends in the abundance indices are not consistent amongst seasons and that there are conflicts in the CPUE indices amongst regions.

Alternative parameterisation of the movement dynamics was investigated. The base four region model simply estimated a single annual set of movement coefficients. Increasing the frequency of movements to occur quarterly did not appreciably improve the model fits to the CPUE indices. Temporal variation in movement was also investigated via linking the movement parameters to an environmental covariate that has the potential to influence the distribution of albacore within the Indian Ocean. The Indian Ocean Dipole Index was selected as a potential candidate based on comparisons of trends in the CPUE indices among regions, especially between LL1 and LL2. However, the resulting temporal variation in the movement parameters, linked to the environmental covariate, actually resulted in a deterioration in the fit to the CPUE indices for most regions.

The two region spatial structure partitioned the western and eastern regions of the Indian Ocean (Figure 25) and assumed different selectivities for the longline fisheries in the north and south, while also estimating regional variation in recruitments (Appendix 1, Table 1A). Three model options were considered that utilised different sets of CPUE indices in each region: the southern (LL3 and LL4) indices only (*R2_CPUE_South*), the northern (LL1 and LL2) indices only (*R2_CPUE_North*), and both the southern and northern indices (*R2_CPUE_All*). The models provided a reasonable fit to the southern CPUE indices although the fits deteriorated with the inclusion of the northern CPUE indices (Table A2 and Figure A2). By comparison, the fits to the northern CPUE indices were quite poor, reflecting the different trends between the two sets of northern CPUE indices (LL1 and LL2). The *R2_CPUE_South* model estimated similar levels of recruitment between the two regions during the mid 1980s to early 2010s, although recruitment differed considerably in the earlier period (Figure A6). The model which incorporated the four sets of CPUE indices (*R2_CPUE_All*) estimated an unrealistically large stock biomass (Table A2).

To further explore the conflict amongst the individual data sets, the two region spatial structure was used to partition the Indian Ocean into two discrete single region models: a western Indian Ocean model and an eastern Indian Ocean model. For each model, both the north (either LL1 or LL2) and south (either LL3 or LL4) longline CPUE indices were incorporated as the abundance indices. The overall fits to the CPUE indices from the two models were not appreciably different from the *R2_CPUE_All* model, indicating little improvement in fit to the CPUE indices achieved from movement between the two regions (Appendix 1 Table A3 and Figure A4). However, the eastern model estimated a huge biomass (Appendix 1 Table A2). This is likely to be due to the lack of the length composition data from the purse seine fishery (western region only) which appears to constrain the upper bound on biomass (see Section 5.1).

The single region Indian Ocean models were formulated with three different configurations based on different sets of CPUE indices, equivalent to the groupings used in the two region models. Equivalent assumptions were also made regarding the differences in the longline selectivities between the northern and southern fisheries (Appendix 1 Table 1A). For the *R1_CPUE_All* option, the fits to the CPUE indices were relatively poor (Appendix 1 Table A3 and Figure A3) and appreciably worse than the corresponding two- and four-region models due to the conflicting trends between the four sets of in the indices and. Similarly, the fits to the CPUE indices from the *R1_CPUE_North* and *R1_CPUE_South* models were worse than the spatially resolved models (Appendix 1 Table A3). On that basis, a further model was configured that only included the single set of CPUE indices from the south-western longline fishery (*CPUE_SouthWest*).

5 Model results – reference model and sensitivities

5.1 Final model selection

The results of the preliminary modelling reveal that a key structural uncertainty is the treatment of the northern LL CPUE indices (inclusion or exclusion of these indices). There is considerable conflict between the northern and southern LL CPUE indices. The only model options that resolved the conflict amongst the CPUE indices were the four region, spatially stratified models which estimated considerable variation in annual recruitments amongst the four regions. However, given the paucity of the length composition data from the key longline fisheries, it is considered that there are insufficient data available to reliably inform these models regarding regional scale trends in recruitment. Nonetheless, the fit to the longline length composition data from

the four region model was substantially worse for the LL3 and LL4 fisheries compared to the single region model, whereas the fit to the LL1 and LL2 data was improved with the more complex model structure. This suggests that the recruitment trends estimated by the four region models are essentially informed by the regional CPUE indices rather than the integration of the regional length composition data.

There are no additional data available to evaluate the reliability of each of the four sets of CPUE indices. However, on balance, it is considered that the southwestern longline indices (LL3) are likely to represent a more reliable indices of stock abundance; the CPUE indices are derived from the longline fisheries data that represent a main target longline fishery for albacore and the length composition data associated with the fishery are considerably less variable than for the northern longline fisheries, suggesting that the operation of the fishery may have remained more consistent over time. There fits to the LL1 CPUE indices revealed marked differences in the seasonal trends in the model residuals that may indicate changes in the operation of the fishery over time. The trends in the LL3 CPUE indices during 1985-2010 are quite similar to the CPUE indices from south-eastern longline fishery (LL4), the other main component of the target albacore fishery. However, there are notable differences between the two sets of CPUE indices; the 1979-1984 CPUE indices from LL3 are considerably higher than the LL4 CPUE indices, while the recent (2011-2017) LL4 CPUE indices are considerably higher than the LL3 CPUE indices. These differences may indicate differences in target behaviour in the fisheries at different times. The recent increase in the LL4 CPUE indices corresponds with an increase in albacore catch by the Japanese fleet in the region and a change in the fishing behaviour of this component of the fleet which may introduce a positive bias in the CPUE indices.

On that basis, the single region *CPUE_SouthWest* model was selected as the reference model, while the *CPUE_South* model (which includes both the LL3 and LL4 CPUE indices) was retained as a sensitivity option. The two models yielded quite different trends in recent stock biomass due to the influence of the more positive LL4 CPUE indices which moderate the decline in the recent LL3 CPUE indices (Table 1).

For the reference model, a likelihood profile was conducted for the recruitment scale parameter (*R0*) to investigate the influence of the various data sets and model assumptions. The minimum total likelihood value of the reference model is achieved at an *R0* value of 9.49 (Figure 26). However, the individual components of the likelihood revealed that upper bound of the parameter is poorly determined and that there is considerable conflict amongst the various data inputs. The minima is primarily informed by the length composition data from the purse-seine fishery with minor additional influence from the recruitment component of the likelihood (influenced by the *SigmaR* parameter), the length composition data from the LL2 fishery, and the DN CPUE indices. The decline in the larger albacore in the samples from the purse-seine fishery since the mid 2000s appears to be particularly influential (Figure 18). Model sensitivities were conducted to investigate the influence of these data (*PSLFupweight* and *PSLFdownweight*) and the LL2 length composition data (*LengthComp_exLL2* and *SelectLL2).* Additional sensitivities examined the influence of the *SigmaR* parameter (*SigmaR60* and *SigmaR80* options).

The suite of model sensitivities also included the presumption that longline efficiency has increased by 1% per annum over the entire period of the fishery (applied to the LL3 CPUE indices) (*LLqIncrease*). An additional sensitivity were also formulated that varied the selectivity function of the southern longline fishery and, thereby, mediated the influence of the principle abundance indices (*SelectDN50*).

There is concern over the reliability of the longline length composition data, especially the data collected by the Taiwanese logbook programme. The *LengthComp_exTWLF* model sensitivity excludes those data from the length composition data sets.

The two alternative parameterisations of natural mortality were also included within the suite of model sensitivities. For the base model configuration, management advice was formulated using a range of values for SRR steepness (0.70, 0.80 and 0.90). For presentation purposes, detailed results were presented for the intermediate value of steepness only.

Table 1: A description of the model sensitivities relative to the single region reference model (base model).

Model	Description	Base model parameters	Alternative parameters
LengthAtAge	Increase variation in length-at-age for males and females.	CVs for length-at-age CV_young 0.06 CV_old 0.025	CV_young 0.10 CV_old 0.10
LengthWeight	Use length-weight parameters from Kitakado et al. (2019)	a = 1.3718e-05 b = 3.0973	a = 6.9e-06 b = 3.2263
LLqIncrease	Increase effective effort of LL3 CPUE indices by 1% per annum.		
Mature1	Use maturity at length from recent western Indian Ocean study (rather than South Pacific reproductive potential at length)	Length based Reproductive Potential from South Pacific albacore.	Length based maturity ogive from Dhrumeea et al (2016)
NatMort1	Decrease natural mortality from 0.30 to 0.2207	M = 0.30 all ages	M = 0.2207 all ages
NatMort2	Age specific natural mortality from 0.40 to 0.2207 (Hybrid)	M = 0.30 all ages	M = 0.2207 4+ ages
SelectDN50	Constrain LL3/LL4 selectivity to 50% selection for largest length classes.		Constraint on terminal parameter of selectivity.
SelectLL2	Estimate separate length based selectivities for LL1 and LL2. Approx. logistic form.	Selectivity shared LL1 and LL2.	Separate selectivities for LL1 and LL2.
SigmaR60	Increase *SigmaR* to 0.60	*SigmaR* = 0.30	*SigmaR* = 0.60
SigmaR80	Increase *SigmaR* to 0.80	*SigmaR* = 0.30	*SigmaR* = 0.80
Steepness70	SRR Steepness 0.70	h = 0.80	h = 0.70
Steepness90	SRR Steepness 0.90	h = 0.80	h = 0.90
CPUE_South	Incorporate LL3 and LL4 CPUE indices in single region model.	LL3 CPUE only	LL3 and LL4 CPUE indices.
CPUE_West	Incorporate LL1 and LL3 CPUE indices in single region model.	LL3 CPUE only	LL1 and LL3 CPUE indices.
LengthComp_exLL2	Exclude length composition data from LL2 fishery.	LL2 LF data included	No LL2 LF data
LengthComp_exTWLF	Exclude all Taiwanese LL logsheet length composition data.	Include TWLF data in length comp	Exclude TWLF data from length comp
PSLFdownweight	Decrease the influence of the PS LF data in the model fit.	PS LF lambda = 1.0	PS LF lambda = 0.5
PSLFupweight	Increase the influence of the PS LF data in the model fit.	PS LF lambda = 1.0	PS LF lambda = 2.0

For comparative purposes, two alternative spatially stratified models were included in the final set of model options: a two region model and a four region model. The four region model (*R4_CPUE_All*) incorporated the four region specific LL CPUE indices with a shared catchability coefficient (q) and a common logistic selectivity function for the longline fisheries. Regional recruitment deviates were estimated for the four regions and movements were estimated amongst regions (Figure 25).

The two region model (*R2_CPUE_South*) incorporated the two southern longline CPUE indices (LL3 and LL4), rescaled with regional scalars that represented the larger regions. The two LL CPUE indices shared a catchability coefficient (q) and a common selectivity function. The LL1 and LL2 longline fisheries also shared a separate selectivity function. Regional recruitment deviates were estimated for the two regions and movements were estimated between the regions (Figure 25).

5.2 Fit diagnostics – reference model

The performance of the model was evaluated by examining the fit to the two data components – the CPUE indices and the fishery-specific length composition data.

- The reference model provides a reasonable fit to the overall trends in the LL3 CPUE indices (Figure 30 and Figure 31). There is considerable variability in the CPUE indices that is not accounted for by the model and the RMSE of the CPUE indices approximates the CV assigned to the indices (CV 0.20). The magnitude of the residuals may be partly attributable to seasonal variation in CPUE in the LL3 fishery. However, estimating separate seasonal catchability coefficients for the CPUE series did not substantially improve the overall fit to the CPUE indices.
- The trends in the vulnerable biomass estimated for the LL1, LL2 and LL4 fisheries from the reference model are not consistent with the respective CPUE indices (Figure 30 and Figure 31).
- The fit to the drift net CPUE indices (nobs=7) is poor for all model options (Figure 32). This relates to the strong decline in the LL3 CPUE indices during the late 1980s that dominates the estimated trend in stock abundance. The assessment model estimated that this abundance trend was partly attributable to a general decline in recruitment during the 1980s. In turn, this would have been expected to affect the magnitude of the stock biomass that was vulnerable to the drift net fishery. However, the trend in declining abundance was not evident in the DN CPUE indices (Figure 32).
- For the LL1−4 fisheries, the single region reference model approximates the overall length composition data from the fisheries (Figure 33). However, the structural assumptions of the model (shared selectivities for LL1/LL2 and LL3/LL4) appear to degrade the overall fit to the length composition data from the LL2 fishery with the model over-estimating the proportion of fish in the 80-110 cm length range.
- For the LL2 and LL4 fisheries, the reference model over-estimates the proportion of fish in individual length classes resulting in "spikes" in the aggregated length compositions. The variation is related to length composition data from periods that occur following higher recruitment estimated by the model, indicating that the estimates of higher recruitment is not apparent in the length composition data from those fisheries.
- The deficiencies in the overall fit to the length composition from the LL1−4 fisheries are considerably more pronounced for the four region model (Figure 34) than the single region reference model (Figure 33). This is likely to be due to the additional constraints imposed on the longline selectivities for the four region model.
- The most comprehensive length composition data is available from the LL3 fishery. From 1990, the reference model predicts a small decline (of approx. 2–3 cm) in the length of fish from the LL3 fishery which is not apparent in the length composition data (Figure 35 and Figure 36). From 2000, there was an increase in the occurrence of larger fish sampled from the LL3 fishery, while the variability in the length composition also increased. The dynamics of the assessment model do not adequately reflect these observations, although the model predicts larger fish in the LL3 catches around 2000, 2010 and 2015 (immediately following periods with higher recruitment estimated by the model). Fluctuations in the size of fish sampled from the LL4 fishery are not predicted by the reference model (Figure 35 and Figure 36).
- For LL1 and LL2, larger fish were sampled from the fisheries around 1990 and from 2015–2017, while smaller fish were sampled during the mid-late 1990s (Figure 35). The reference model approximates the observed trends in length from these fisheries, although the extent of the variation is under-estimated by the model (Figure 36).
- There is a high degree of variation in the individual length samples from the longline fisheries that cannot be accounted for by the model. The high degree of variability is assumed to be indicative of a high degree of sampling error and consequently the length frequency data sets were all assigned a relatively low weighting in the final model options (Figure 35). There may also be seasonal variation in fish size which is not adequately represented by the model.
- For the DN and PS 1 fisheries, there is a reasonable overall fit to the aggregated length composition data (Figure 33). The DN length composition data are from a limited period only. The longer time series of length composition data from the purse seine fishery reveal a decline in the average length of albacore

sampled. The extent of the decline in fish length over the last decade is under-estimated by the model (Figure 35 and Figure 36).

5.3 Model parameter estimates

5.3.1 Selectivity

A common double normal selectivity function was estimated for the southern longline fisheries (LL3 & LL4). The selectivity function estimates that fish are fully vulnerable over a relatively narrow length range of about 75–90 cm (Figure 40). Larger fish are estimated to have a considerably lower vulnerability to the southern longline fisheries.

A common selectivity function was estimated for the northern longline fisheries (LL1 & LL2). The selectivity function was parameterised using a double normal although it was constrained to maintain full selectivity for the largest length classes. Full selectivity was estimated to be attained from about 95 cm (Figure 40).

The selectivity of the PS 1 fishery indicates the fishery catches the larger fish in the population with full vulnerability at about 100 cm. The selectivity function was constrained to fully select the larger length classes (Figure 40). The selectivity function for the drift net fisheries was estimated to have a narrow selection range between 57–77 cm (Figure 40). The four "Other" fisheries were assumed to have a selectivity function that was equivalent to the drift net fisheries.

5.3.2 Recruitment parameters

Annual recruitment deviates from the SRR were estimated for 1975–2015 (Figure 41). The model assumes recruitment deviates are from a distribution with a standard deviation of 0.3 (*sigmaR*) which was comparable to the realised variation in the recruitment deviates from initial model options. The recruitment deviates are estimated with a relatively high level of uncertainty reflecting the limited data available to inform the model of the magnitude of individual year classes. There is no strong temporal trend in the recruitment deviates, although higher recruitment deviates tended to be estimated during the early 1980s followed by lower recruitment in the early 1990s (Figure 41). Recruitment was estimated to be low for the two most recent years in the series (2014 and 2015).

5.4 Stock dynamics

5.4.1 Recruitment

The assessment models are configured to constrain recruitment to be at the equilibrium level for 1950–1974 (Figure 42) with variation in annual recruitments estimated for 1975–2015. Overall, the reference model estimated relatively low variation in recruitment. Recruitment is estimated to have been above average during the late 1970s and early 1980s and lower during 1986–1987. This pattern in the annual recruitments corresponds with the sharp decline in the LL3 CPUE indices during the late 1980s. Annual recruitment fluctuated during the 1990s and 2000s with short periods of higher recruitment in 1993, 1998–2000, 2006 and 2012 (Figure 42) immediately preceding periods of higher CPUE from the LL3 fishery (in 1995–1999, 2002, 2008 and 2013). Recruitment was estimated to be below average in 2014 and 2015 which corresponded to the sharp decline in the CPUE indices in the most recent years. The model option that incorporated the south-eastern LL CPUE indices (LL4) moderated the recent decline in the estimated recruitment.

Model options with a higher assumed variation in recruitment deviates (SigmaR 0.6 or 0.8) did not estimate an appreciably different pattern in the annual recruitments compared to the reference model, although the overall scale of recruitment was marginally higher than the reference model (by 4% and 8%, respectively).

5.4.2 Biomass

For the reference model, spawning biomass is estimated to have declined gradually during 1950–1980 (Figure 43) following the general increase in annual catches. The spawning biomass declined sharply during 1990–1995 following the high catches from the drift net fishery (in 1986–1991) and a corresponding decline in estimated annual recruitments (1986–1987). Spawning biomass continued to decline during 1999–2002 following high catches by the western longline fisheries (LL1 and LL3) during the same period. Over the last decade, spawning biomass remained relatively stable at an historically low level (Figure 43).

These overall trends in stock abundance are comparable for the range of model options (Figure 43 and Figure 44) although the overall extent of the stock decline is lower for the model option that incorporates the north-western longline CPUE indices (LL1) (*CPUE_West*) (Figure 43). Recent trends in spawning biomass are slightly more optimistic for the model option that incorporates the south-eastern CPUE indices (LL4) (*CPUE_South*), while the recent trend in biomass is more pessimistic for the model that incorporates an increase in longline efficiency (*LLqIncrease*) (Figure 43). The model is also sensitive to the parameterisation of the selectivity function for the LL3 fishery as this mediates the CPUE index.

The overall scale of the spawning biomass and stock depletion is influenced by assumptions related to the spawner-recruitment relationship (steepness and sigmaR) and the magnitude of natural mortality (Figure 44). The results are also sensitive to the degree of variation in length-at-age as this presumably influences of the purse seine length composition data in the model; a higher variation in length-at-age will be interpreted as a higher level of depletion as fewer of the larger fish are observed.

For the reference model, there is a relatively high level of precision associated with the estimate of initial spawning biomass and the level of spawning biomass during the period prior to 1975 (Figure 45). The level of precision is a function of the assumption of equilibrium recruitment during the early period and the fixed level of steepness for the SSR. There is a higher level of uncertainty associated with the estimates of spawning biomass during main data period of the model (1975–2017) that includes the estimation period for the recruitment deviates.

5.4.3 Fishing mortality

Fishing mortality rates for each fishery are defined as apical fishing mortality rates; i.e. the fishing mortality for the fully selected length class (or length classes). The fishing mortality rates are an approximation of the Baranov continuous *F* (Methot & Wetzel 2013).

Longline fishing mortality rates are estimated to be higher for the southern longline fisheries (LL3 & LL4) than the northern fisheries (LL1 & LL2). For LL4, fishing mortality rates have increased relatively steadily since 1990, while LL3 fishing mortality rates are estimated to have increased rapidly over the last decade (Figure 46). Relatively high fishing mortality rates were estimated for the two drift net fisheries during the late 1980s and early 1990s (Figure 46). Fishing mortality rates for the "Other" fisheries were negligible throughout the model period.

Aggregated, age-specific fishing mortality rates were derived for the terminal year (2017) of the model (following Methot & Wetzel 2013). Aggregate fishing mortality rates were highest for age classes 2–3 years (reflecting the age composition of the catch from the southern longline fisheries) and decline for the older age classes (Figure 47). The aggregate, age-specific fishing mortality from 2017 is the basis for the derivation of the *MSY* based reference points.

6 Stock status

6.1 Current status and yields

Current (2017) stock status was defined relative to the *MSY* based biomass (SB_{MSY}) and fishing mortality (F_{MSY}) reference points. For the reference model structure, the yield analysis incorporates the SRR into the equilibrium biomass and yield computations with three alternative values of steepness assumed for the SRR (0.70, 0.80 and 0.90). For comparative purposes, the range of model sensitivities (CPUE options and natural mortality options) assumed the intermediate value of steepness (0.80). The time-series of model estimates of spawning biomass and recruitment are uninformative regarding the value of steepness (Figure 48).

Equilibrium yield and biomass (spawning) were computed as a function of the 2017 aggregate fishing mortality-at-age (Figure 47). Estimates of *MSY* from the range of single region model options based on the LL3 CPUE index are 29,700–44,800 mt (Table 7), although the upper range of the *MSY* values is not considered plausible due to the higher level of recruitment variability assumed (SigmaR 0.8). The more credible range of *MSY* values (29,700–38,000 mt) is broadly comparable to the average annual catch from 2013–2017 (35,737 mt) (Table 3).

The estimates of *MSY* were relatively insensitive to the inclusion of additional sets of CPUE indices within the single region model (*CPUE_West* and *CPUE_South*) (Table 7). The four region model option also

yielded a similar estimate of *MSY* (Table 8), while the two region model incorporating the southern CPUE indices (LL3 and LL4) estimated a substantially higher estimate of yield (*MSY* 87,900 mt).

The *MSY* reference spawning biomass is estimated to be a relatively small proportion of the equilibrium unexploited spawning biomass i.e. SB_{MSY}/SB_0 of 0.205–0.215 for the 0.8 steepness options (Table 7). The relatively low SB_{MSY}/SB_0 ratio appears to be related to the lower vulnerability of the older, mature age classes.

For the reference model option, the spawning biomass is estimated to have remained above the SB_{MSY} level throughout the history of the fishery (1950–2017) (Figure 49). Prior to 1985, exploitation rates were low and spawning biomass remained well above SB_{MSY} (Figure 49 and Figure 50). Fishing mortality increased sharply in the late 1980s and exceeded the F_{MSY} level in 1990, at the peak of the drift net fishery. Fishing mortality rates were lower immediately following the cessation of the drift net fishery in the early 1990s, but have generally increased over the last two decades and are estimated to have exceeded the F_{MSY} level in 2016–2017.

Spawning biomass is estimated to have declined during the 1990s–early 2000s, approaching the SB_{MSY} level in the early 2000s and remaining at about that level over the last decade. For the reference model option, the point estimate of current (2017) biomass is above SB_{MSY} (SB_{2017}/SB_{MSY} 1.246, confidence interval 0.804–1.689) (Figure 51 and Table 7), although there is an associated 13.5% probability of the stock being below the SB_{MSY} threshold. Fishing mortality in 2017 is estimated to have exceeded the F_{MSY} level (F_{2017}/F_{MSY} 1.227, confidence interval 0.832–1.623) with a high degree of certainty ($\Pr(F_{2017}/F_{MSY} > 1) = 0.868$)) (Figure 51).

All of the single region model options estimate fishing mortality to be approaching or have exceeded the F_{MSY} level (F_{2017}/F_{MSY} 0.891–1.676) (Table 7). The range of model options are more equivocal in terms of the level of depletion. While the reference model estimates the stock to be above the SB_{MSY} level, model options that have lower productivity parameters (lower natural mortality and lower SRR steepness) estimate current (2017) biomass to be at or below the SB_{MSY} level. Similarly, model sensitivities that mediate the principle abundance indices (LL3 CPUE indices), either via the estimation of selectivity or increased longline efficiency, also estimate current (2017) biomass to be below the SB_{MSY} level. Estimates of stock status are also sensitive to the relative weighting of the purse seine length composition data; greater influence of these data in the model resulted in a more pessimistic stock status with current biomass estimated to be below the SB_{MSY} level.

The estimates of stock status were similar between the single region reference model and the four region model (Table 8). However, the two region model (R2_CPUE_South) estimated substantially higher estimates of stock size and seemingly unrealistically high estimates of yield (Table 8).

A retrospective analysis of the reference model, progressively excluding the last 1-5 years of the assessment period, indicates that the model tends to under-estimate the biomass level (relative to SB_{MSY}) in the terminal year of the model (Figure 52), while over-estimating the level of fishing mortality (Figure 53) as the model generally under-estimated recruitment in the last four years of the model period.

6.2 Projections

Stock projections were conducted for the reference model option. The projections were conducted for a 10 year period (2018–2027) with a constant level of catch at multiples (60%, 70%, 80%, 90%, 100%, 110%, 120%, 130%, 140%) of the 2017 fishery catches (total of 38,168 mt). Recruitment during the projection period was at the equilibrium level (derived from the SRR with steepness of 0.80). The uncertainty associated with the projected biomass was derived from the covariance matrix. Uncertainty in the projected biomass promulgates rapidly reflecting the uncertainty associated with recent biomass, recent recruitment and the equilibrium recruitment level. For each stock scenario, the probabilities of the biomass being below the SB_{MSY} level and the 40% SB_{MSY} limit after 3 years (2020) and 10 years (2027) were determined. Similarly, the probabilities of exceeding the F_{MSY} level and the 140% F_{MSY} limit were also determined.

For the reference model, recent recruitment is estimated to have been below average and current (2017) level of catch exceeds the equilibrium surplus production (*MSY* 33,300 mt). Consequently, the biomass is projected to decline rapidly to below the SB_{MSY} level over the first three years of the projection period and continues to decline, at a lower rate, for the remainder of the projection period. Annual catches of 120% of the current catch level are projected to cause the stock to crash within the 10 year projection period, while catches stabilise above the SB_{MSY} level at the 80% catch level (Table 9). There is a high probability that fishing mortality will continue to exceed the F_{MSY} level at the current level of catch (100%) during the projection period with a relatively high probability of also exceeding the 140% F_{MSY} limit (Table 10).

7 Discussion and conclusions

7.1 Comparison with previous (2016) assessment results

The overall scale of the stock biomass from the current assessment is lower, by approximately one third, than the biomass estimated from the 2016 reference model. There is also a higher level of depletion estimated by the current assessment (Table 7). There have been four main changes to the 2019 assessment from the previous assessment models. Firstly, the spatial distribution of albacore catches from the Indian Ocean longline fishery has been refined resulting in increases in the annual catches from the LL1 (40% increase overall) and LL2 (13% increase) longline fisheries and decreases to the annual catches from the LL3 (17% decrease) and LL4 (25% decrease). This has resulted in a change in the overall exploitation pattern of the albacore fishery. Substituting the catches from the 2016 assessment into the current model substantially increased the estimate of overall biomass and *MSY* yield (Table 11).

The primary CPUE indices included in the current assessment (LL3) differ considerably from the indices incorporated in the previous assessment (Hoyle et al 2019). The revised and extended LL3 CPUE indices exhibit a greater decline than the previous set of indices which corresponds to a higher degree of stock depletion. New growth parameters, specific to Indian Ocean albacore tuna, have been included in the current assessment, including different values for the variation of length-at-age. The new growth parameters increased the magnitude of the spawning biomass and decreased the level of depletion relative to the previous growth parameters. Finally, for the current assessment, there have been changes to the configuration of the length composition data from the longline fishery which reduced the magnitude of the overall biomass and appreciably increase the estimate of current fishing mortality (Table 11). There are likely to be interactions between the various data components that complicate the comparisons between the current and previous (2016) stock assessment models.

Collectively, these four main changes appear to account for most of the difference in the overall model results from the previous assessment. Other model changes (such as reducing *SigmaR* 0.6 to 0.3) appear to have resulted in relatively small changes to the results.

7.2 Current assessment results

The current assessment depends largely on the time series of southwestern longline CPUE indices and the catch history from the entire fishery. The LL3 CPUE indices declined considerably during the late 1980s–early 1990s and continued to decline at a lesser rate during the remainder of the 1990s and 2000s. There is a reasonable correspondence between the declining trends in the CPUE indices and the overall catch from the fishery.

There is also a reasonable correspondence between the trends in the LL3 CPUE indices and the southeastern LL (LL4) CPUE indices, although the two sets of indices diverge over the last decade. The LL3 CPUE indices declined sharply over the last 5 years, while CPUE indices from LL4 increased considerably over the last decade. The increase in albacore catch by the Japanese fleet in LL4 may indicate that the level of targeting of albacore has increased and may be positively biasing the LL4 CPUE indices. Further evaluation of the CPUE indices is required to determine the reliability of these two sets of CPUE indices

Overall, the magnitude of the decline in the LL3 CPUE indices is more pronounced than evident from the CPUE indices from the equatorial regions (LL1 and LL2). The differences between the sets of CPUE indices are mediated by the different selectivities assumed for the equatorial and southern longline fisheries. The model results are sensitive to the extent that the larger length classes are vulnerable to the southern longline fisheries. The selectivity functions for these fisheries are informed by the length composition data from the fisheries. However, these length data are highly variable, over time and between fleets, and the reliability of the data from some sectors of the fleet has been questioned. While these data were assigned a relatively low weight in the assessment modeling, the data will still influence the estimation of the selectivity parameters of the longline fisheries.

Estimates of current stock status are strongly influenced by the length composition data from the purse seine fishery. The decline in the length of fish sampled from the purse seine fishery are more consistent with a lower overall stock size and a higher level of depletion. The purse seine fishery operates in the western equatorial region where larger albacore predominate, although catches from the fishery are relatively small, averaging about 650 t over the last decade. The decline in the size of fish sampled from this fishery appears to

be influential in bounding the upper range of the overall productivity of the stock through the interaction with the fishery selectivity parameters and albacore natural mortality and growth parameters (including the variation in length-at-age) from the recent study. Sampling of albacore catches from the purse seine fishery has provided a comprehensive set of length composition data from this fishery. However, it is unknown whether these data encompass the entire upper length range of the albacore population. Further, the declining trend in fish size may be influenced by change in the operation of the purse seine fishery, including the spatial distribution of catch and increased reliance of FADs, although a detailed examination of the available data did not reveal any substantial changes in fish size that were attributable to set type, fleet or area fished.

The drift net CPUE indices have negligible influence in the assessment models due to the relatively low weighting assigned to the indices and the small number of indices relative to the number of LL3 CPUE observations in the corresponding period. The current assessment is the first time that historical length composition data have been included from the Indian Ocean drift net fishery. These data confirm previous assumptions regarding the size composition of the drift net catch. Overall, the CPUE indices from the drift net fishery are not very influential in the assessment; excluding these data did not appreciably change estimates of stock status and yield.

The recent estimates of growth for Indian Ocean albacore represent an improvement in our understanding of the biology of the species. However, further reaserch is required to refine our knowledge regarding other key life history parameters. In the absence of studies specific to the Indian Ocean, it is necessary to adopt parameters from albacore studies in other Oceans. For example, reproductive potential is assumed to be equivalent to an estimate of reproductive potential at length from South Pacific albacore which, in turn, influences the determination of spawning biomass reference points. The assessment results are also sensitive to the other key productive assumptions, especially SRR steepness and natural mortality. Estimates of natural mortality, such as those derived from observations of longevity, are limited for Indian Ocean albacore and have been based on the values used in the assessment of other albacore stocks. The value of natural mortality (M=0.3) included in the reference assessment model resulted in a considerably better fit to the length composition data compared to the model options with a lower level of natural mortality for adult fish (M=0.2207). This observation only provides a weak basis for preferentially selecting the higher M option because the fit to the length composition data is also dependent on the estimation of selectivity and other life history parameters (especially growth).

Estimates of overall stock size are also likely to be influenced by assumptions regarding the population structure during the early period of the model. The range of model options are based on the assumption that the stock is at unexploited, equilibrium conditions at the start of the model (1950) and recruitment prior to 1975 is simply a function of the SRR. Model testing indicated that estimating recruitment during the earlier period (prior to 1975) may result in a different biomass trajectory during the early period, although the biomass trajectories from alternative models tended to converge during the late 1980s–early 1990s. The models can account for the higher catches during the subsequent years either by having a higher level of equilibrium biomass or by increasing recruitment immediately prior to the period of higher catch (early recruitment options). There is very limited information to inform the model about the population age structure during this crucial period due to the lack of information to inform the model about the age composition of the population at that period (due to the uninformative length composition data). Nonetheless, the estimation of the early recruitments may influence the overall level of equilibrium recruitment and, hence the estimates of the overall productivity of the stock.

The current assessment has highlighted a considerable conflict between key sources of data included in the model (longline CPUE indices and length composition data). The estimates of stock status are, in part, influenced by the selection of the primary abundance index (LL3) and the relative weighting assigned to the individual data sets within the model. Consequently, the current stock status is considered to be uncertain as indicated by the relatively broad range of estimates from the range of model sensitivities (SB_{2017}/SB_{MSY} 0.887–1.764) and the uncertainty associated with individual model estimates of stock status. Correspondingly, estimates of current levels of fishing mortality (F_{2017}/F_{MSY} 0.80–1.68) are also uncertain, although almost all model options indicate fishing mortality rates are either approaching or have exceeded the reference level, indicating the overfishing is likely to be occurring.

The *MSY* based reference points correspond to a low overall level of stock size relative to unexploited conditions (SB_{MSY} approximately 20% SB_0). The recent level of catch (2013–2017 average of 35,737 t) is about the middle of the range of estimates of *MSY* for the stock (*MSY* 30,000–38,000 t).

Stock projections were conducted to evaluate the impact of current (2017) level of catch. The projections are not intended to provide a reliable prediction of future stock status due to the simplifying assumptions of equilibrium recruitment (from SRR), constant catch and unconstrained fishing mortality. Instead, the projections provide an indication of relative trends in stock biomass under different catch assumptions. For the reference model option, the stock was projected to decline below SB_{MSY} over the next 10 years.

8 Acknowledgements

The stock assessment was funded by FAO and IOTC and the project was managed by Paul de Bruyen. The IOTC Secretariat staff of Fabio Fiorellato and James Geehan provided the initial data sets. Simon Hoyle (IOTC Consultant) provided input regarding the longline CPUE indices.

9 References

Bartoo, N., Holts. D. (1993). Estimated drift gillnet selectivity for albacore *Thunnus alalunga*. *Fishery Bulletin* 92:371–378.

Bromhead, D., B., A. Williams and S. D. Hoyle (2009). Factors affecting size composition data from south Pacific albacore longline fisheries.

Chang, F.-C., C.-Y. Chen, L.-K. Lee and S.-Y. Yeh (2012). Assessment on Indian albacore stock based mainly on Taiwanese longline data. Fourth Working Party on Temperate Tunas, Shanghai, China, 20–22 August 2012. . Indian Ocean Tuna Commission. **IOTC-2012-WPTmT04-19**.

Chang, S., H. Liu (1995). Adjusted Indian Ocean albacore CPUE series of Taiwanese longline and drift net fisheries. Sixth session of the Expert Consultations on Indian Ocean tunas, Colombo, Sri Lanka 25–29 September 1995. **IOTC-1995-EC602-26.**

Chang, S., H. Liu and C.-C. Hsu (1993). "Estimation of vital parameters for Indian albacore through length frequency data." Journal of the Fisheries Society of Taiwan **20**(1): 1-17.

Chen, I. C., P. F. Lee and W. N. Tzeng (2005). "Distribution of albacore (*Thunnus alalunga*) in the Indian Ocean and its relation to environmental factors." Fisheries Oceanography **14**(1): 71-80.

Chen, K. S., T. Shimose, T. Tanabe, C. Y. Chen and C. C. Hsu (2012). "Age and growth of albacore Thunnus alalunga in the North Pacific Ocean." Journal of fish biology **80**(6): 2328-2344.

Dhurmeea, Z.; Chassot, E.; Augustin, E.; Assan, C.; Nikolic, N.; Bourjea, J. et al. (2016). Morphometrics of albacore tuna (*Thunnus alalunga*) in the Western Indian Ocean. Seventh Working Party on Temperate Tunas: Data Preparatory Meeting, Kuala Lumpa, Malaysia, 14–17 January 2019. Indian Ocean Tuna Commission. **IOTC-2019-WPTmT07(DP)-INF02**.

Dhurmeea, Z.; Zudaire, I.; Chassot, E.; Cedras, M.; Nikolic, N.; Bourjea, J. et al. (2016) Reproductive Biology of Albacore Tuna (*Thunnus alalunga*) in the Western Indian Ocean. PLoS ONE 11(12): e0168605. doi:10.1371/journal.pone.0168605

Farley, J.H.; Eveson, J.P.; Bonhommeau, S.; Dhurmeea, Z.; West, W.; Bodin, N. (2019). Growth of albacore tuna (*Thunnus alalunga*) in the western Indian Ocean using direct age methods. Seventh Working Party on Temperate Tunas: Data Preparatory Meeting, Kuala Lumpa, Malaysia, 14–17 January 2019. Indian Ocean Tuna Commission. **IOTC-2019-WPTmT07(DP)-21**.

Farley, J. H., S. D. Hoyle, J. P. Eveson, A. J. Williams, C. R. Davies and S. J. Nicol (2014). "Maturity Ogives for South Pacific Albacore Tuna (Thunnus alalunga) That Account for Spatial and Seasonal Variation in the Distributions of Mature and Immature Fish." PloS one **9**(1): e83017.

Farley, J., A. Williams, N. Clear, C. Davies and S. Nicol (2013). "Age estimation and validation for South Pacific albacore Thunnus alalunga." Journal of fish biology **82**(5): 1523-1544.

Farley, J.H., A.J. Williams, S. D. Hoyle, C. R. Davies and S. J. Nicol (2013). "Reproductive dynamics and potential annual fecundity of South Pacific albacore tuna *(Thunnus alalunga*)." PLoS ONE **8**(4): e60577.

Fonteneau, A. (2015). Indian Ocean albacore stock: review of its fishery, biological data and results of its 2014 stock assessment. IOTC/2015/XXX.

Francis, R. I. C. C. (2011). "Data weighting in statistical fisheries stock assessment models." Canadian Journal of Fisheries and Aquatic Sciences **68**(6): 1124-1138.

Geehan, J. and S. Hoyle (2013). Review of length frequency data of the Taiwan,China distant water longline fleet, IOTC-2013-WPTT15-41 Rev_1. Indian Ocean Tuna Commission Working Party on Tropical Tunas, San Sebastian, Spain, 23–28 October, 2013.

Guan, W.; Zhu, J.; Xu, L.; Dai, X, (2016). Using a Bayesian biomass dynamics model to assess Indian Ocean albacore. Sixth Working Party on Temperate Tunas, Shanghai, China, 18–21 July 2016. Indian Ocean Tuna Commission. **IOTC-2014-WPTmT06-22**.

Gunn, J. S., N. P. Clear, T. I. Carter, A. J. Rees, C. A. Stanley, J. H. Farley and J. M. Kalish (2008). "Age and growth in southern bluefin tuna,< i> Thunnus maccoyii</i>(Castelnau): Direct estimation from otoliths, scales and vertebrae." Fisheries Research **92**(2): 207-220.

Hoyle, S.D. (2019). Regional scaling factors for Indian Ocean albacore tuna. Seventh Working Party on Temperate Tunas: Data Preparatory Meeting, Kuala Lumpa, Malaysia, 14–17 January 2019. Indian Ocean Tuna Commission. **IOTC-2019-WPTmT07(DP)-13**.

Hoyle, S., J. Hampton and N. Davies (2012). Stock assessment of albacore tuna in the South Pacific ocean. Scientific Committee, Eighth Regular Session, 7-15 August 2012, Busan, Republic of Korea**:** 90.

Hoyle, S. D. (2008). Adjusted biological parameters and spawning biomass calculations for south Pacific albacore tuna, and their implications for stock assessments. WCPFC Scientific Committee. Nouméa, New Caledonia**:** 20.

Hoyle, S. D., A. D. Langley and R. A. Campbell (2014). "Recommended approaches for standardizing CPUE data from pelagic fisheries."

Hoyle, S.D., R. Sharma, M. Herrera (2014). Indian Ocean albacore assessment. Fifth Working Party on Temperate Tunas, Busan, Korea, 28–31 July 2014. Indian Ocean Tuna Commission. **IOTC-2014-WPTmT05-24**.

Hoyle, S.D. Yin Chang, Doo Nam Kim, Sung Il Lee, Takayuki Matsumoto, Kaisuke Satoh, and Yu-Min Yeh (2016). Collaborative study of albacore tuna CPUE from multiple Indian Ocean longline fleets. Sixth Working Party on Temperate Tunas, Shanghai, China, 18–21 July 2016. Indian Ocean Tuna Commission. IOTC-WPTmT06-19a.

Hoyle, S.D.; Chassot, E.; Fu, D.; Kim, D.N.; Lee, S.; Matsumoto, T.; Satoh, K.; Wang, S.; Kitakado, T. (2019). Collaborative study of albacore tuna CPUE from multiple Indian Ocean longline fleets in 2019. Seventh Working Party on Temperate Tunas: Data Preparatory Meeting, Kuala Lumpa, Malaysia, 14–17 January 2019. Indian Ocean Tuna Commission. **IOTC-2019-WPTmT07(DP)-19**.

Hoyle, S.D.; Yeh, Y.M.; Chang, S.T.; Wu, R.F. (2015). Descriptive analysis of the Taiwanese Indian Ocean longlie fishery, focussing on tropical areas. Seventeenth Working Party on Tropical Tunas, Montpellier, France, 23–28 October, 2015. Indian Ocean Tuna Commission. IOTC-2015-WPTT17-INF09.

Huang, H.; Liu, K. (2010). Bycatch and discards by the Taiwanese large-scale tuna longline fleets in the Indian Ocean. Fisheries Research **106**: 261-270

Huang, H., C.-L. Wu, C. Kuo and W. Su (1991). "Age and growth of Indian Ocean albacore (Thunnus alalunga) by scales."

Ianelli, J., M. Maunder and A. E. Punt (2012). Independent review of 2011 WCPO bigeye tuna assessment.

IOTC Secretariat (2013). Report and documentation of the Indian Ocean Tuna Fisheries of Indonesia Albacore Catch Estimation Workshop: Review of Issues and Considerations. Bogor-Jakarta, 21-25 June 2013. IOTC Technical Report. No. 2013/01. Bogor-Jakarta, IOTC. 2013. 40 pp.

IOTC (2014). Report of the Fifth Session of the IOTC Working Party on Temperate Tunas. Fifth Working Party on Temperate Tunas, Busan, Korea, 28–31 July 2014. Indian Ocean Tuna Commission. **IOTC-2014-WPTmT05-R[E]**.

IOTC (2016). Report of the Sixth Session of the IOTC Working Party on Temperate Tunas. Sixth Working Party on Temperate Tunas, Shanghai, China, 18–21 July 2016. Indian Ocean Tuna Commission. **IOTC-2016-WPTmT06-R[E]**.

IOTC (2019). Report of the Seventh Session of the IOTC Working Party on Temperate Tunas (Data Preparatory Session). Seventh Working Party on Temperate Tunas: Data Preparatory Meeting, Kuala Lumpa, Malaysia, 14–17 January 2019. Indian Ocean Tuna Commission. **IOTC-2019-WPTmT07(DP)-RE**.

ISSF (2011). Report of the 2011 ISSF Stock Assessment Workshop: Rome, Italy, March 14-17, 2011. . ISSF Technical Report 2011-02, http://iss-foundation.org/wp-content/uploads/downloads/2011/08/ISSF-2011-02-Report-2011-ISSF-WS.pdf. McLean, Virginia, USA, International Seafood Sustainability Foundation.

Karakulak, F. S., E. Özgür, M. Gökoğlu, I. T. Emecan and A. Başkaya (2011). "Age and growth of albacore (Thunnus alalunga Bonnaterre, 1788) from the eastern Mediterranean." Turkish Journal of Zoology **35**(6): 801-810.

Kitakado, T.; Fiorellato, F.; De Bruyn, P. (2019). Allometric curve for the Indian Ocean albacore. Seventh Working Party on Temperate Tunas: Data Preparatory Meeting, Kuala Lumpa, Malaysia, 14–17 January 2019. Indian Ocean Tuna Commission. **IOTC-2019-WPTmT07XX**.

Kitakado, T., E. Takashima, T. Matsumoto, T. Ijima and T. Nishida (2012). First attempt of stock assessment using Stock Synthesis III (SS3) for the Indian Ocean albacore tuna (*Thunnus alalunga*). IOTC Working Party on Temperate Tunas, Shanghai, China, 20–22 August 2012, Indian Ocean Tuna Commission.

Lan, K.; Kawamura, H.; Lee, M.; Lu, H.; Shimada, T.; Hosoda, K.; Saikaida, F. (2011). Relationship between albacore (*Thunnus alalunga*) fishing grounds in the Indian Ocean and the thermal environment revealed by cloud-free microwave sea surface temperature. Fisheries Research **113**: 1-7

Langley, A.D.; Hoyle, S.D. (2016). Stock assessment of albacore tuna in the Indian Ocean using Stock Synthesis. Sixth Working Party on Temperate Tunas, Shanghai, China, 18–21 July 2016. Indian Ocean Tuna Commission. IOTC-WPTmT06-25.

Lee, H. H., M. N. Maunder, K. R. Piner and R. D. Methot (2012). "Can steepness of the stock-recruitment relationship be estimated in fishery stock assessment models?" Fisheries Research.

Lee, L.-K., C.-C. Hsu and F.-C. Chang (2014). Albacore (*Thunnus alalunga*) CPUE Trend from Indian Core Albacore Areas based on Taiwanese longline catch and effort statistics dating from 1980 to 2013.

Lee, Y. C. and H. C. Liu (1992). "Age determination, by vertebra reading, in Indian albacore, *Thunnus alalunga* (Bonnaterre)." Journal of the Fisheries Society of Taiwan **19**(2): 89-102.

Lorenzen, K. (1996). "THE RELATIONSHIP BETWEEN BODY WEIGHT AND NATURAL MORTALITY IN JUVENILE AND ADULT FISH - A COMPARISON OF NATURAL ECOSYSTEMS AND AQUACULTURE [Review]." Journal of Fish Biology **49**(4): 627-647.

Matsumoto, T., T. Kitakado and T. Nishida (2014). Standardization of albacore CPUE by Japanese longline fishery in the Indian Ocean, IOTC–2014–WPTmT05–18 Indian Ocean Tuna Commission Working Party on Temperate Tuna (WPTmT)**:** 16.

Matsumoto, T., T. Nishida and T. Kitakado (2012). Stock and risk assessments of albacore in the Indian Ocean based on ASPIC. Fourth Working Party on Temperate Tunas, Shanghai, China, 20–22 August 2012. . Indian Ocean Tuna Commission. **IOTC-2012-WPTmT04-20**.

Matsumoto, T., T. Nishida and T. Kitakado (2014). Stock and risk assessments of albacore in the Indian Ocean based on ASPIC. Fifth Working Party on Temperate Tunas, Busan, Korea, 28–31 July 2014. Indian Ocean Tuna Commission. **IOTC-2014-WPTmT05-22 Rev_1**.

Matsumoto, T. (2016). Stock and risk assessments of albacore in the Indian Ocean based on ASPIC. Sixth Working Party on Temperate Tunas, Shanghai, China, 18–21 July 2016. Indian Ocean Tuna Commission. **IOTC-2014-WPTmT06-20**.

McAllister, M. K. and J. N. Ianelli (1997). "Bayesian stock assessment using catch-age data and the sampling-importance resampling algorithm." Canadian Journal of Fisheries and Aquatic Sciences **54**(2): 284-300.

Megalofonou, P. (2000). "Age and growth of Mediterranean albacore." Journal of Fish Biology **57**(3): 700-715.

Methot, R.D. (2015). User Manual for Stock Synthesis model Version 3.24s. 11 February 2015.

Methot, R. D., Jr and I. G. Taylor (2011). "Adjusting for bias due to variability of estimated recruitments in fishery assessment models." Canadian Journal of Fisheries and Aquatic Sciences **68**(10): 1744-1760.

Methot, R. D. and C. R. Wetzel (2013). "Stock synthesis: A biological and statistical framework for fish stock assessment and fishery management." Fisheries Research **142**: 86-99.

Nikolic, N., Fonteneau, A., Hoarau, L., Morandeau, G., Puech, A., Bourjea, J. (2013). Short review on biology, structure, and migration of *Thunnus alalunga* in the Indian Ocean. Fifth Working Party on Temperate Tunas, Busan, Korea, 28–31 July 2014. Indian Ocean Tuna Commission. **IOTC-2014-WPTmT05-13**.

Nishida, T.; Dhurmeea, Z. (2019). Review of Indian Ocean albacore biological parameters for stock assessments. Seventh Working Party on Temperate Tunas: Data Preparatory Meeting, Kuala Lumpa, Malaysia, 14–17 January 2019. Indian Ocean Tuna Commission. **IOTC-2019-WPTmT07(DP)-12**

Nishida, T., T. Matsumoto and T. Kitakado (2012). Stock and risk assessments on albacore (Thunnus alalunga) in the Indian Ocean based on AD Model Builder implemented Age-Structured Production Model (ASPM).

Nishida, T.; Sato, K.; Chang, Y.; Matsumoto, T.; Lee, Y.C.; Kitakado, T. (2016). Stock assessments of albacore (Thunnus alalunga) in the Indian Ocean using Statistical-Catch-at-Age (SCAA). Age-Structured Production Model (ASPM). Sixth Working Party on Temperate Tunas, Shanghai, China, 18–21 July 2016. Indian Ocean Tuna Commission. **IOTC-2014-WPTmT06-21**.

Saji, N.H.; Yamagata, T. (2003). Possible impacts of Indian Ocean Dipole mode events on global climate. Climate Research 25(2) 151-169.

Santiago, J. and H. Arrizabalaga (2005). "An integrated growth study for North Atlantic albacore (*Thunnus alalunga*, Bonn. 1788)." ICES Journal of Marine Science **62**(4): 740-749.

Wells, R. J. D., S. Kohin, S. L. H. Teo, O. E. Snodgrass and K. Uosaki (2013). "Age and growth of North Pacific albacore (Thunnus alalunga): Implications for stock assessment." Fisheries Research **147**: 55-62.

Williams, A. J., J. H. Farley, S. D. Hoyle, C. R. Davies and S. J. Nicol (2012). "Spatial and sex-specific variation in growth of albacore tuna (Thunnus alalunga) across the South Pacific Ocean." PLoS One **7**(6): e39318.

Xu, Y., T. Sippel, S. L. H. Teo, K. Piner, K.-S. Chen and R. J. Wells (2014). A comparison study of North Pacific albacore (*Thunnus alalunga*) age and growth among various sources, ISC/14/ALBWG/04 ISC Albacore Working Group Meeting, 14-28 April 2014, La Jolla, CA, 92037, USA.

Yeh, S.; Hui, C.; Treng, T.; Kuo, C. (1995). Indian Ocean albacore stock structure studies by morphometric and DNA sequence methods. Sixth Session of the Expert Consultations on Indian Ocean Tunas, Columbo, Sri Lanka, 25–29 September 1995. Indian Ocean Tuna Commission. IOTC-1995-EC602-25.

Zhu, J., Y. Chen, X. Dai, S. J. Harley, S. D. Hoyle, M. N. Maunder and A. M. Aires-da-Silva (2012). "Implications of uncertainty in the spawner–recruitment relationship for fisheries management: An illustration using bigeye tuna (Thunnus obesus) in the eastern Pacific Ocean." Fisheries Research **119-120**: 89-93.

Table 2. Definition of fisheries for the albacore assessment models.

Fishery	Nationality	Gear	Area
1. LL1	All	Longline	1
2. LL2	All	Longline	2
3. LL3	All	Longline	3
4. LL4	All	Longline	4
5. DN3	CN-TW	Drift net	3
6. DN4	CN-TW	Drift net	4
7. PS1	All	Purse seine	1
8. Other1	All	Other gears	1
9. Other2	All	Other gears	2
10. Other3	All	Other gears	3
11. Other4	All	Other gears	4

Table 3: Recent albacore tuna catches (mt) by fishery included in the stock assessment model. The annual catches are presented for 2016 and 2017 and the average annual catch is presented for 2013-17.

Fishery	Time period		
	2013-17	2016	2017
1. LL1	8,519	7,774	9,033
2. LL2	1,857	1,333	1,477
3. LL3	14,803	16,145	17,286
4. LL4	9,462	9,030	9,320
5. DN3	0	0	0
6. DN4	0	0	0
7. PS1	488	433	438
8. Other1	99	87	142
9. Other2	507	476	472
10. Other3	3	6	0
11. Other4	0	0	0
Total	35,737	35,284	38,168

Table 4. Main structural assumptions of the albacore tuna reference model and details of estimated parameters. The specifications of the contrasting four region model are in grey italics.

Category	Assumptions	Parameters
Spatial structure	Single region *Four regions*	
Recruitment	Occurs at the start of fourth quarter as 0 age fish. Recruitment is a function of Beverton-Holt stock-recruitment relationship (SRR). Temporal recruitment deviates from SRR, 1975–2015. *Overall regional recruitment distribution.* *Temporal variation in regional recruitment distribution 1980–2015*	LNR_0 No prior*;* h = 0.80 *SigmaR* = 0.3, 41 deviates. *4 parameters (3 estimated, 1 fixed)* *108 parameters*
Initial population	A function of the equilibrium recruitment assuming population in an unexploited state prior to 1950. Initial fishing mortality fixed at zero for all fisheries.	
Age and growth	Two sexes with 14 age-classes, with the last representing a plus group. Growth parameterised using VonBert growth model. CV of length-at-age based varies as a linear function of age. Mean weights (w_j) from the weight-length relationship $W = aL^b$.	Female *Lage1* = 52.60, *Linfinity* = 103.8cm, *k* = 0.38 Male *Lage1* = 52.04, *Linfinity* = 110.6cm, *k* = 0.34 CVyoung =0.06, CVold =0.025 *a* = 1.3718e-05, *b* = 3.0973
Natural mortality	Invariant with age.	Fixed parameter 0.30
Reproductive potential	Length based female reproductive potential. Fecundity is directly related to female biomass (Wt) i.e. eggs=Wt*(a+b*Wt) with a=0 and b=1.	Specified by length class
Movement	*Age specific*	*Estimated*

Selectivity	Length based selectivity, parameterised with double normal function. LL3 and LL4 fisheries (and CPUE) share a common double normal selectivity. LL1 and LL2 fisheries share a common double normal selectivity constrained to approximate full selectivity for the largest length classes. Drift net fisheries have common selectivity. Double normal. Purse seine double normal selectivity. Other (1-4) fisheries fixed selectivity, equivalent to DN. *All LL fisheries (and CPUE) share a common selectivity.* *Constrained to approximate full selectivity for the largest length classes.*	 4 estimated parameters, no priors. 4 estimated parameters, no priors. 3 estimated parameters, no priors. 3 estimated parameters, no priors. *4 estimated parameters, no priors.*
Catchability	No seasonal variation in catchability for LL CPUE. LL CPUE indices have CV of 0.2. *Shared base catchability estimated for four sets of LL CPUE indices.*	1 base parameter estimated
Fishing mortality	Hybrid approach (method 3, see Methot & Wetzel 2013).	
Length composition	Multinomial error structure. Length samples assigned an ESS of nfish/400 with a maximum ESS of 5. Nfish is the number of fish sampled.	

Table 5. Main objective function components for the single region reference model and model sensitivities. NA indicates that the data component was not included in the model likelihood.

Model	Total	Total LF Comp	CPUE indices				
			LLCPUE1	LLCPUE2	LLCPUE3	LLCPUE4	DNCPUE
R1_CPUE_SouthWest Reference	881.4	1053.8	NA	NA	-134.8	NA	-5.0
LengthAtAge	880.3	1045.0	NA	NA	-127.8	NA	-4.9
LengthComp_exLL2	771.2	944.6	NA	NA	-134.9	NA	-5.0
LengthComp_exTWLF	373.6	549.2	NA	NA	-136.0	NA	-5.3
LengthWeight	881.7	1054.1	NA	NA	-134.8	NA	-5.0
LLqIncrease	889.7	1058.3	NA	NA	-132.8	NA	-4.8
Mature1	881.3	1053.6	NA	NA	-134.7	NA	-5.0
NatMort1	915.0	1085.7	NA	NA	-133.5	NA	-5.0
NatMort2	913.2	1084.2	NA	NA	-133.9	NA	-5.1
SelectDN50	899.5	1068.8	NA	NA	-132.8	NA	-5.0
SelectLL2	876.0	1048.3	NA	NA	-134.7	NA	-5.0
SigmaR60	898.9	1052.9	NA	NA	-135.6	NA	-5.0
SigmaR80	908.2	1054.1	NA	NA	-136.0	NA	-4.9
Steepness70	882.0	1054.9	NA	NA	-135.3	NA	-5.0
Steepness90	881.2	1053.0	NA	NA	-134.4	NA	-5.0
CPUE_South	793.9	1054.7	NA	NA	-123.1	-100.2	-4.7
CPUE_West	769.8	1056.4	-117.1	NA	-132.0	NA	-5.3

Table 6. Main objective function components for the set of stock assessment models with different spatial components. NA indicates that the data component was not included in the model likelihood.

Model	Total	Total LF Comp	CPUE indices				
			LLCPUE1	LLCPUE2	LLCPUE3	LLCPUE4	DNCPUE
R1_CPUE_SouthWest Reference	881.4	1053.8	NA	NA	-134.8	NA	-5.0
R1_CPUE_South	793.9	1054.7	NA	NA	-123.1	-100.2	-4.7
R1_CPUE_West	769.8	1056.4	-117.1	NA	-132.0	NA	-5.3
R2_CPUE_South	748.0	1022.5	NA	NA	-141.8	-119.6	-5.1
R4_CPUE_ALL	510.5	1047.3	-142.9	-161.1	-131.2	-111.1	-4.6

Table 7. Estimates of management quantities for the set of one region stock assessment models. The 95% confidence intervals for the current stock status metrics are provided for the single region reference model. The estimates of 2014 stock status from the 2016 reference model are included for comparison.

Model	SB_0	SB_{MSY}	SB_{MSY}/SB_0	SB_{2017}	SB_{2017}/SB_0	SB_{2017}/SB_{MSY}	F_{2017}/F_{MSY}	MSY
R1_CPUE_SouthWest *Reference*	103,612	21,321	0.206	26,567	0.256	1.246 (0.804-1.689)	1.227 (0.832-1.623)	33,302
LengthAtAge	91,320	19,115	0.209	15,816	0.173	0.827	1.676	30,132
LengthComp_exLL2	104,036	21,426	0.206	26,780	0.257	1.250	1.211	33,491
LengthComp_exTWLF	95,488	19,553	0.205	18,329	0.192	0.937	1.445	31,677
LengthWeight	106,166	22,025	0.207	27,322	0.257	1.240	1.230	33,252
PSLFdownweight	117,970	24,218	0.205	39,564	0.335	1.634	0.936	37,563
PSLFupweight	94,650	19,561	0.207	17,883	0.189	0.914	1.565	30,782
LLqIncrease	103,549	21,319	0.206	19,009	0.184	0.892	1.568	33,351
Mature1	130,753	28,236	0.216	37,031	0.283	1.311	1.132	34,266
NatMort1	145,778	31,293	0.215	27,767	0.190	0.887	1.630	29,740
NatMort2	134,060	27,776	0.207	24,627	0.184	0.887	1.619	29,871
SelectDN50	92,680	19,445	0.210	18,190	0.196	0.935	1.552	30,707
SelectLL2	102,880	21,179	0.206	25,529	0.248	1.205	1.250	33,146
SigmaR60	118,578	24,380	0.206	30,670	0.259	1.258	1.156	37,977
SigmaR80	137,097	28,160	0.205	34,122	0.249	1.212	1.085	43,777
Steepness70	115,116	28,913	0.251	30,633	0.266	1.060	1.404	31,290
Steepness90	95,638	14,365	0.150	24,352	0.255	1.695	0.996	36,399
CPUE_South	105,415	21,721	0.206	32,902	0.312	1.515	0.986	33,814
CPUE_West	120,162	24,679	0.205	43,542	0.362	1.764	0.891	38,257
Reference 2016 (CPUEsouth)	*146,434*	*30,030*	*0.205*	*54,089**	*0.37**	*1.801* 1.154–2.448*	*0.846* 0.421–1.271*	*38,812*

Table 8. Estimates of management quantities for the set of for the set of stock assessment models with different spatial components. The estimates of 2014 stock status from the 2016 reference model are included for comparison.

Model	SB_0	SB_{MSY}	SB_{MSY}/SB_0	SB_{2017}	SB_{2017}/SB_0	SB_{2017}/SB_{MSY}	F_{2017}/F_{MSY}	MSY
R1_CPUE_SouthWest *Reference*	103,612	21,321	0.206	26,567	0.256	1.246 (0.804-1.689)	1.227 (0.832-1.623)	33,302
R1_CPUE_South	105,415	21,721	0.206	32,902	0.312	1.515	0.986	33,814
R1_CPUE_West	120,162	24,679	0.205	43,542	0.362	1.764	0.891	38,257
R2_CPUE_South	284,716	59,369	0.209	198,336	0.697	3.341	0.214	87,920
R4_CPUE_All	108,135	23,083	0.213	38,227	0.354	1.656	0.850	35,213
Reference 2016 (CPUEsouth)	*146,434*	*30,030*	*0.205*	*54,089**	*0.37**	*1.801* 1.154–2.448*	*0.846* 0.421–1.271*	*38,812*

Table 9. Projected stock status relative to SB_{MSY} and the probability of being below SB_{MSY} and 40% SB_{MSY} in 3- and 10 years for projections conducted using multiples of the 2017 level of catch (38,168 mt) for the single region *CPUE_SouthWest* model.

Model option	3 years (2020)			10 year (2027)		
	SB/SB_{MSY}	Pr($SB<SB_{MSY}$)	Pr($SB<0.4SB_{MSY}$)	SB/SB_{MSY}	Pr($SB<SB_{MSY}$)	Pr($SB<0.4SB_{MSY}$)
Catch 60%	1.048	0.421	0.003	1.800	0.043	0.00
Catch 70%	0.990	0.529	0.003	1.472	0.165	0.015
Catch 80%	0.933	0.601	0.011	1.143	0.392	0.064
Catch 90%	0.875	0.691	0.011	0.815	0.665	0.205
Catch 100%	0.818	0.804	0.032	0.489	0.877	0.456
Catch 110%	0.762	0.852	0.056	0.178	0.972	0.693
Catch 120%	0.705	0.909	0.078	0.000	1.000	1.000
Catch 130%	0.649	0.947	0.133	0.000	1.000	1.000
Catch 140%	0.593	0.967	0.195	0.000	1.000	1.000

Table 10. Projected fishing mortalityrelative to F_{MSY} and the probability of being above F_{MSY} in 3- and 10 years for projections conducted using multiples of the 2017 level of catch (38,168 mt) for the for the single region *CPUE_SouthWest* model.

Model option	3 years (2020)			10 year (2027)		
	F/F_{MSY}	Pr($F>F_{MSY}$)	Pr(F>1.4F_{MSY})	F/F_{MSY}	Pr($F>F_{MSY}$)	Pr(F>1.4F_{MSY})
Catch 60%	0.616	0.001	0.000	0.476	0.000	0.000
Catch 70%	0.757	0.068	0.000	0.624	0.009	0.000
Catch 80%	0.913	0.341	0.011	0.826	0.243	0.005
Catch 90%	1.088	0.623	0.124	1.142	0.617	0.306
Catch 100%	1.286	0.807	0.365	1.764	0.711	0.599
Catch 110%	1.513	0.885	0.589	4.234	1.000	1.000
Catch 120%	1.776	0.936	0.742	NA	1.000	1.000
Catch 130%	2.084	0.945	0.829	NA	1.000	1.000
Catch 140%	2.455	0.938	0.864	NA	1.000	1.000

Table 11. Estimates of 2014 stock status from retrospective stepwise changes from the current single region reference model to incorporate components of the 2016 assessment for comparison with the 2016 reference model.

Model	SB_0	SB_{MSY}	SB_{MSY}/SB_0	SB_{2014}	SB_{2014}/SB_0	SB_{2014}/SB_{MSY}	F_{2014}/F_{MSY}	MSY
R1_CPUE_SouthWest *Reference 2019*	103,612	21,321	0.206	26,103	0.252	1.224	1.227	33,302
Step1 2016 LL catch	146,897	30,072	0.205	63,720	0.434	2.119	0.649	46,342
Step2 2016 LL3 CPUE	135,689	27,781	0.205	65,122	0.480	2.344	0.685	42,826
Step3 2016 Growth	118,719	24,685	0.208	38,906	0.328	1.576	1.206	32,912
Step4 2016 SigmaR	122,730	25,477	0.208	37,667	0.307	1.478	1.794	33,806
Step5 2016 Maturity	125,762	26,043	0.207	38,159	0.303	1.465	1.607	33,201
Step6 2016 LFs	156,099	32,259	0.207	63,996	0.410	1.984	0.853	41,607
Step7 MSYRef2014	156,099	32,037	0.205	63,996	0.410	1.998	0.837	41,104
Reference 2016 (CPUEsouth)	*146,434*	*30,030*	*0.205*	*54,089*	*0.37*	*1.801* *1.154–2.448*	*0.846* *0.421–1.271*	*38,812*

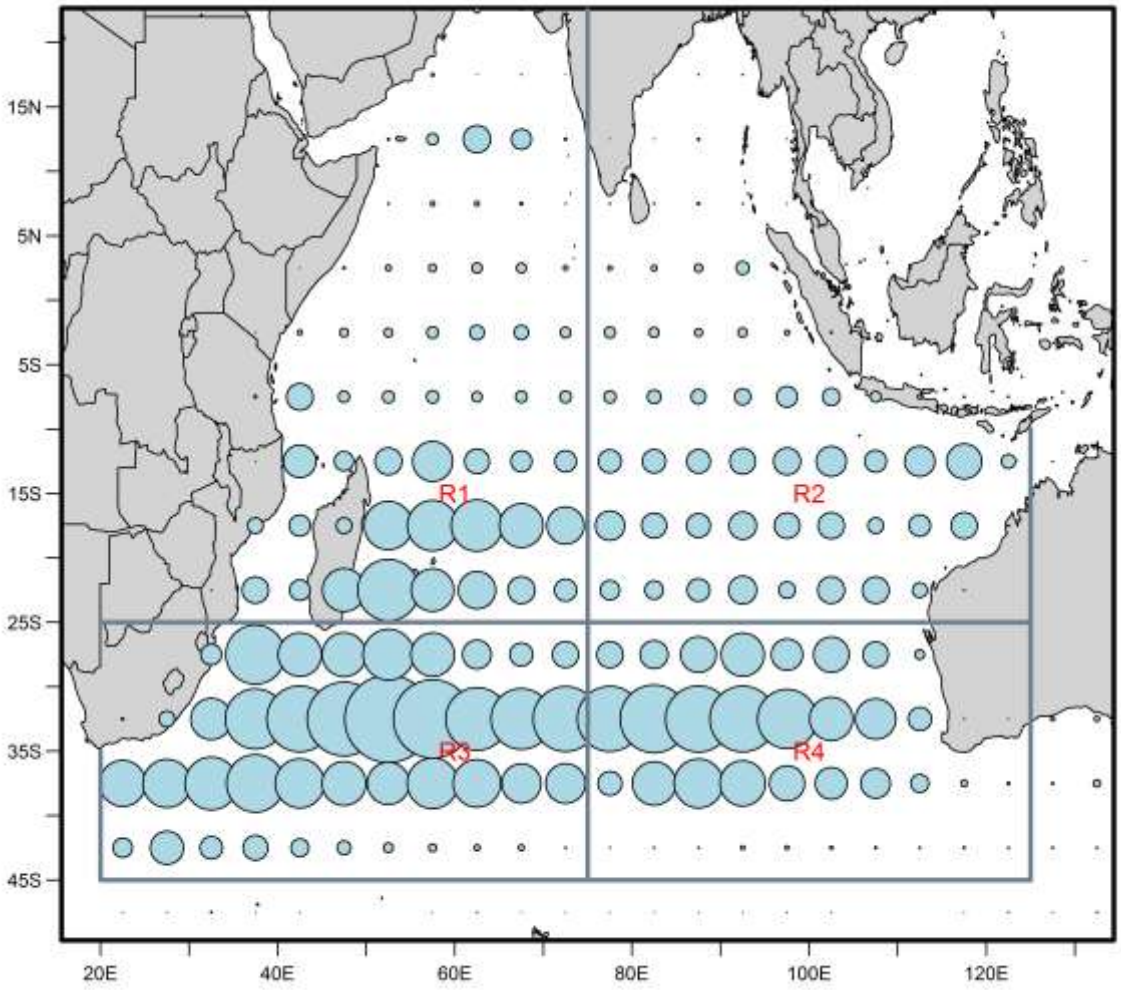

Figure 1. Spatial stratification of the Indian Ocean for the definition of the fisheries. The blue circles represent the aggregated Japanese and TW LL albacore catch (numbers of fish) by 5 degree cell from 1952-2017. The area of the circle is proportional to the magnitude of the catch (the largest circle represents a catch of 2.45 million fish).

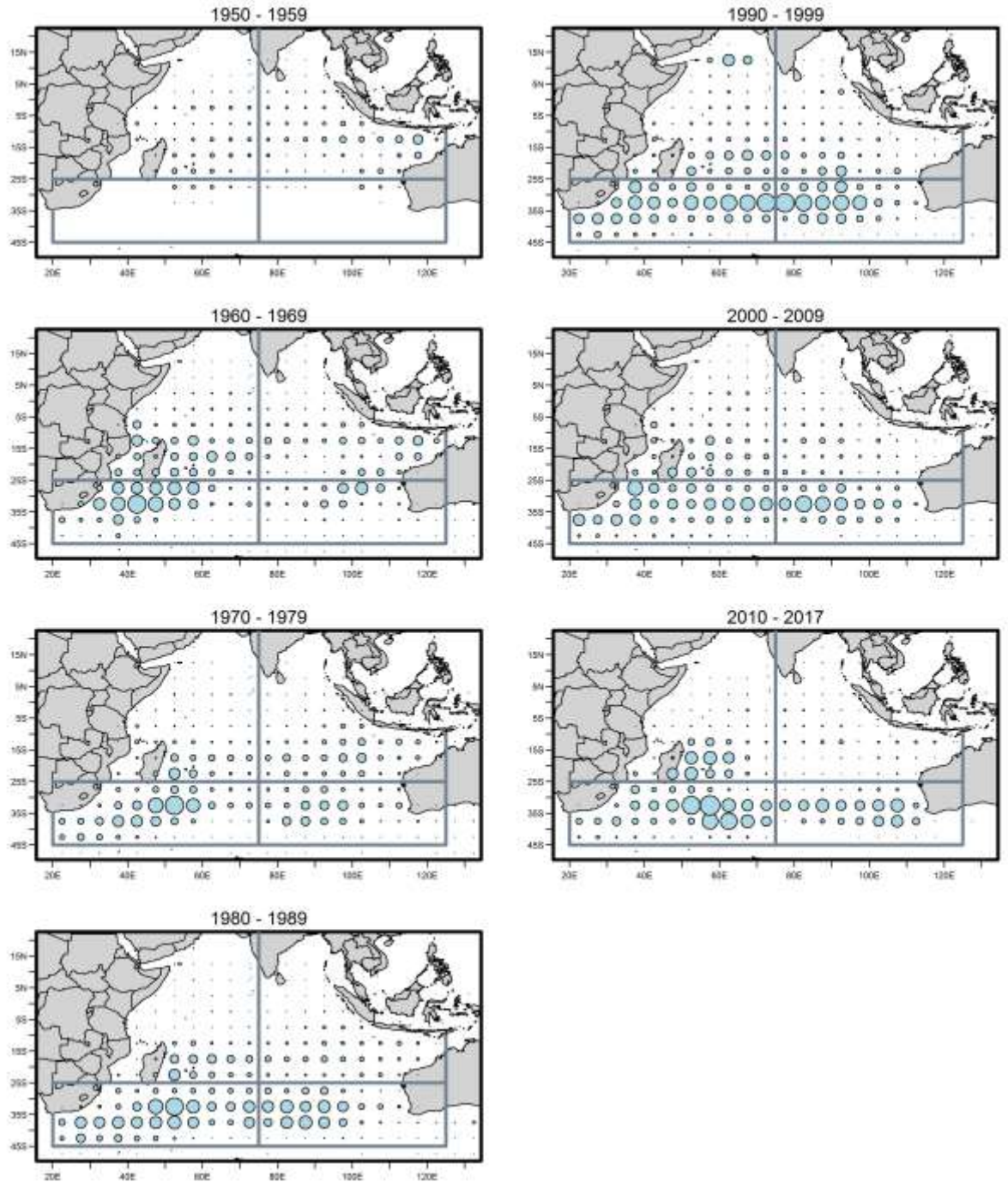

Figure 2. Distribution of Indian Ocean albacore longline catches by decade. The blue circles represent the aggregated Japanese and TW LL albacore catch (numbers of fish) by 5 degree cell. The area of the circle is proportional to the magnitude of the catch (the largest circle represents a catch of 692737 fish).

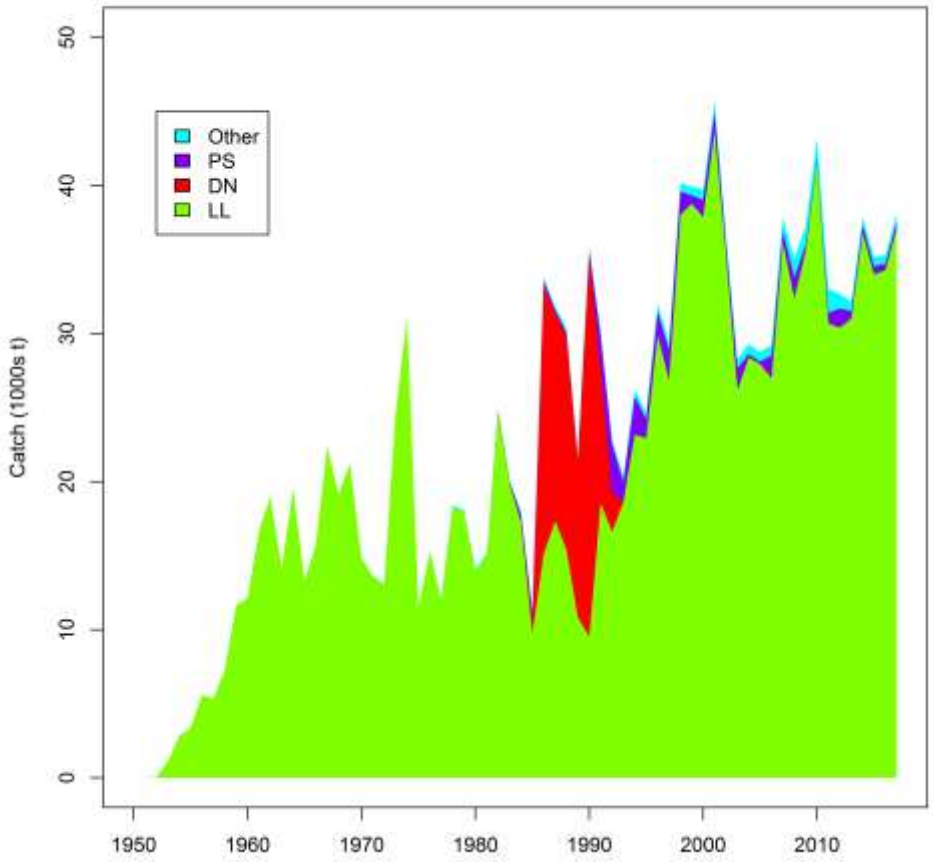

Figure 3. Total annual catch (1000s mt) of albacore tuna by fishing method from 1950 to 2017 (LL, longline; PS, purse-seine; OT, other; DN, drift net).

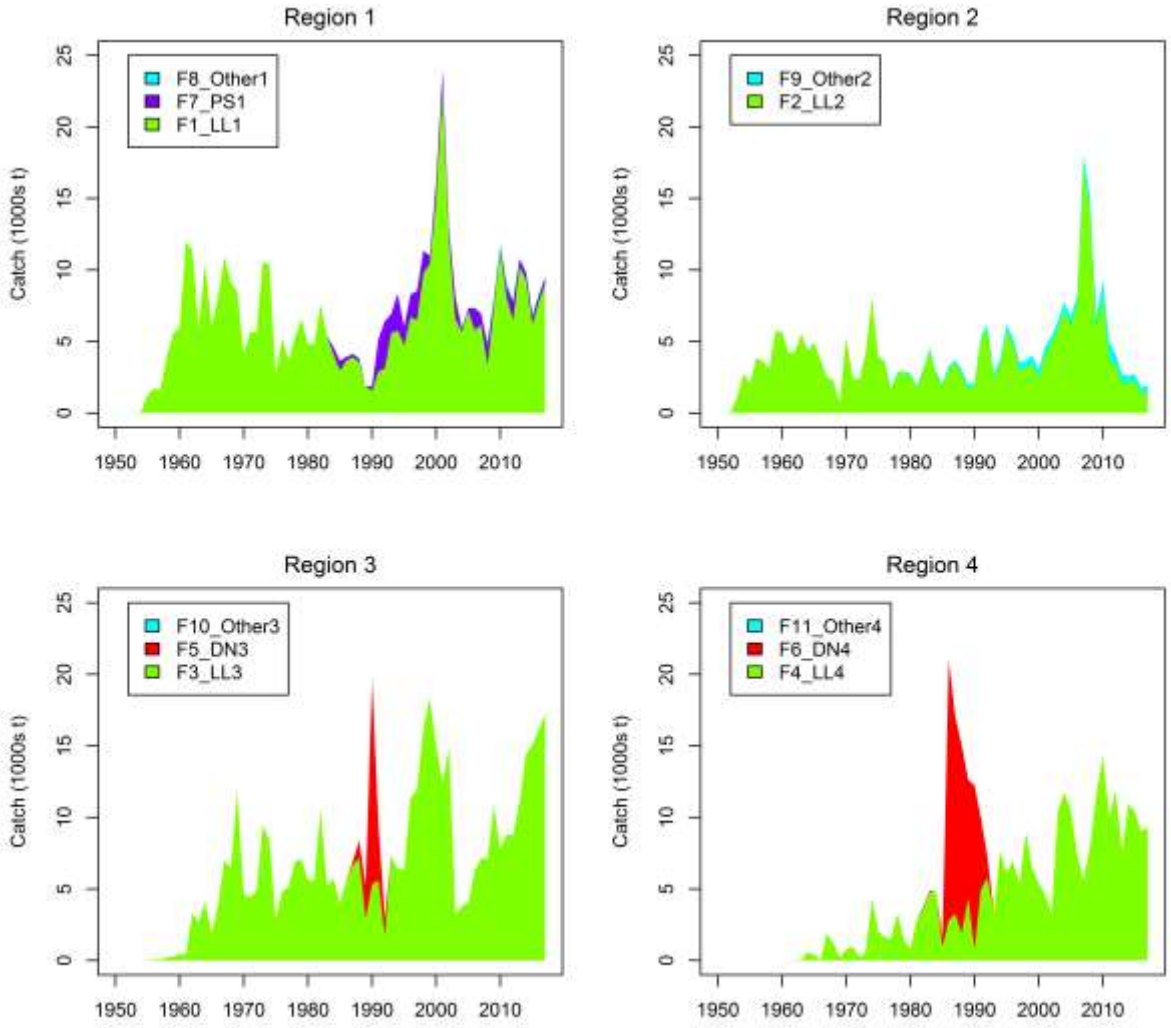

Figure 4. Total annual catch (1000s mt) of albacore tuna by fishing method and region from 1950 to 2017 (LL, longline; PS, purse-seine; OT, other; DN, drift net).

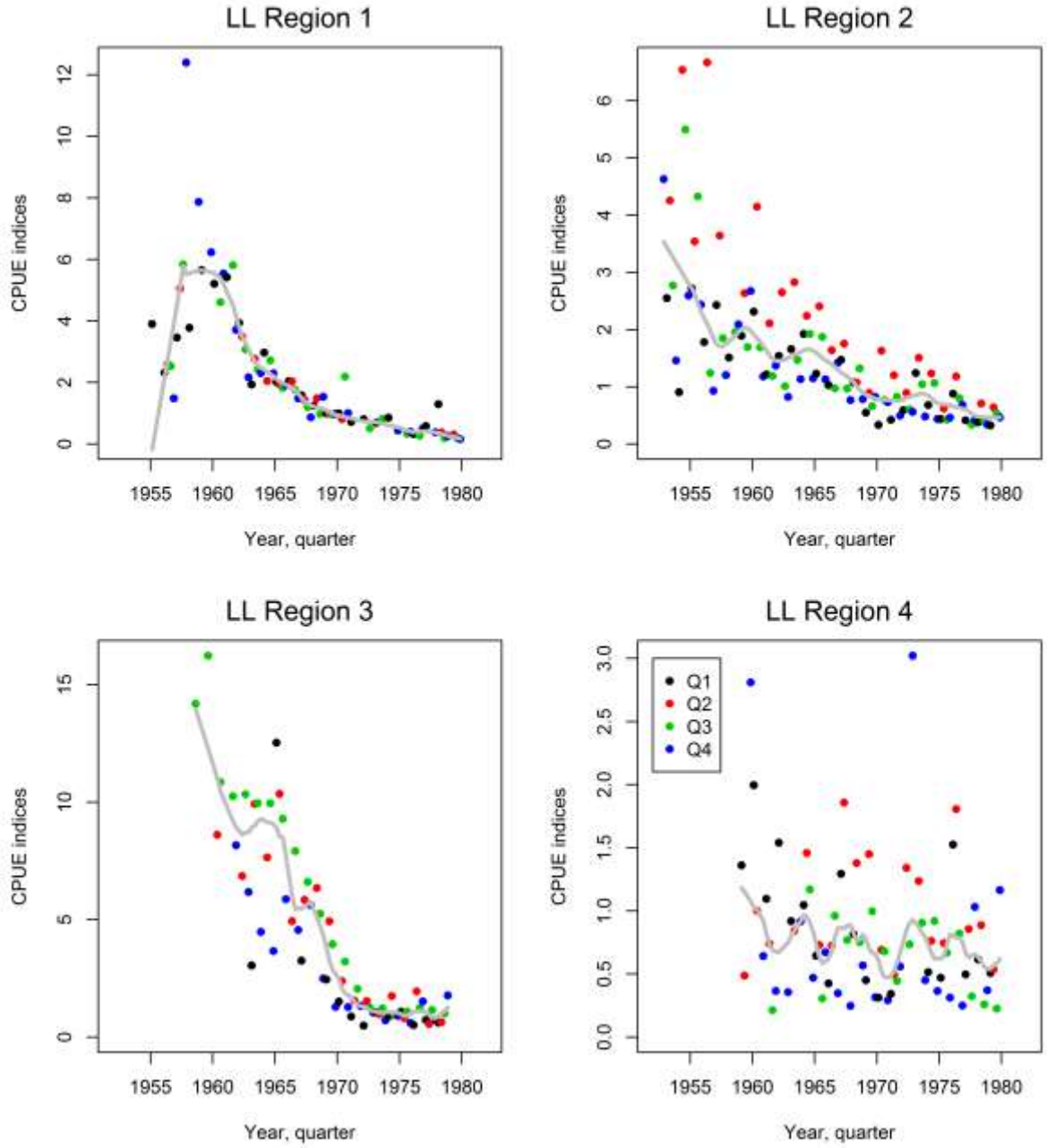

Figure 5. Quarterly GLM standardised catch-per-unit-effort (CPUE) for the longline fisheries (LL 1–4) (*novess_5279* series) (source Hoyle et al 2019). Each set of indices is scaled by the respective regional scaling factor. The lines represent a lowess smooth fit to each set of indices.

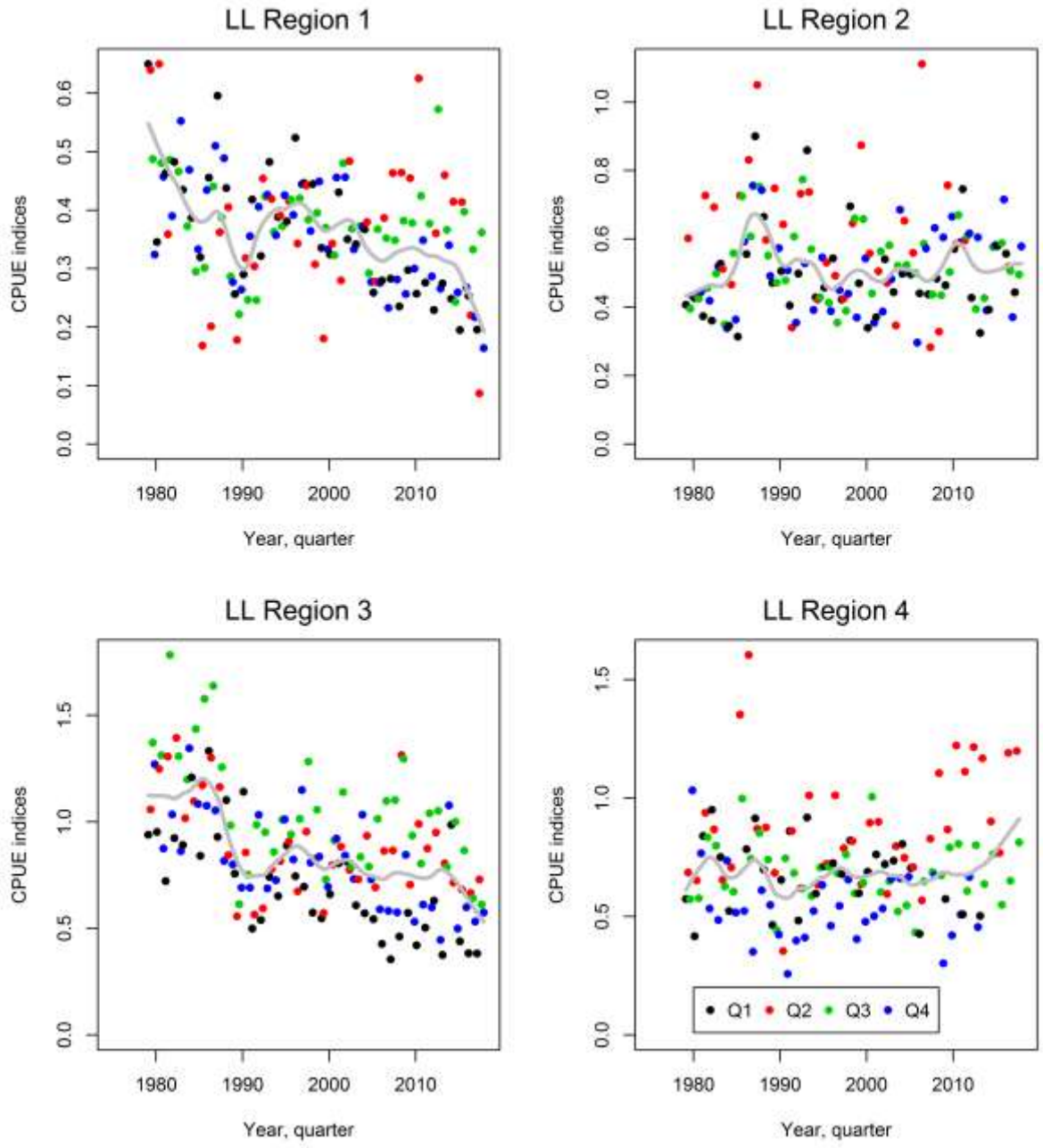

Figure 6. Quarterly GLM standardised catch-per-unit-effort (CPUE) for the longline fisheries (LL 1–4) from 1979-2017 (*vessid_79nd* series) (source Hoyle et al 2019). Each set of indices is scaled by the respective regional scaling factor. The lines represent a lowess smooth fit to each set of indices.

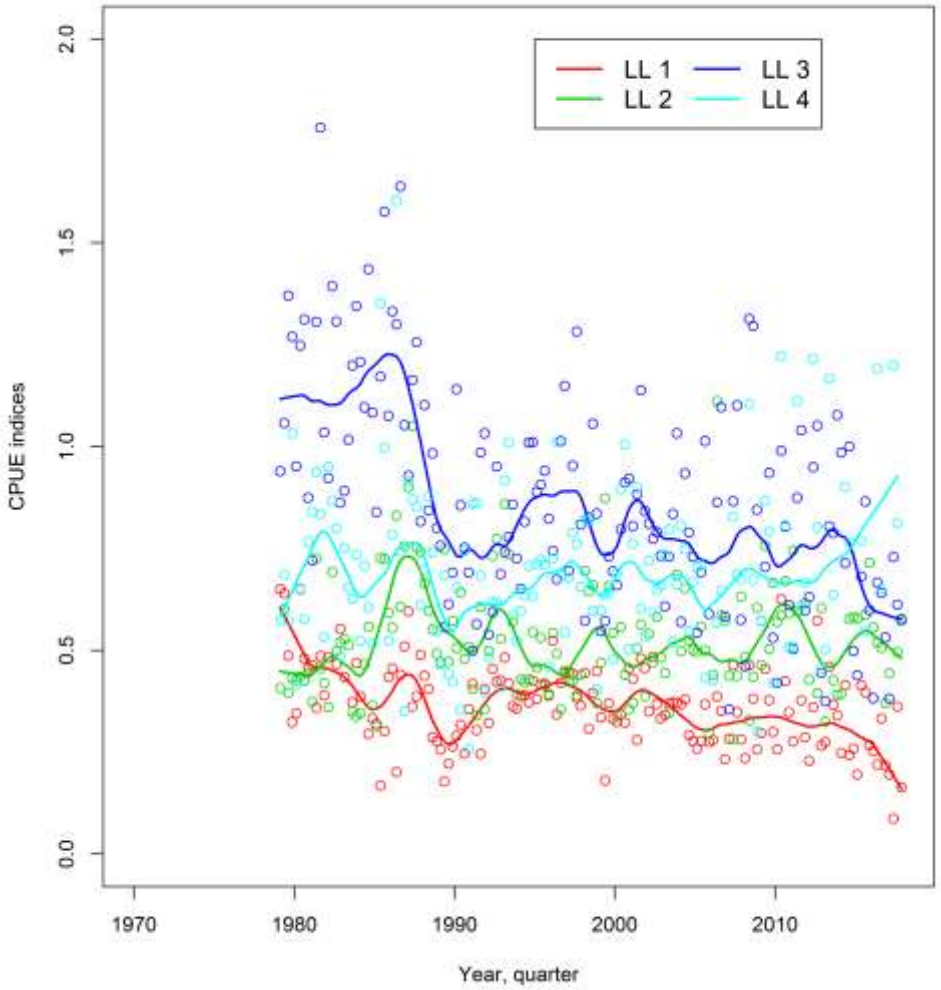

Figure 7: A comparison of the regional CPUE indices for the longline fisheries (LL 1–4) from 1979-2017 (*vessid_79nd* series) (source Hoyle et al 2019). Each set of indices is scaled by the respective regional scaling factor. The lines represent a lowess smooth fit to each set of indices.

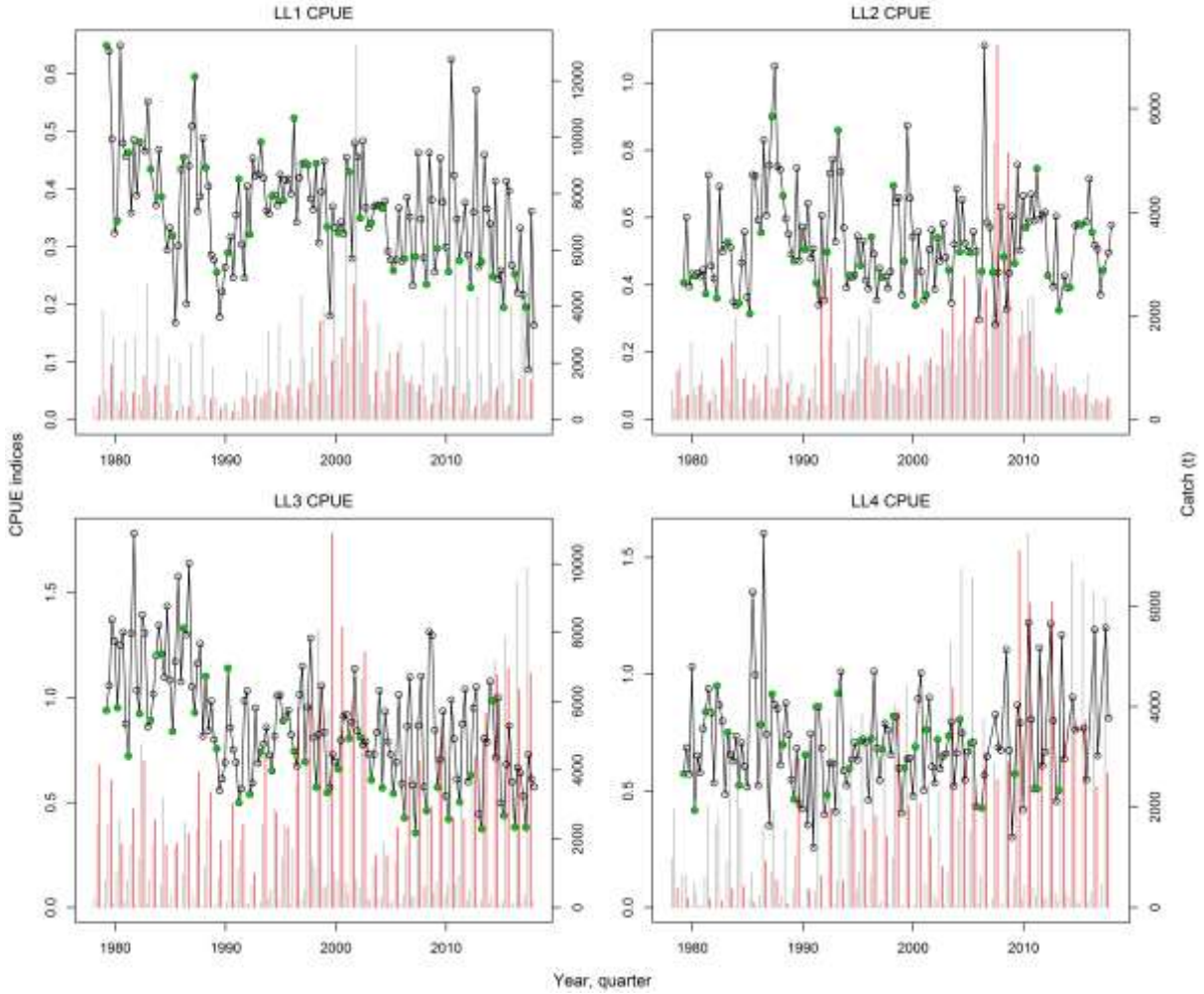

Figure 8. A comparison of the regional CPUE indices for the longline fisheries (LL 1–4) from 1979-2017 (*vessid_79nd* series) (points) and the quarterly catch (bars). The green points correspond to the CPUE indices from the first quarter 1 (Q1) of the year. The red bars correspond to the catch from the 3rd quarter (Q3).

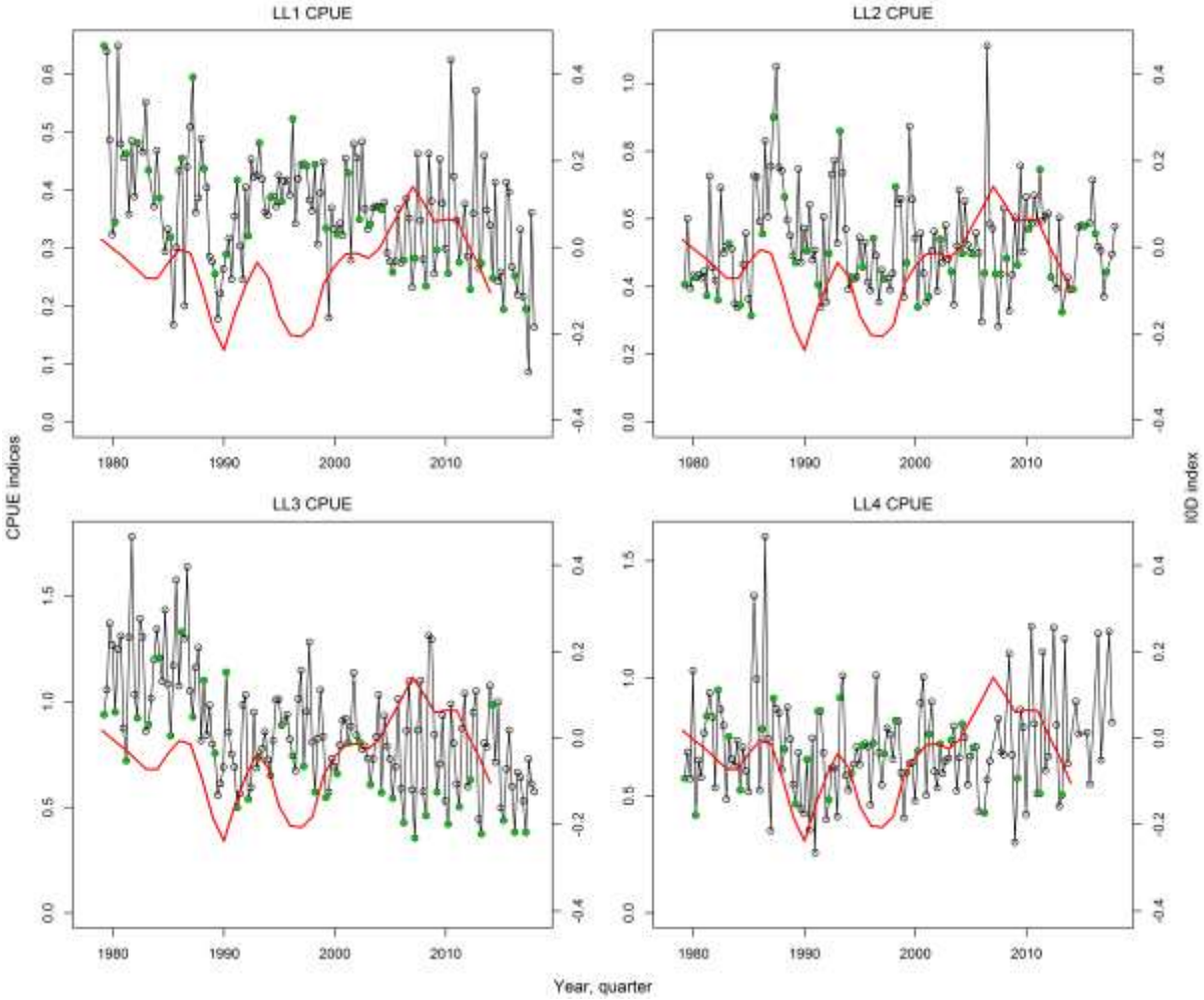

Figure 9. A comparison of the regional CPUE indices for the longline fisheries (LL 1–4) from 1979-2017 (*vessid_79nd* series) (points) and the trend in the Indian Ocean Dipole (IOD) index (red line). The green points correspond to the CPUE indices from the first quarter 1 (Q1) of the year.

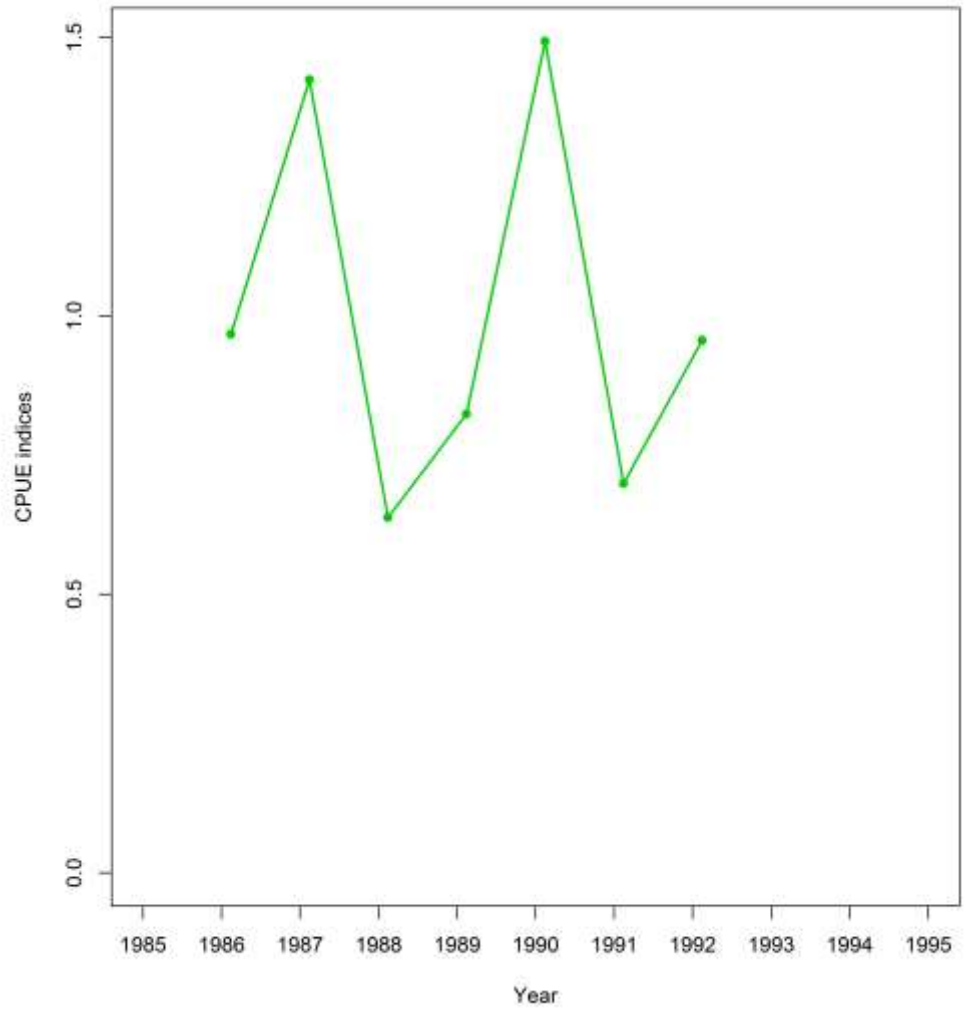

Figure 10. Annual drift net CPUE indices (source: Chang & Liu 1995).

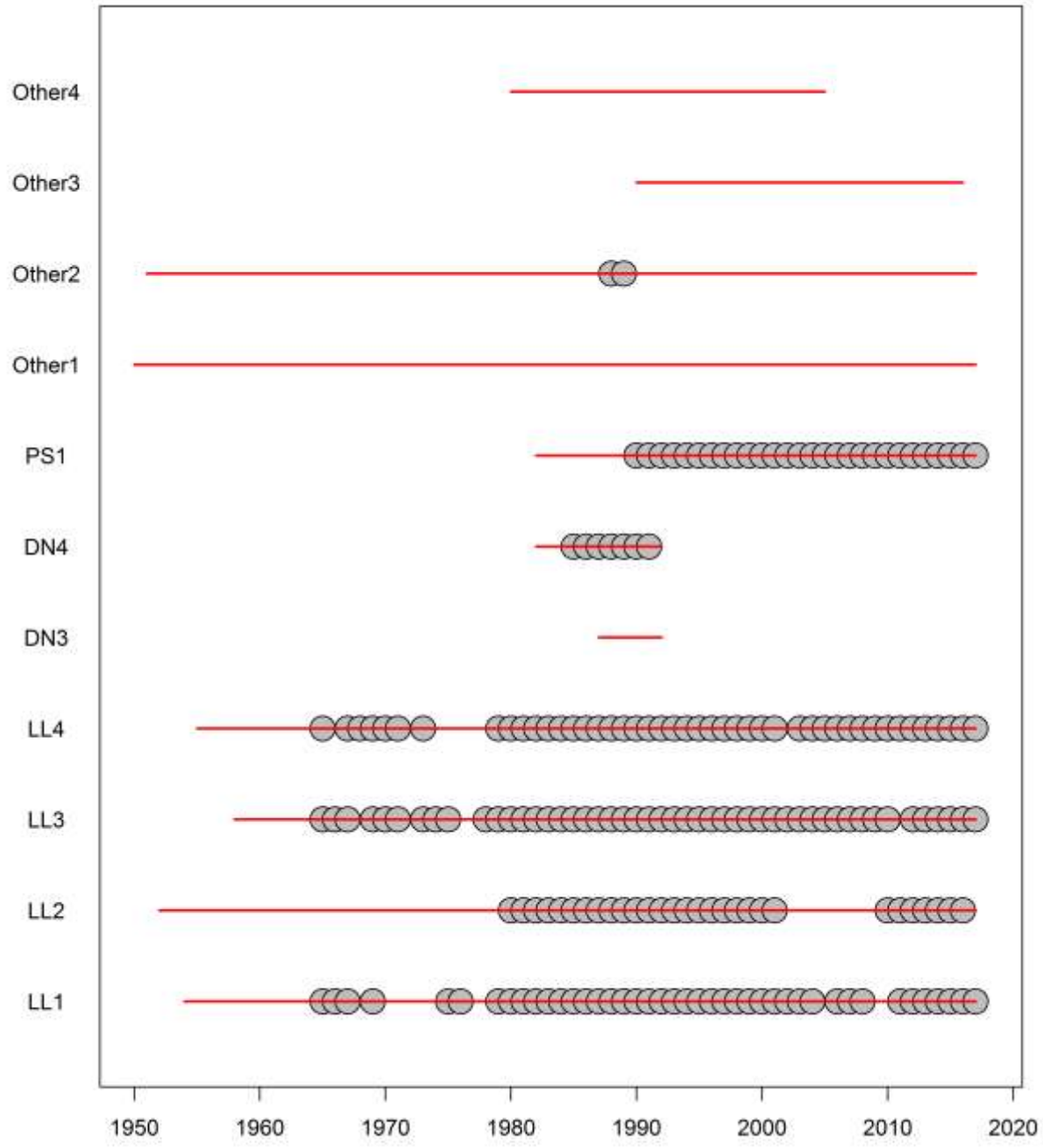

Figure 11. The availability of length sampling data from each fishery by year. The grey circles denote the presence of samples in a specific year. The red horizontal lines indicate the time period over which each fishery operated.

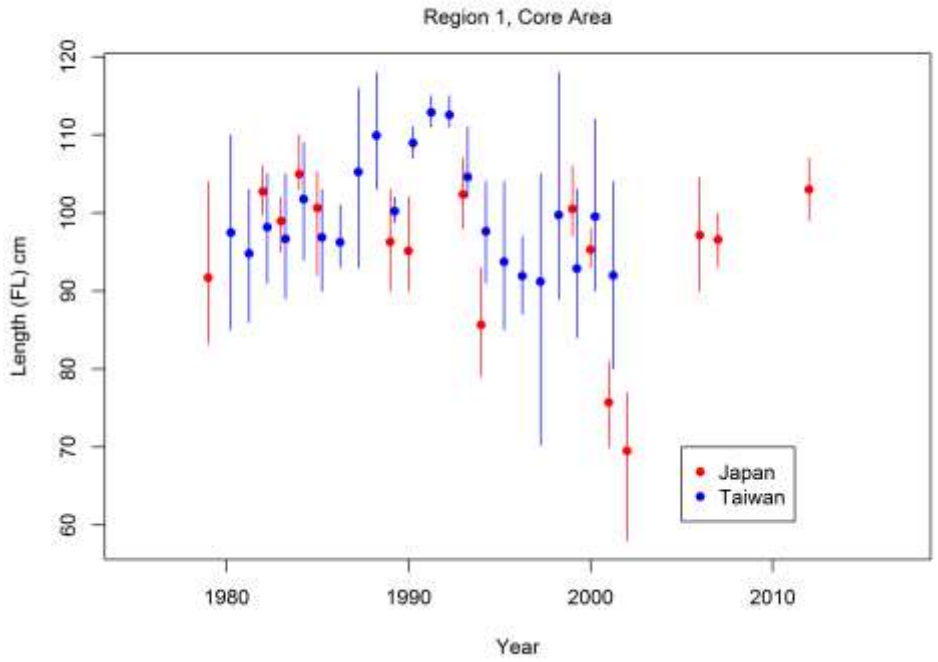

Figure 12. A comparison of the annual average length (fork length) and quartile range of albacore sampled from the Japanese and Taiwanese longline fleets within the core area of Region 1. Length samples collected via logbook from the Taiwanese fleet from 2003-2017 are excluded.

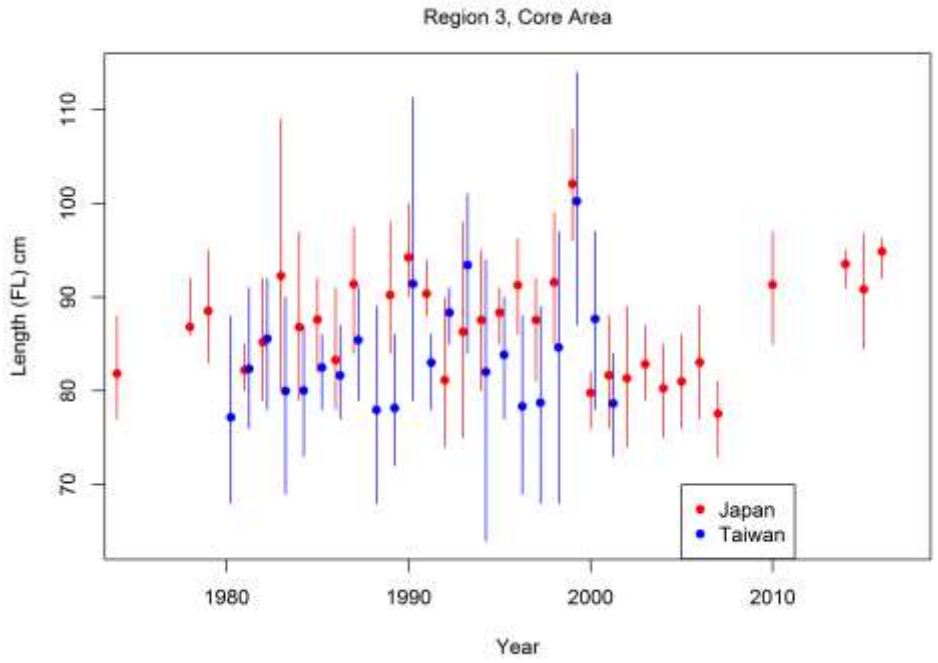

Figure 13. A comparison of the annual average length (fork length) and quartile range of albacore sampled from the Japanese and Taiwanese longline fleets within the core area of Region 3. Length samples collected via logbook from the Taiwanese fleet from 2003-2017 are excluded.

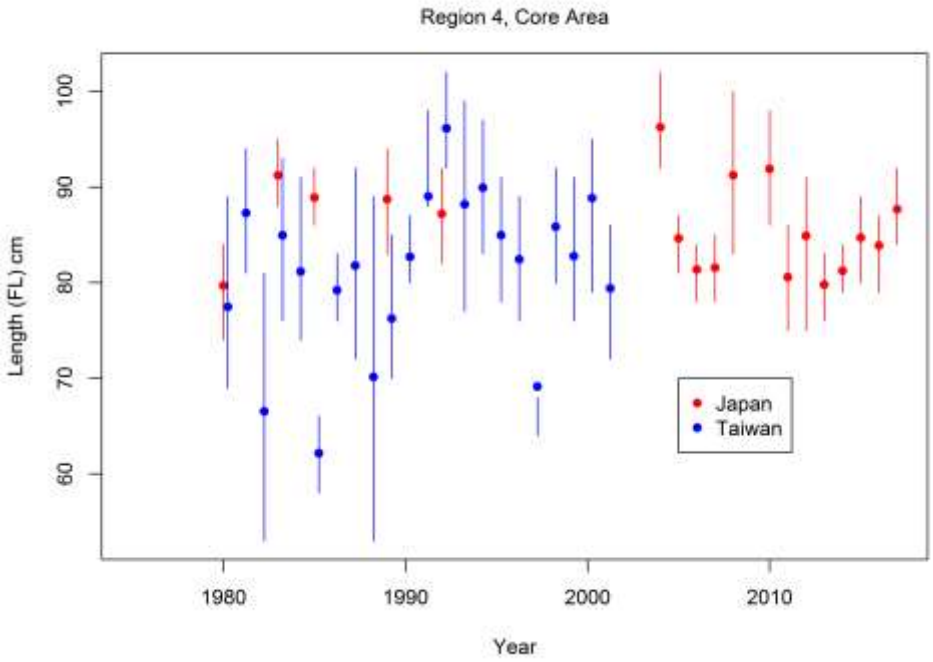

Figure 14. A comparison of the annual average length (fork length) and quartile range of albacore sampled from the Japanese and Taiwanese longline fleets within the core area of Region 4. Length samples collected via logbook from the Taiwanese fleet from 2003-2017 are excluded.

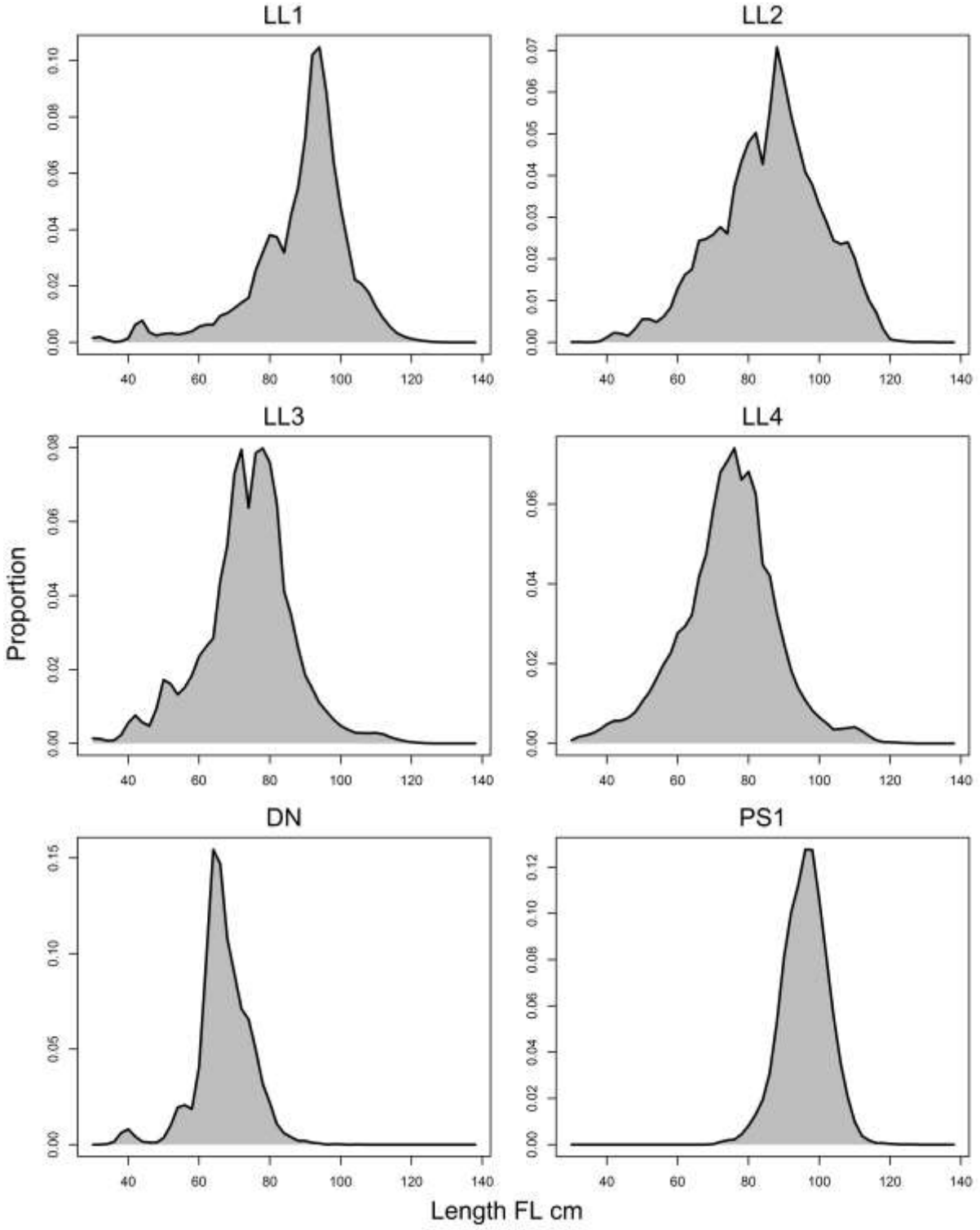

Figure 15. Aggregated length compositions of albacore sampled from the main fisheries, all years combined.

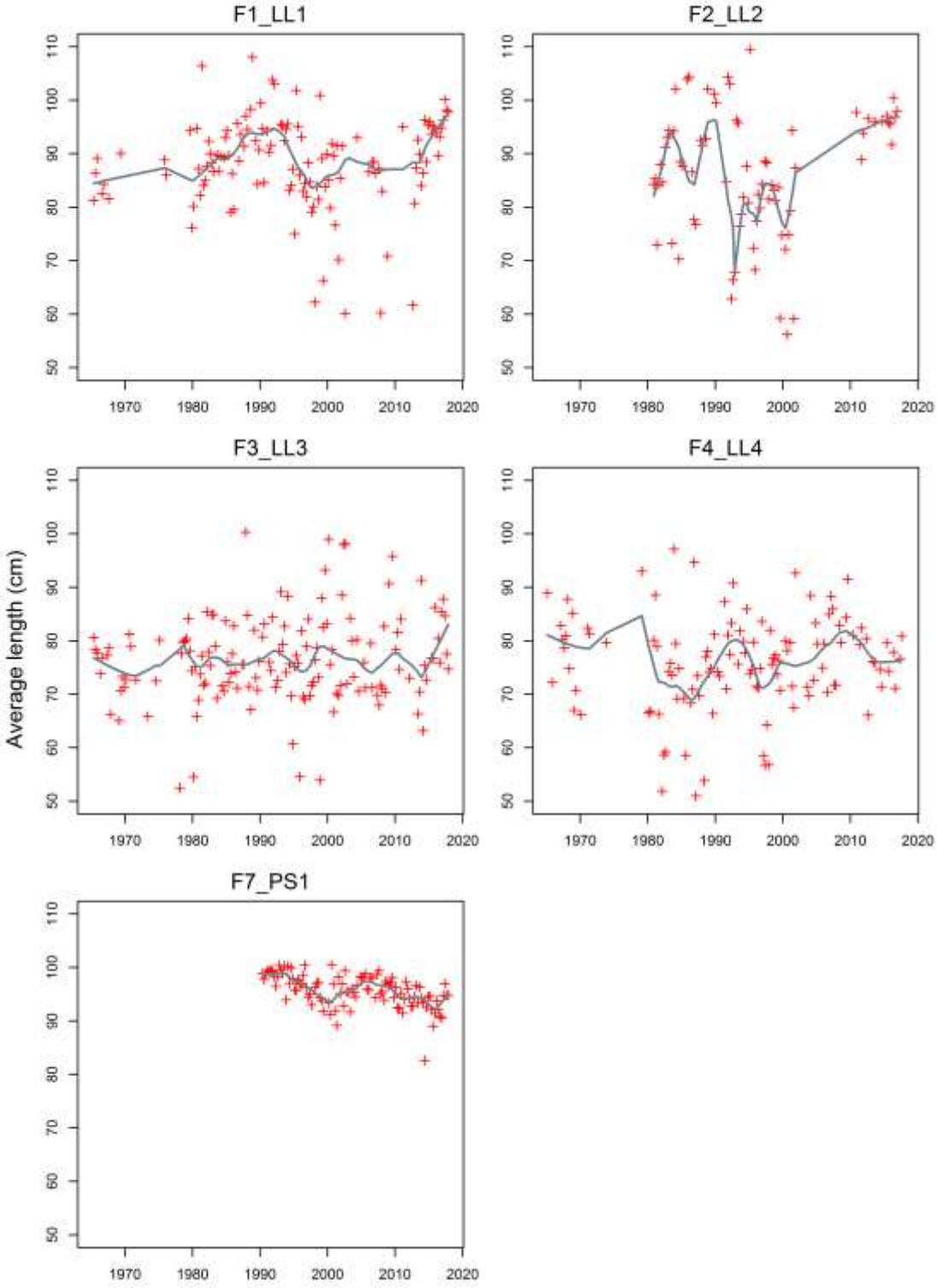

Figure 16. Mean length (fork length, cm) of albacore sampled from the main fisheries by quarter. The grey line represents the fit of a lowess smoother to each data set (including Taiwanese logbook data prior to 2003).

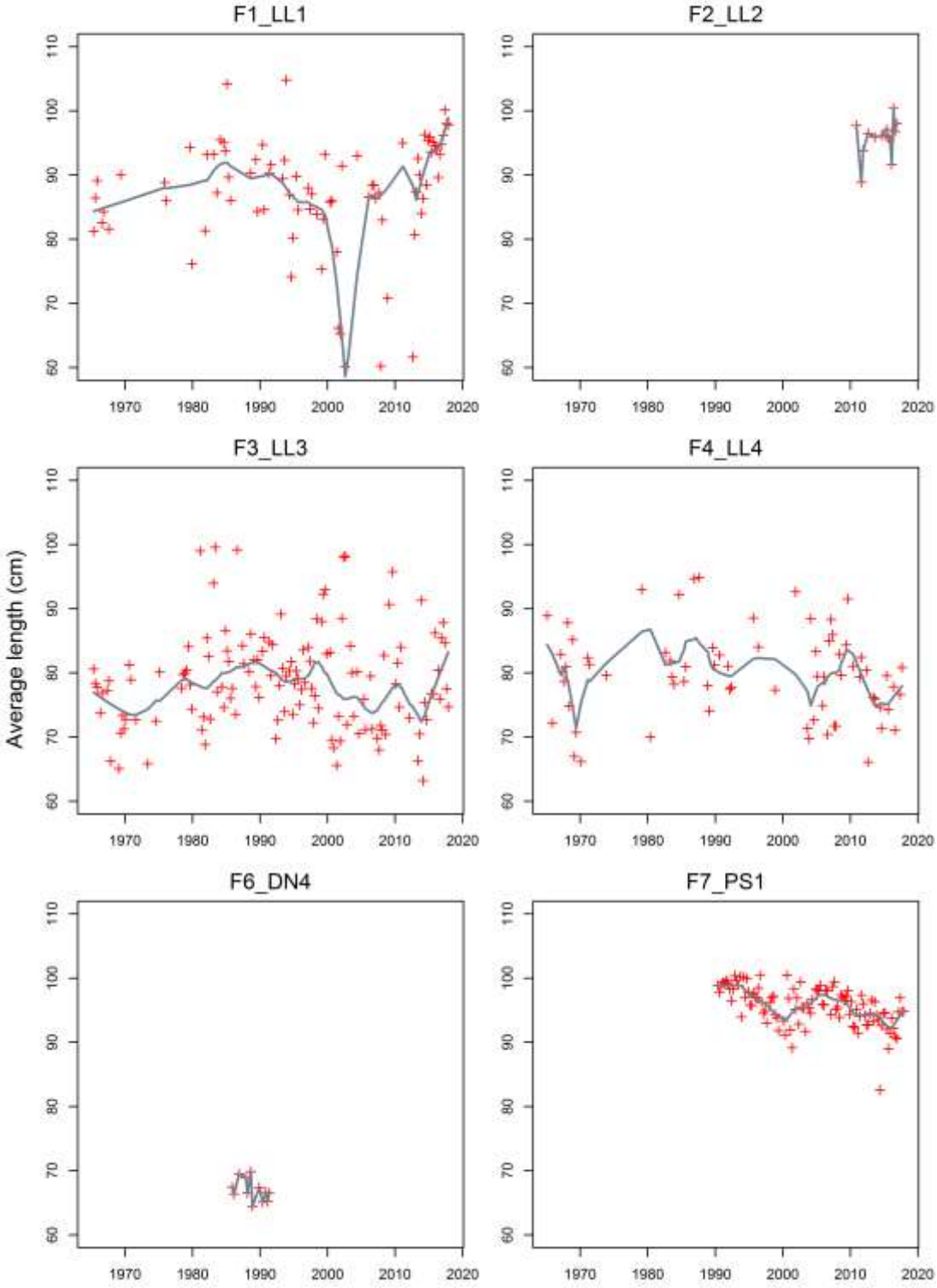

Figure 17. Mean length (fork length, cm) of albacore sampled from the main fisheries by quarter. The grey line represents the fit of a lowess smoother to each data set (excluding Taiwanese logbook data prior to 2003).

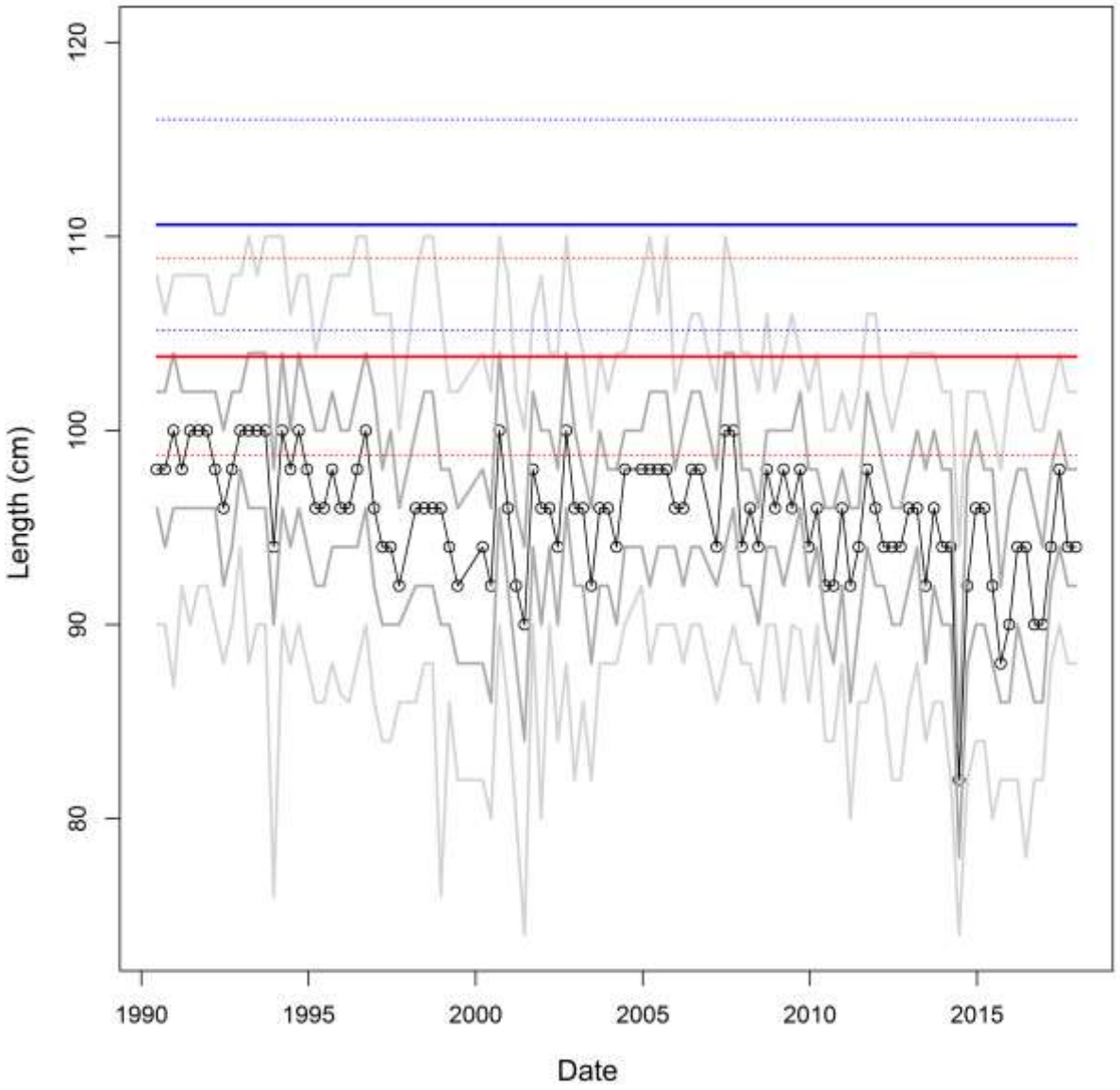

Figure 18. Median length of albacore sampled from the purse seine fishery (points), 5% and 95% quantiles of length (light grey) and 25% and 75% quantiles of length (dark grey). For comparison the maximum length-at-age (Linfinity and 95% distribution) of male (blue) and female (red) are also plotted.

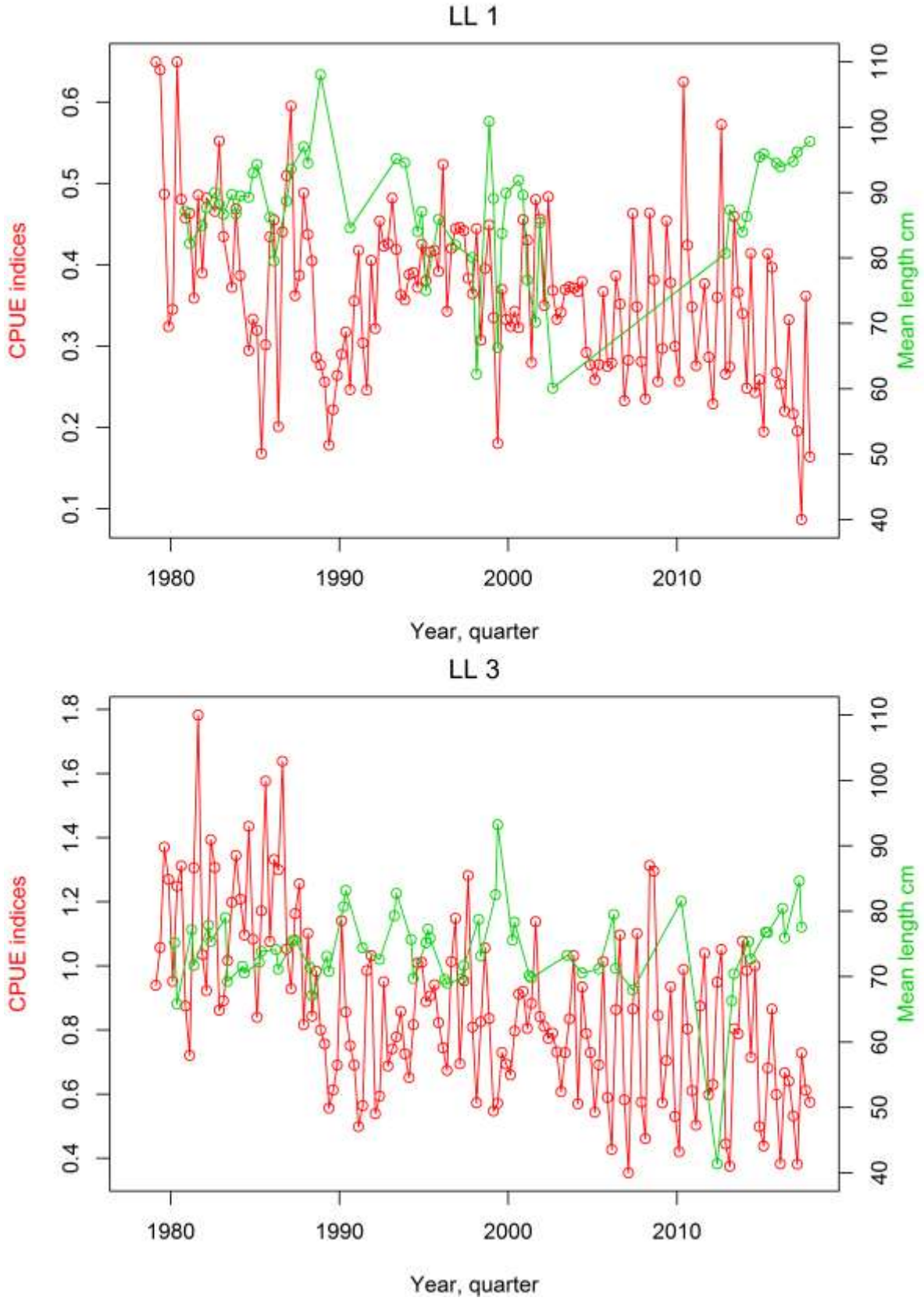

Figure 19. A comparison of the trends LL CPUE indices and average length of albacore sampled from the longline fisheries from the LL1 and LL3 fisheries.

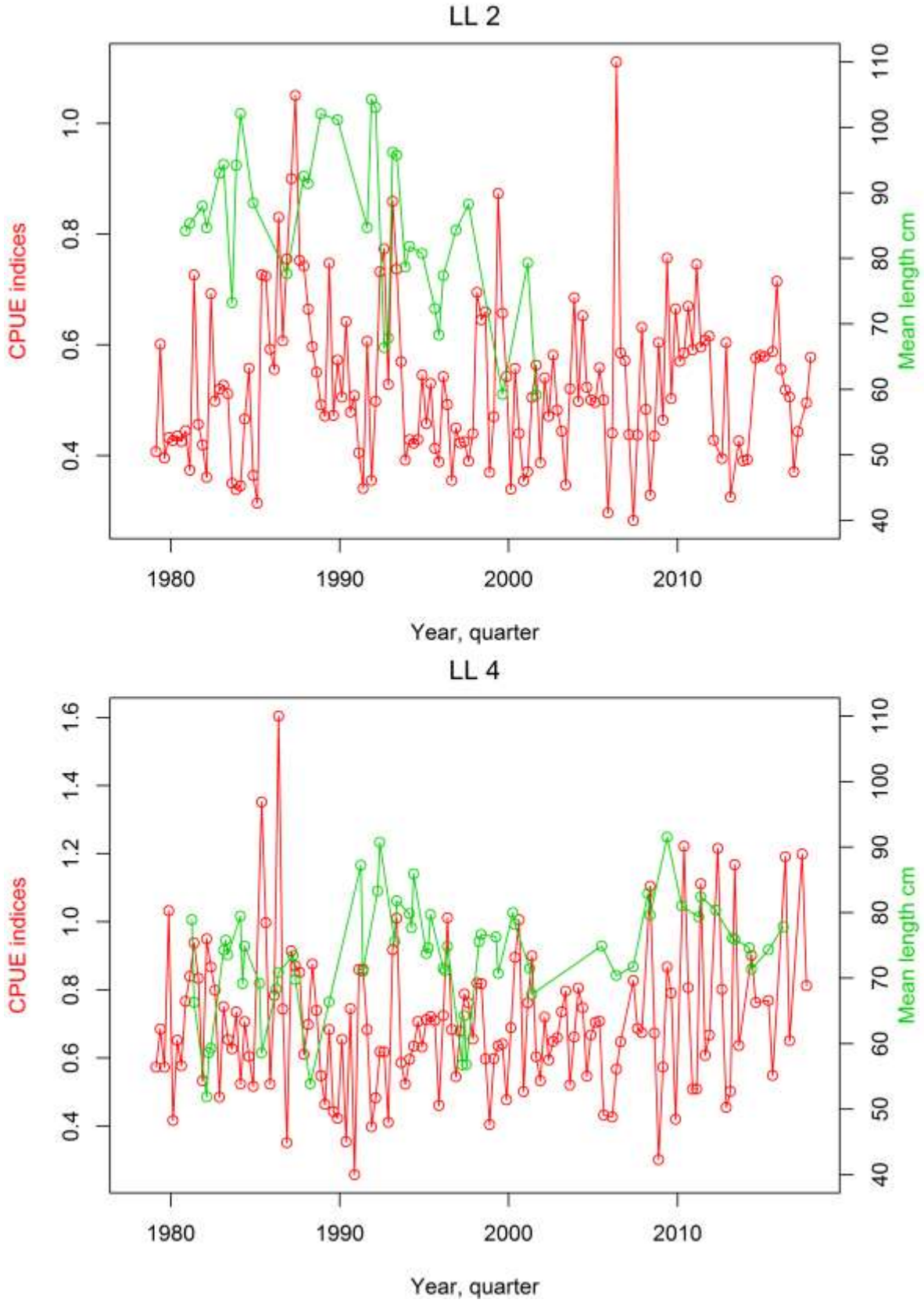

Figure 20. A comparison of the trends in LL CPUE indices and average length of albacore sampled from the longline fisheries from the LL2 and LL4 fisheries.

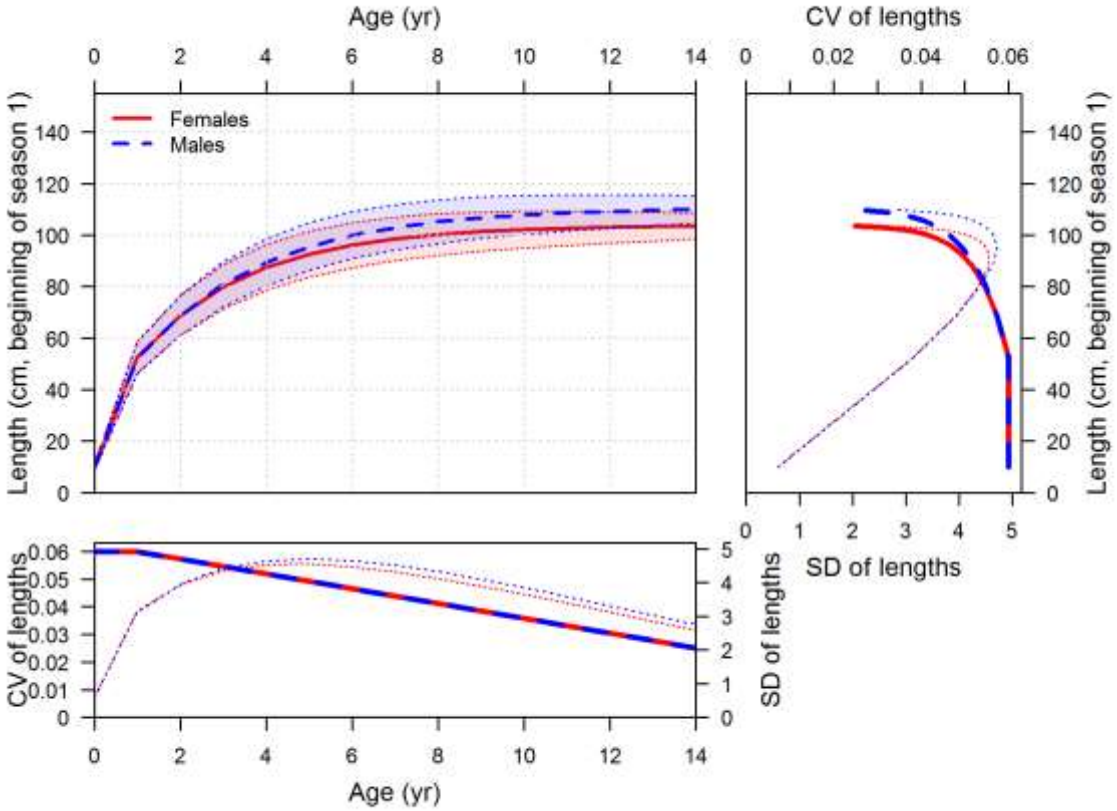

Figure 21. Growth function for female and male albacore.

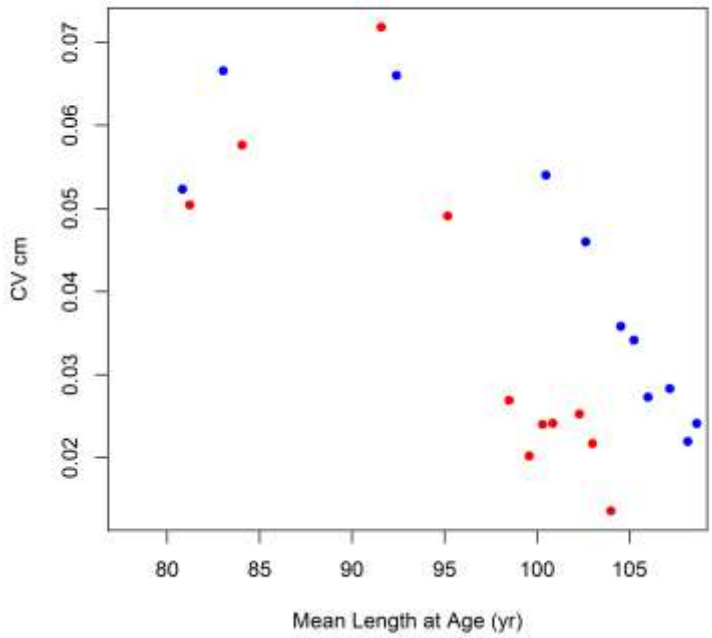

Figure 22. Coefficient of variation (CV) of the mean length at age of female (red) and male (blue) albacore tuna from the western Indian Ocean derived from recent otolith ageing (Farley et al 2019).

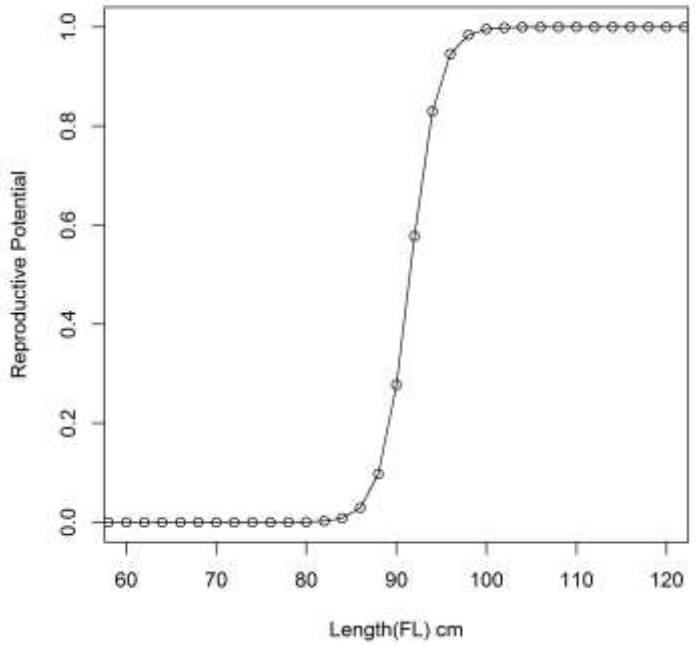

Figure 23. Reproductive potential by length class for female albacore.

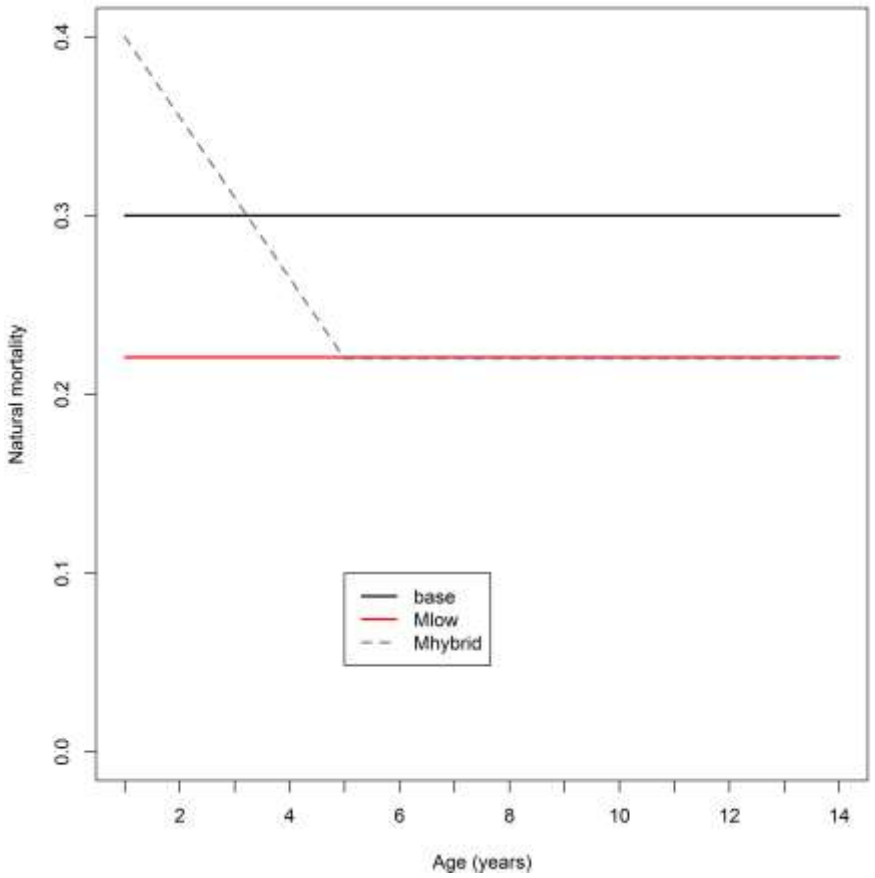

Figure 24. The age-specific natural mortality schedule assumed for the assessment model (*Base*) and other age-specific *M* schedules from various model options (see text for details).

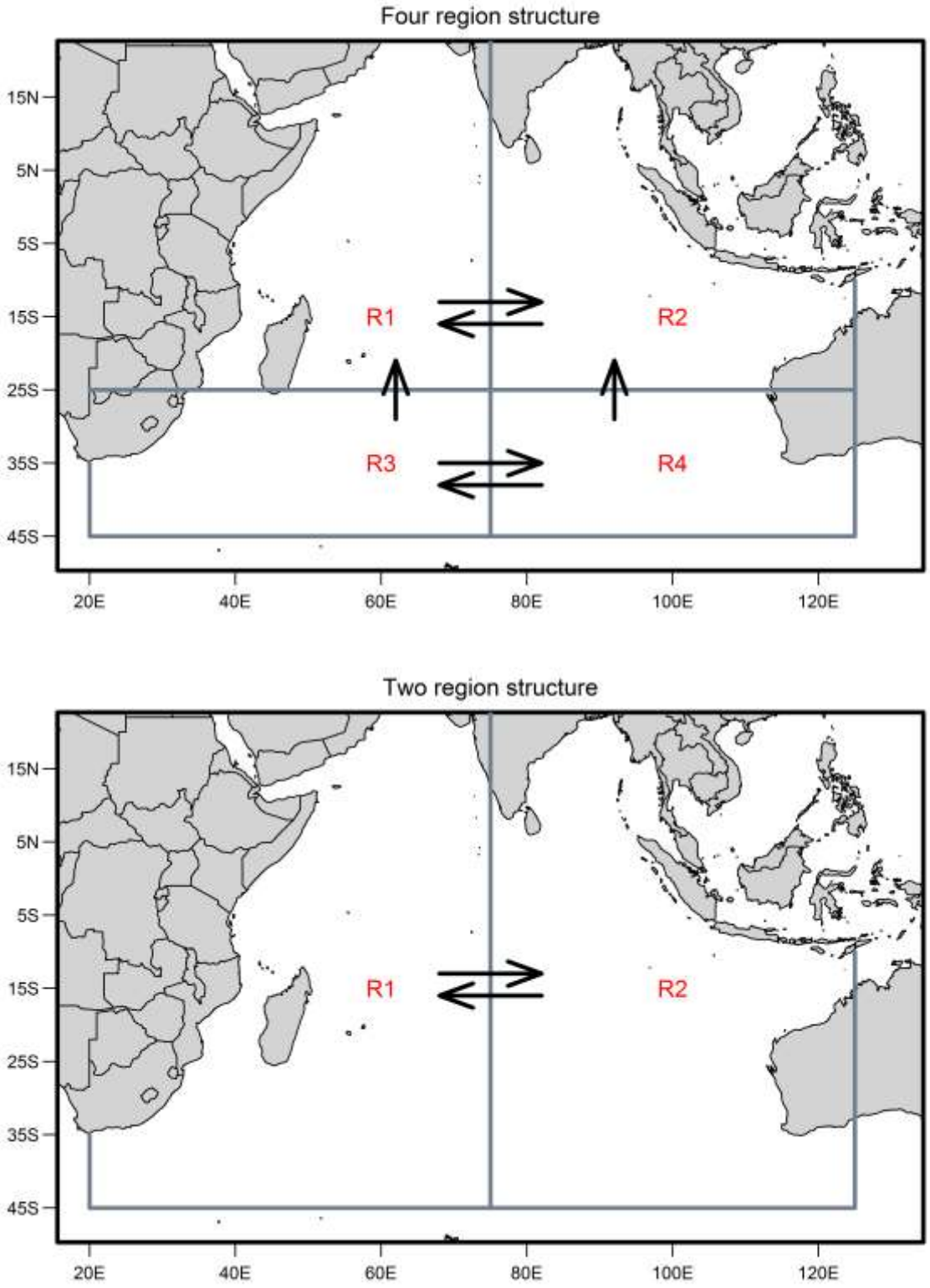

Figure 25. Alternative spatial structures investigated during the stock assessment modelling.

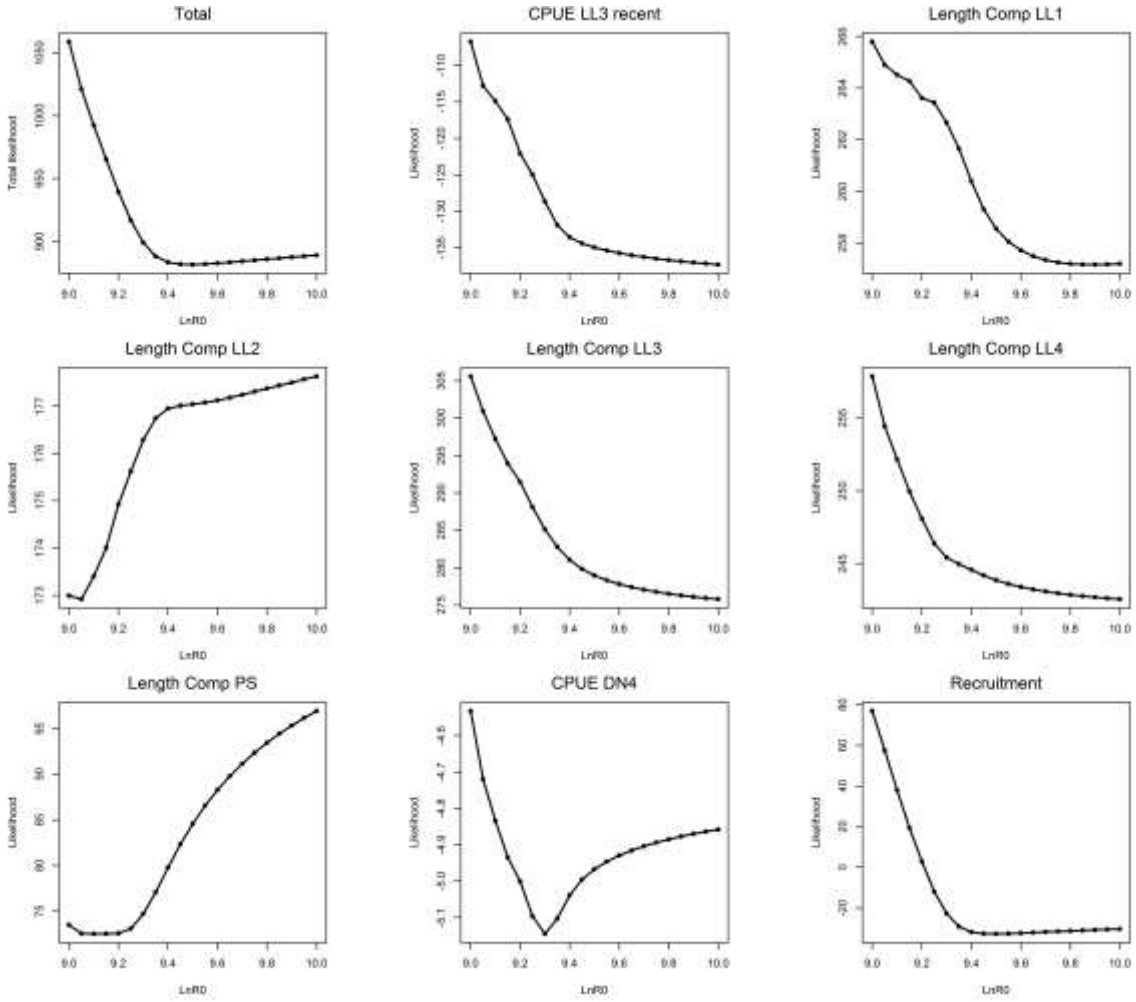

Figure 26. Likelihood profile of the R0 parameter for each of the main likelihood components included in the reference model.

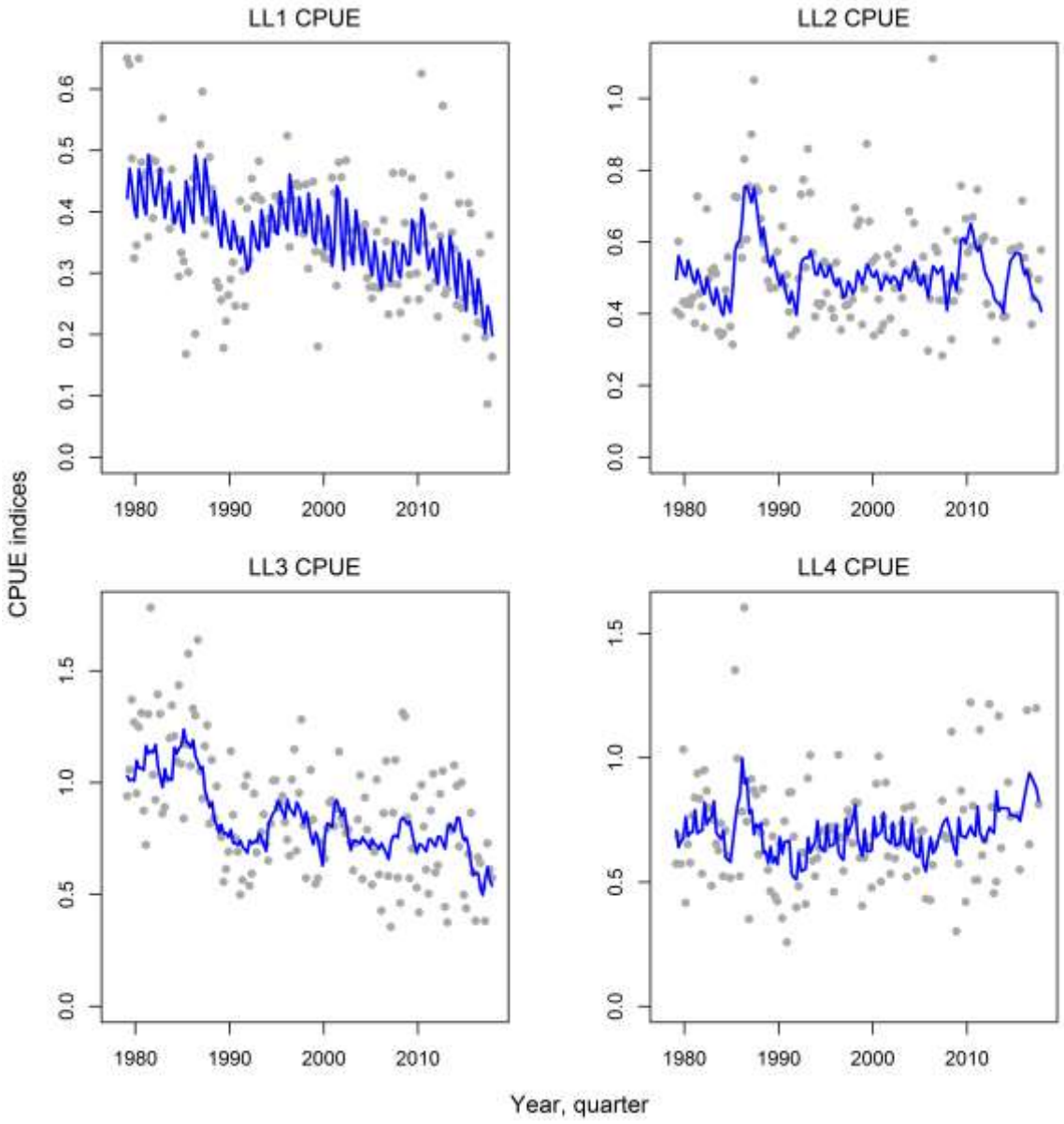

Figure 27. Fit to the longline CPUE indices for the four region reference model (R4_SelectAll).

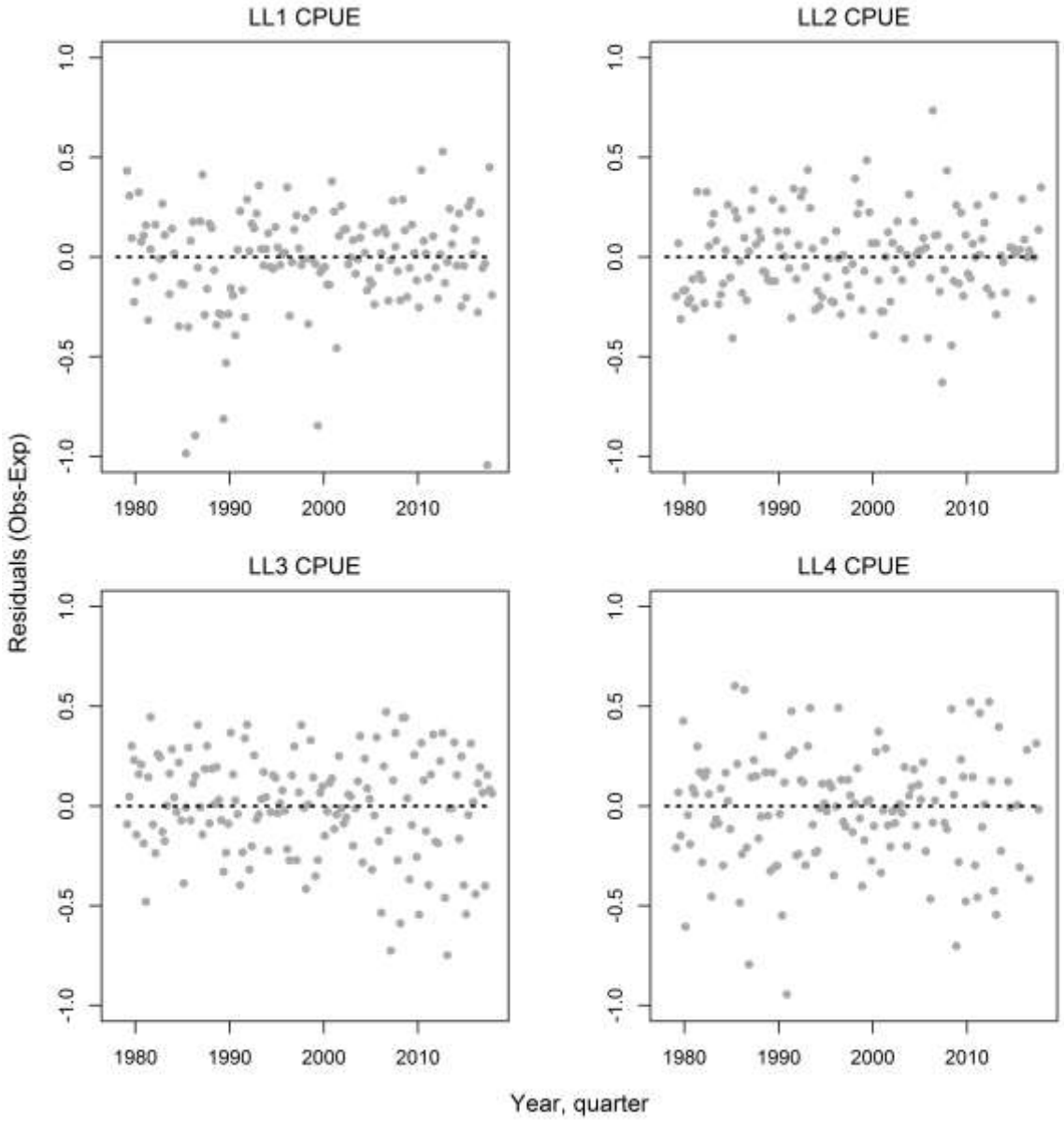

Figure 28. Residuals (observed – expected) from the fit to the longline CPUE indices for the four region reference model.

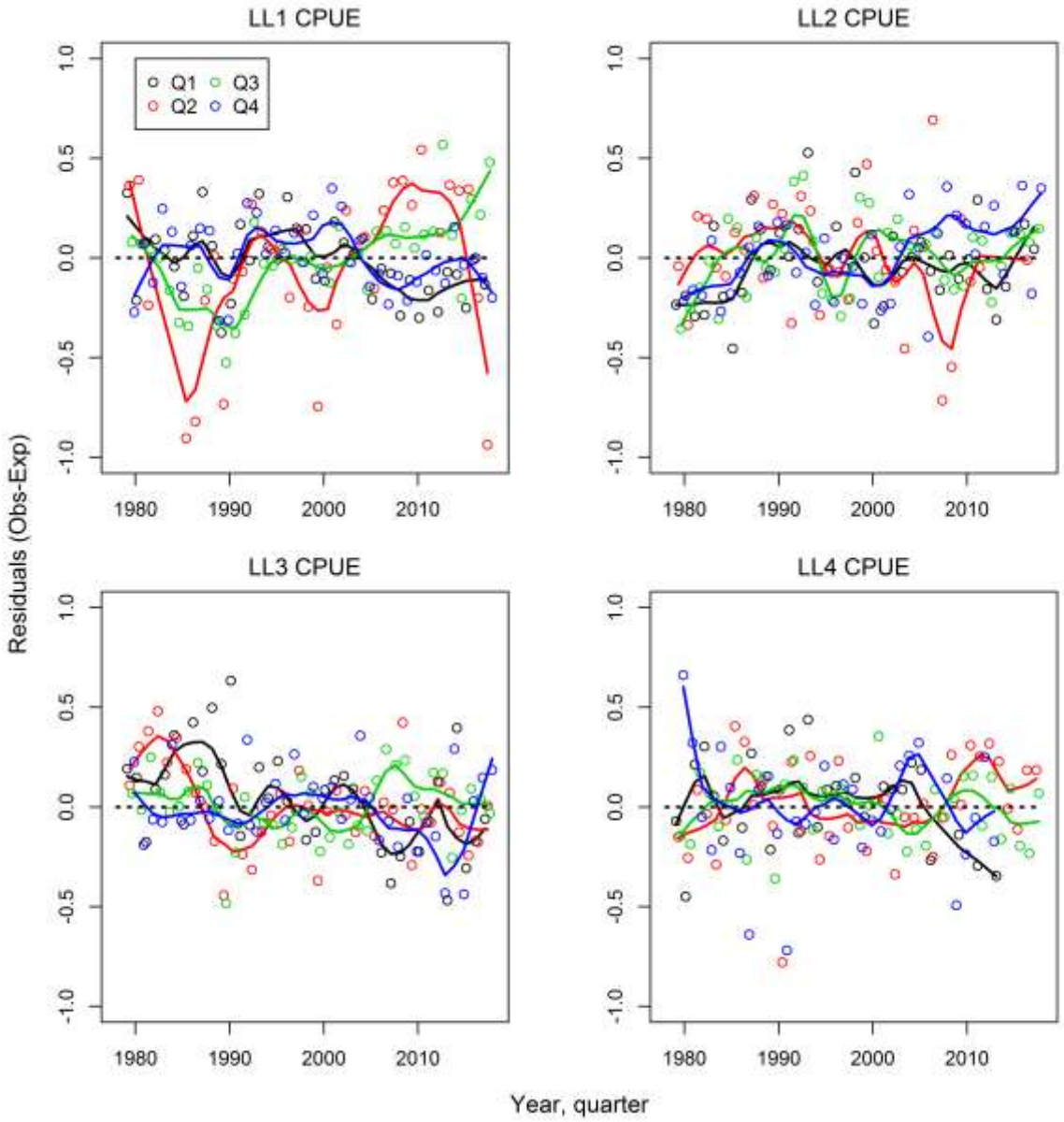

Figure 29. Residuals (observed – expected) from the fit to the longline CPUE indices for the four region seasonal CPUE model. The lines represent lowess smooth fits to the residuals from each quarter CPUE series.

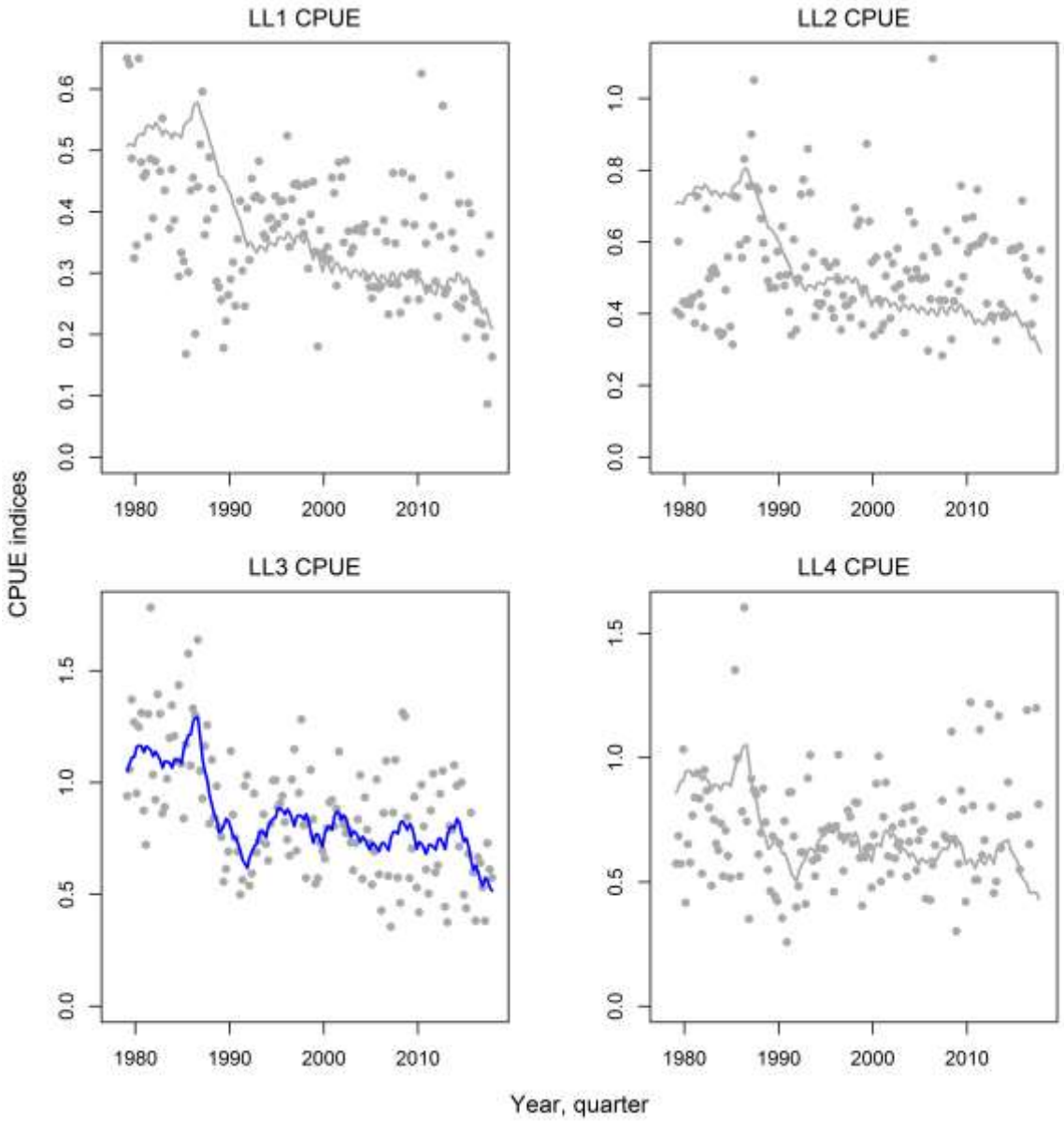

Figure 30. Fit to the longline CPUE indices for the single region reference model. Only the LL3 CPUE indices are included in the model likelihood.

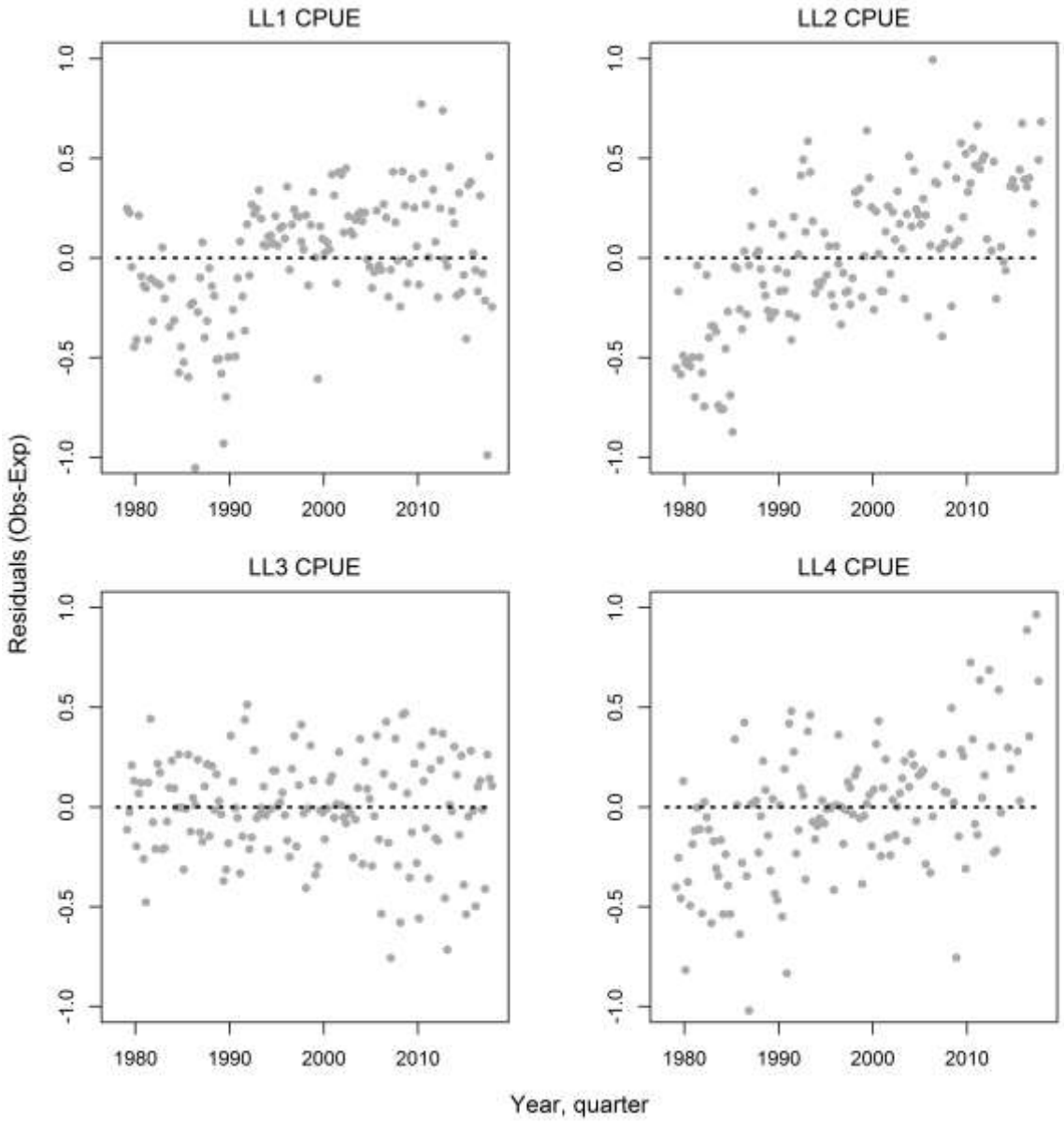

Figure 31. Residuals (observed – expected) from the fit to the longline CPUE indices for the single region reference model. Only the LL3 CPUE indices are included in the model likelihood.

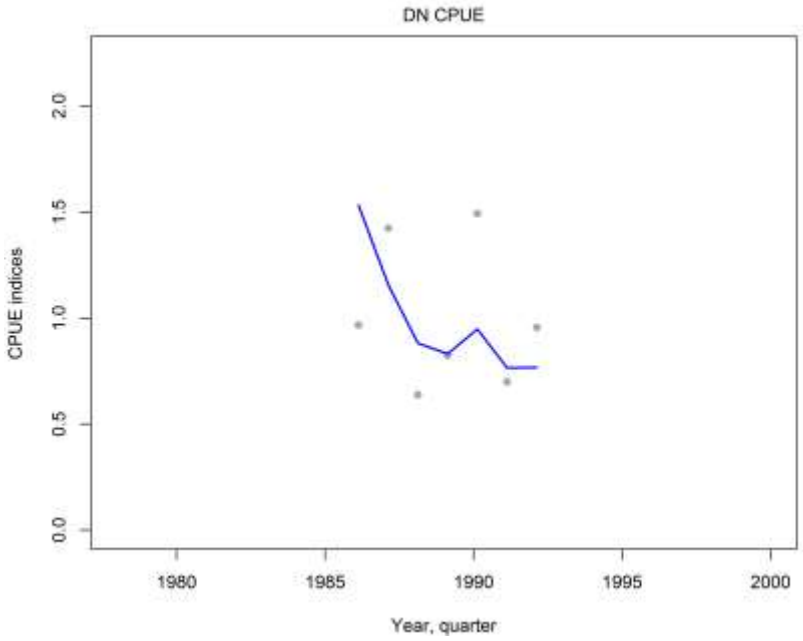

Figure 32. Fit to the drift net CPUE indices for the single region reference model.

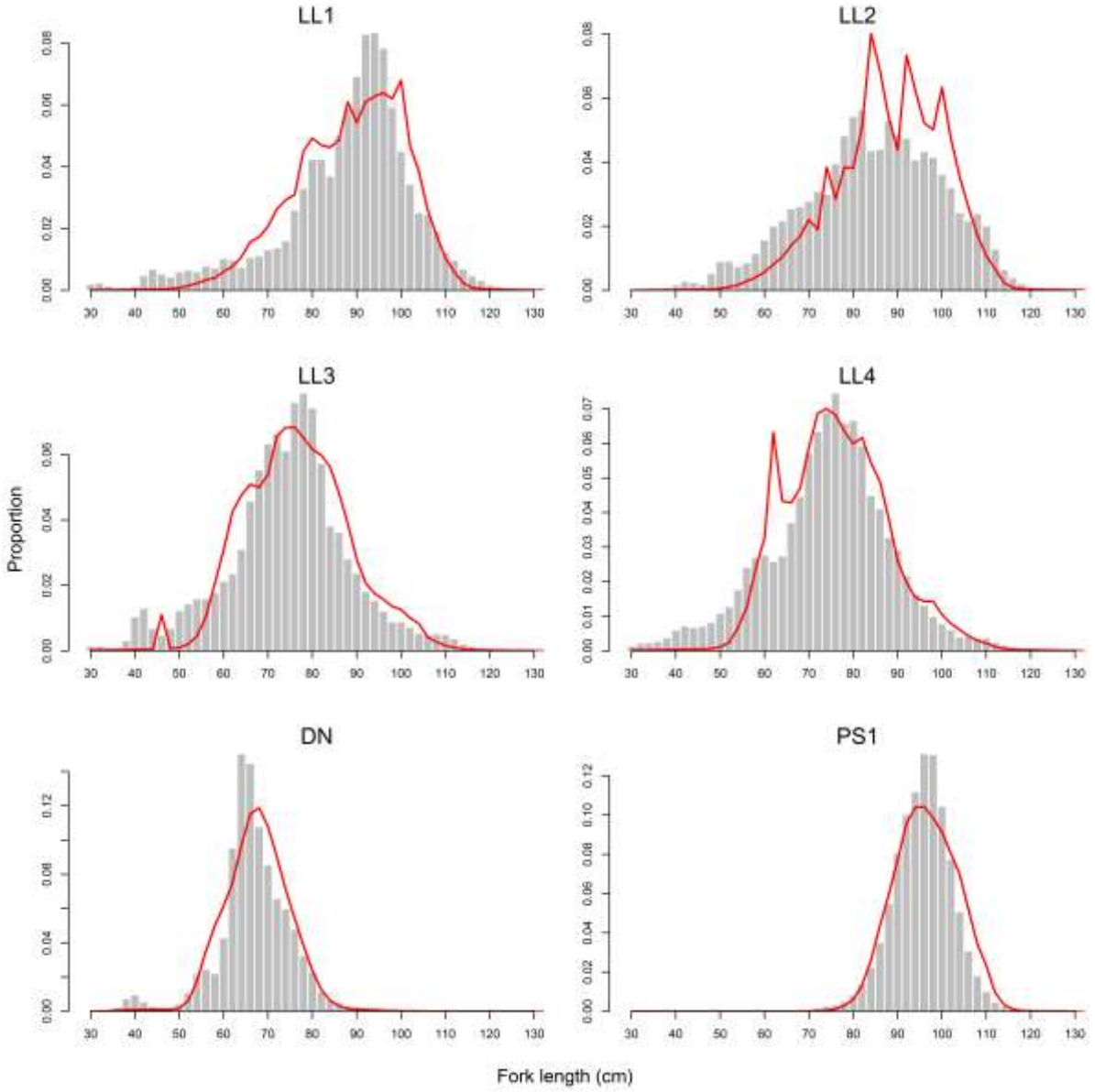

Figure 33. Observed (grey bars) and predicted (red line) length compositions (in 2 cm intervals) for each fishery aggregated over time from the single region reference model.

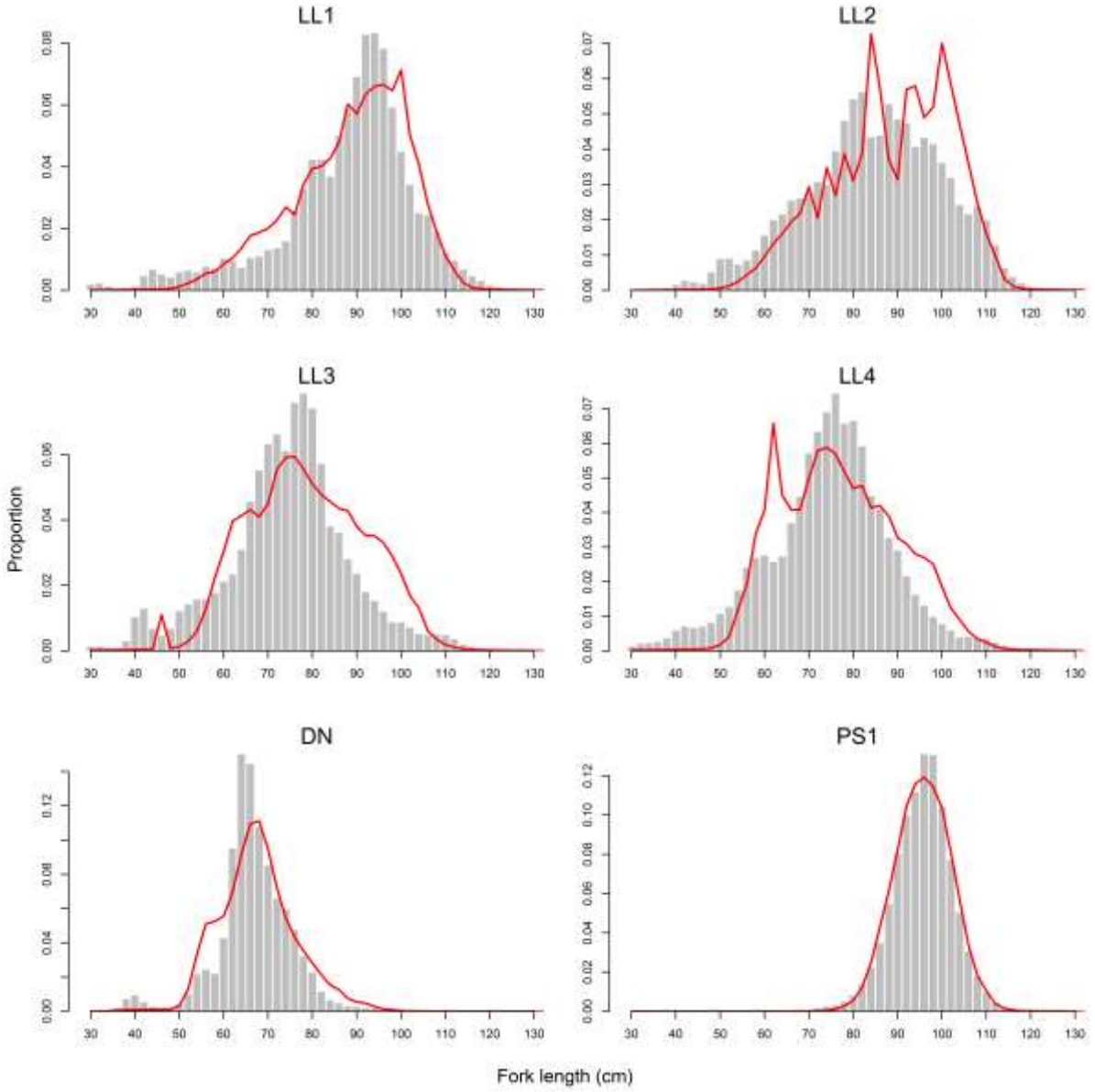

Figure 34. Observed (grey bars) and predicted (red line) length compositions (in 2 cm intervals) for each fishery aggregated over time from the four region reference model.

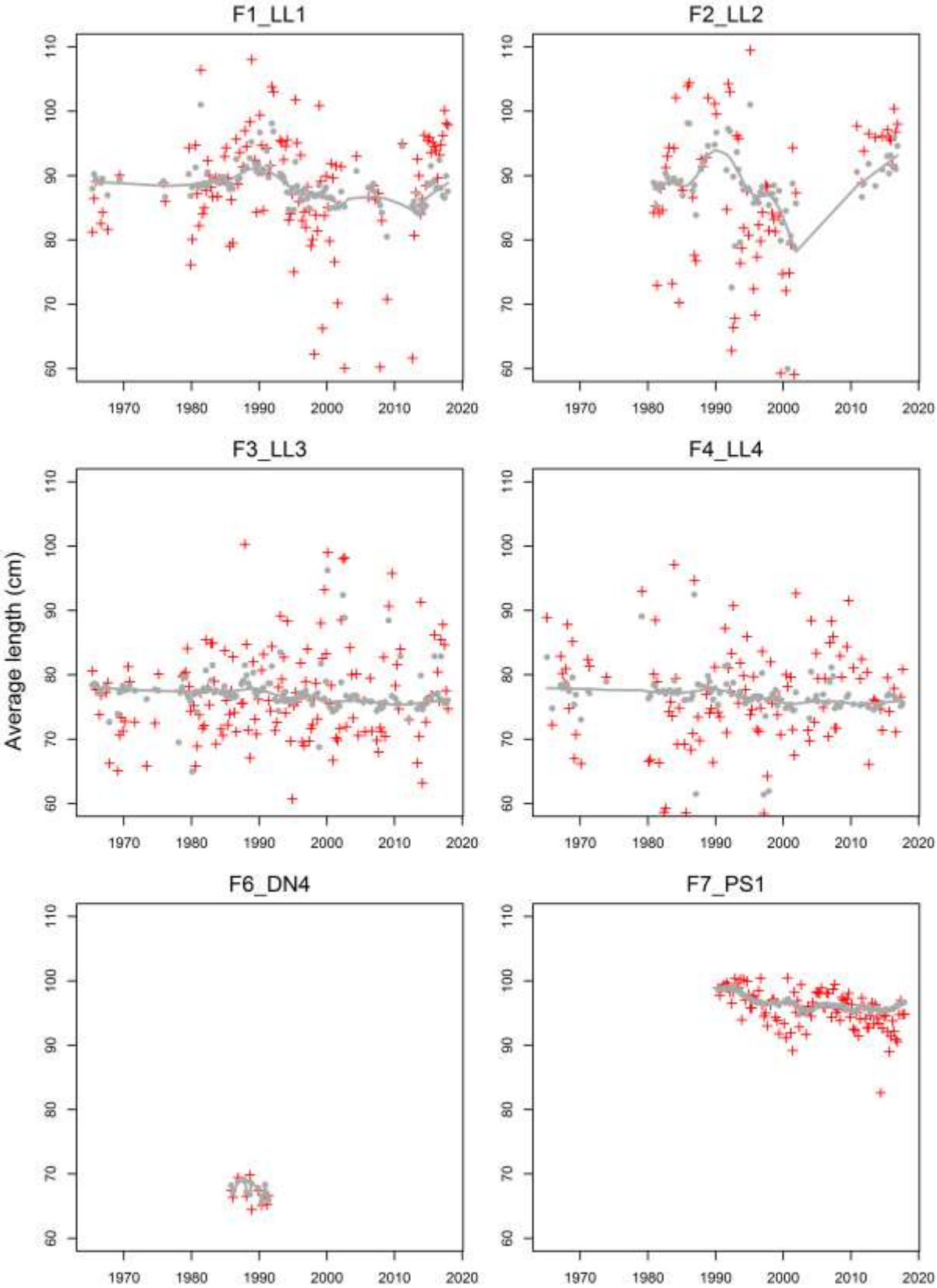

Figure 35: A comparison of the observed (red points) and predicted (grey points) average fish length (FL, cm) of albacore tuna by fishery for the single region reference model.

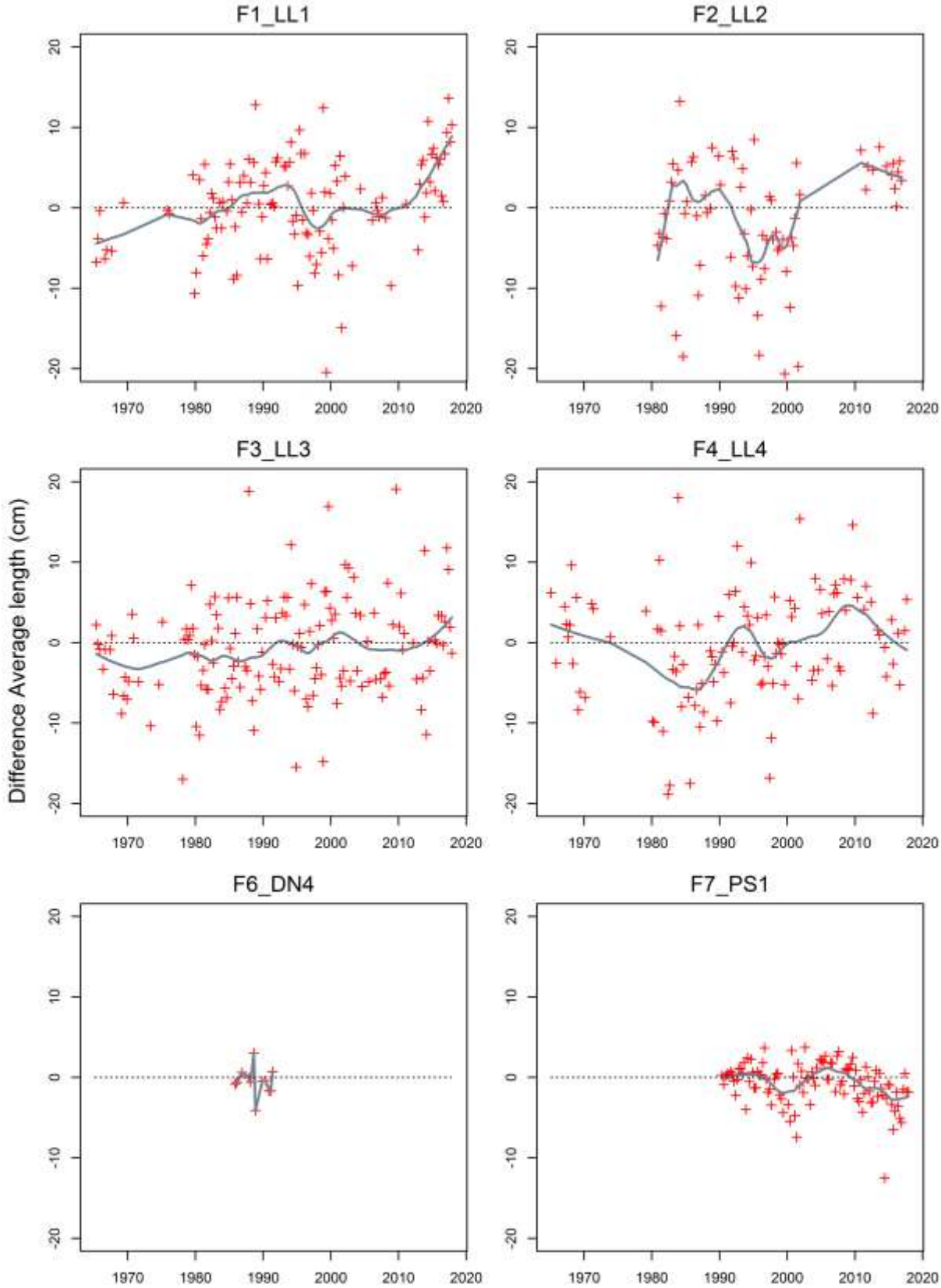

Figure 36: Trends in the difference between the observed and predicted average fish length (FL, cm) of albacore tuna by fishery fishery for the single region reference model. The grey line represents a lowess smoothing fit the the data points.

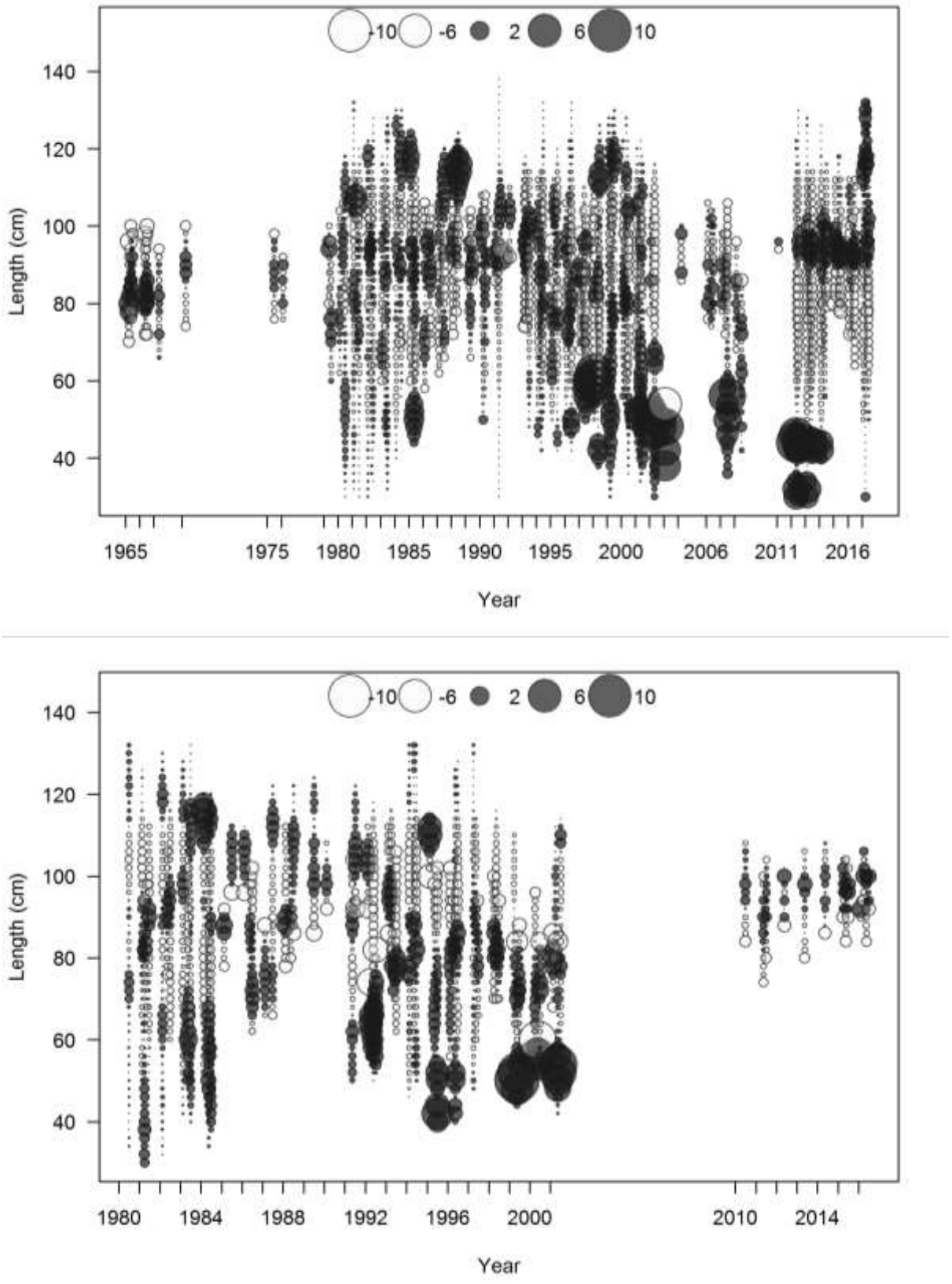

Figure 37. Pearson residuals from the fit to the length composition data from the LL1 (top) and LL2 (bottom) fisheries (single reference model). Positive residuals are plotted as filled circles; negative residuals are plotted as open circles; the magnitude of the residual is proportional to the area of the circle.

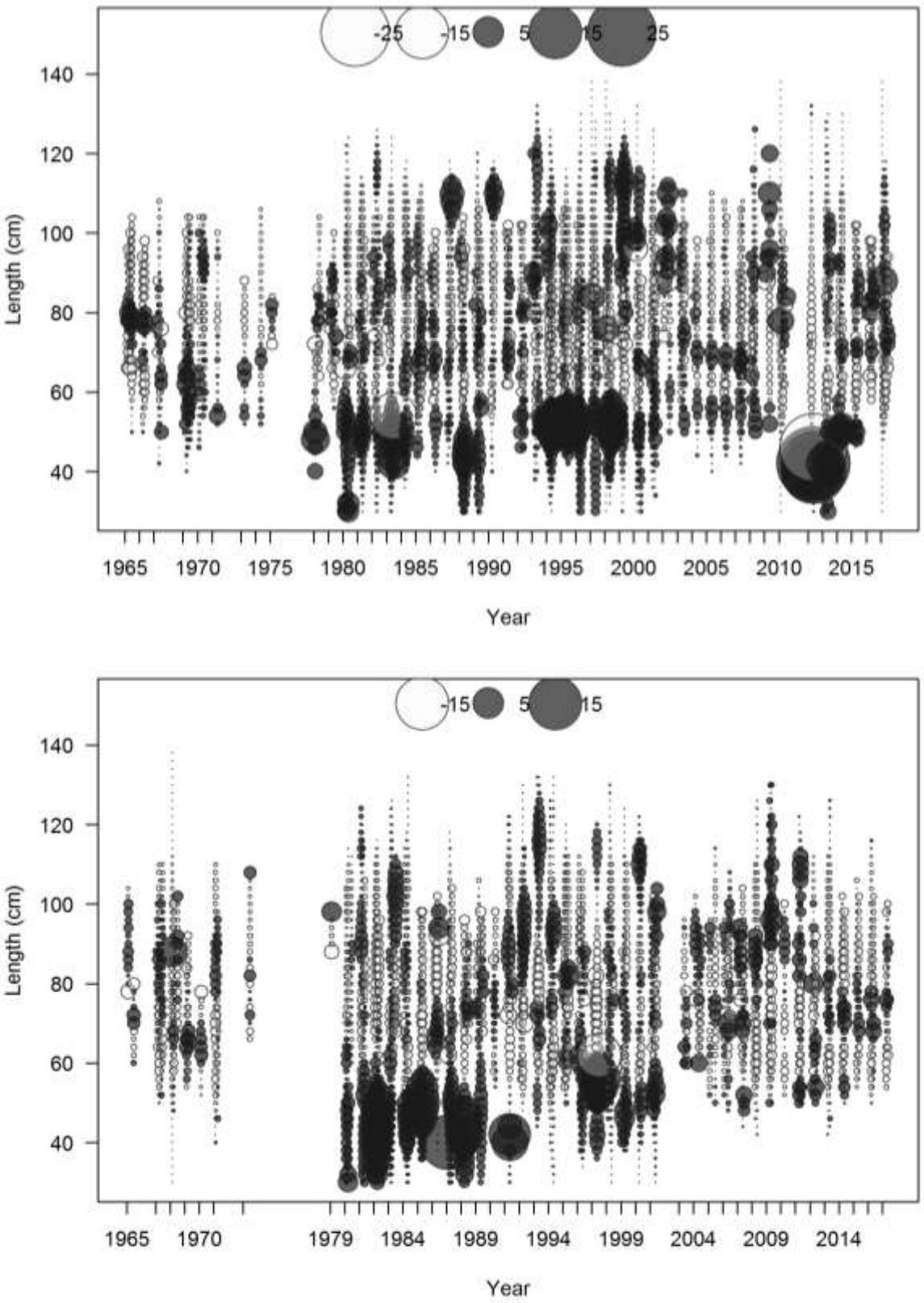

Figure 38. Pearson residuals from the fit to the length composition data from the LL3 (top) and LL4 (bottom) fisheries (single reference model). Positive residuals are plotted as filled circles; negative residuals are plotted as open circles; the magnitude of the residual is proportional to the area of the circle.

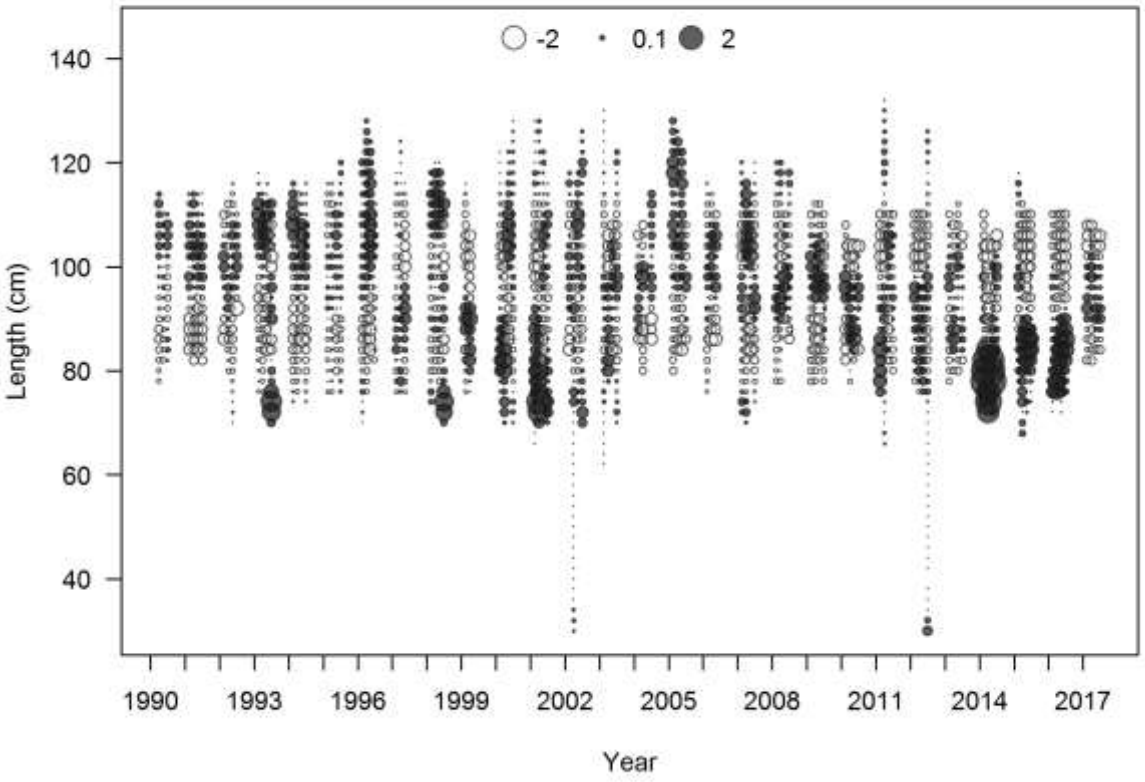

Figure 39. Pearson residuals from the fit to the length composition data from the PS1 fishery (single region reference model). Positive residuals are plotted as filled circles; negative residuals are plotted as open circles; the magnitude of the residual is proportional to the area of the circle.

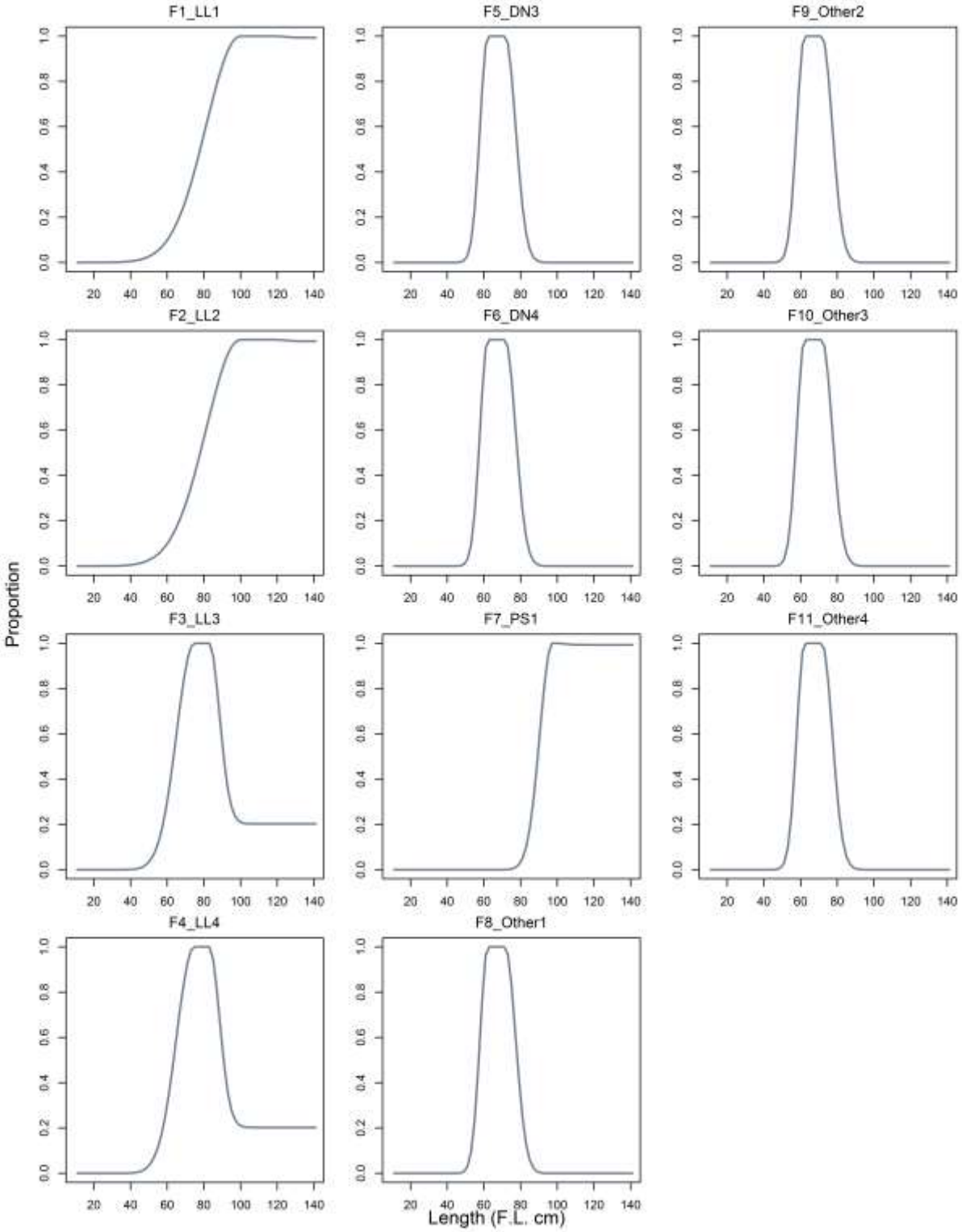

Figure 40. Length specific selectivity by fishery for the single region reference model.

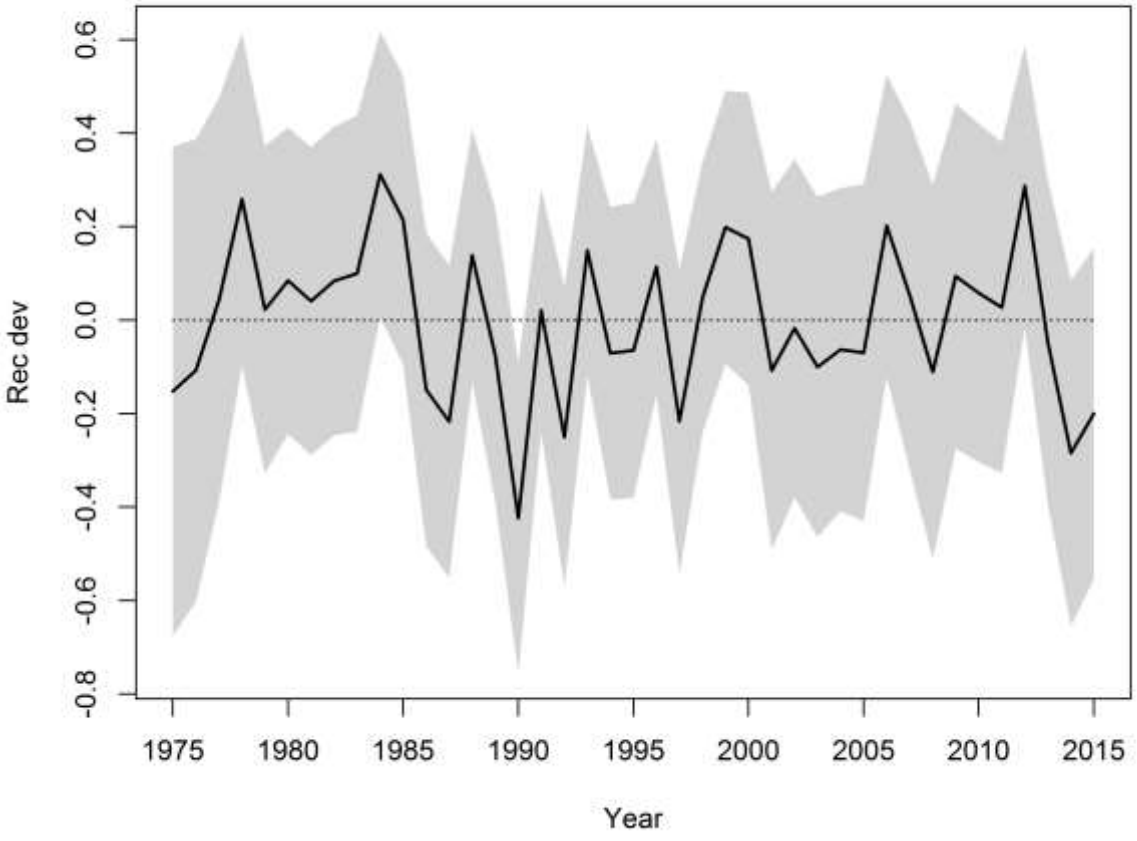

Figure 41. Estimated recruitment deviates and the associated 95% confidence interval for the single region reference model.

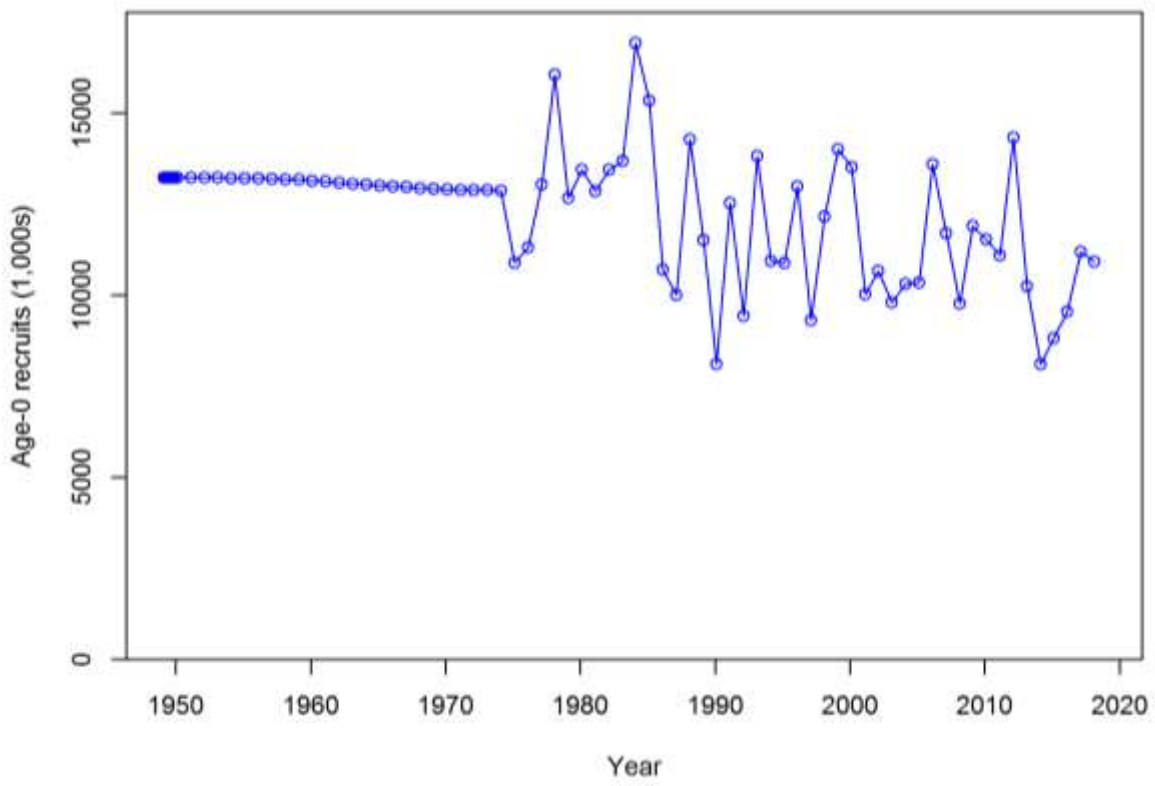

Figure 42. Estimated annual recruitment for the reference single region model.

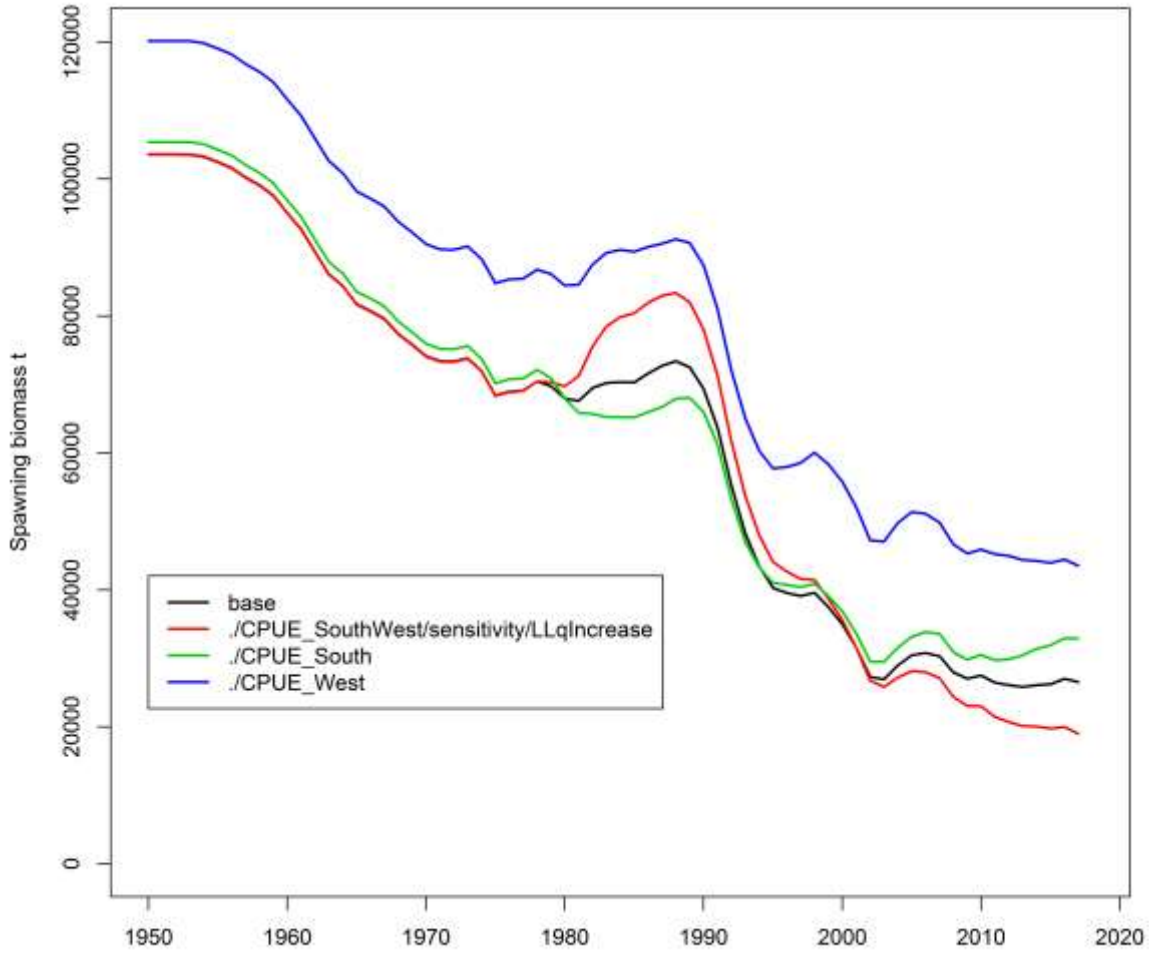

Figure 43. A comparison of the spawning biomass trajectory for the reference model and the alternative CPUE options.

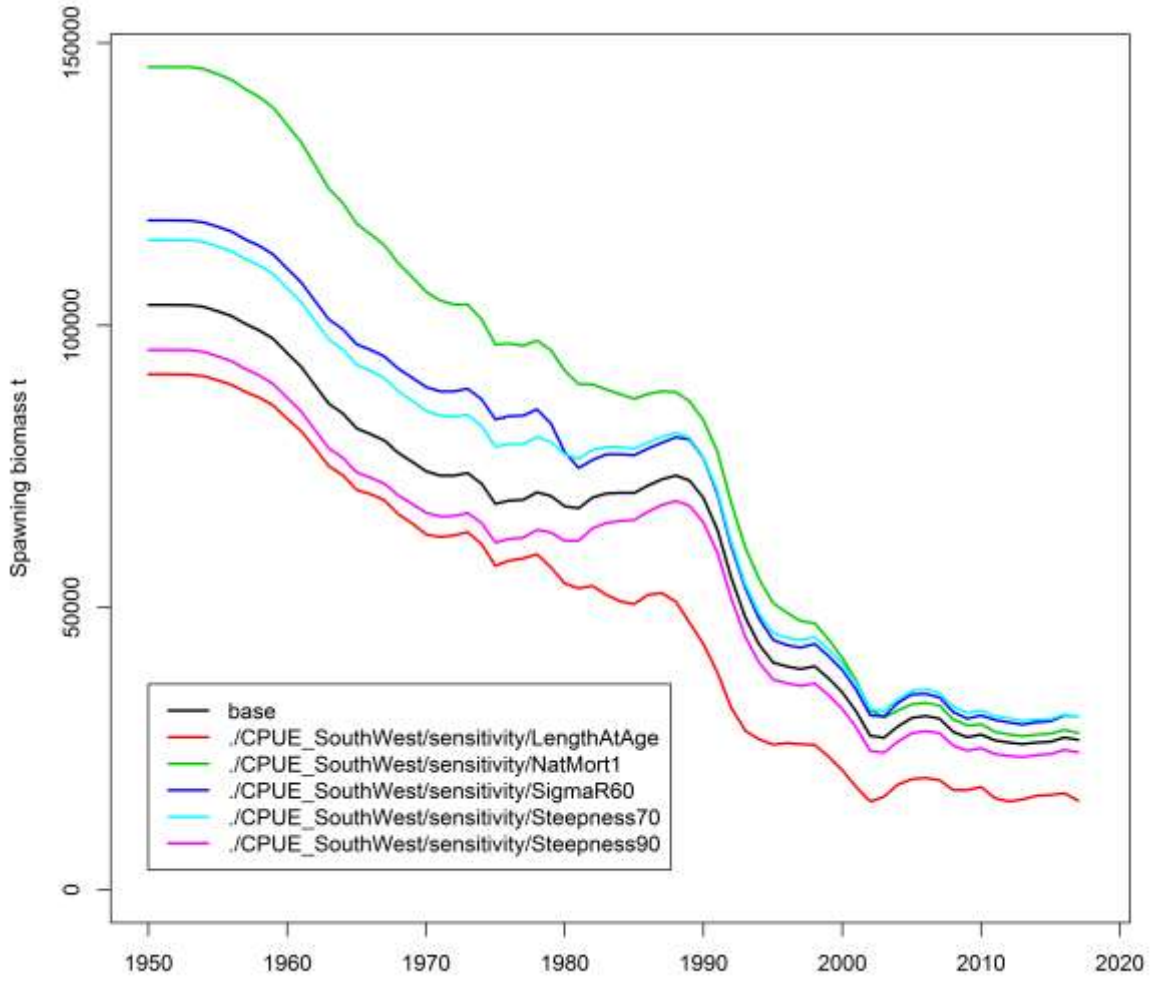

Figure 44. A comparison of the spawning biomass trajectory for the reference model and the model options with alternative biological parameters.

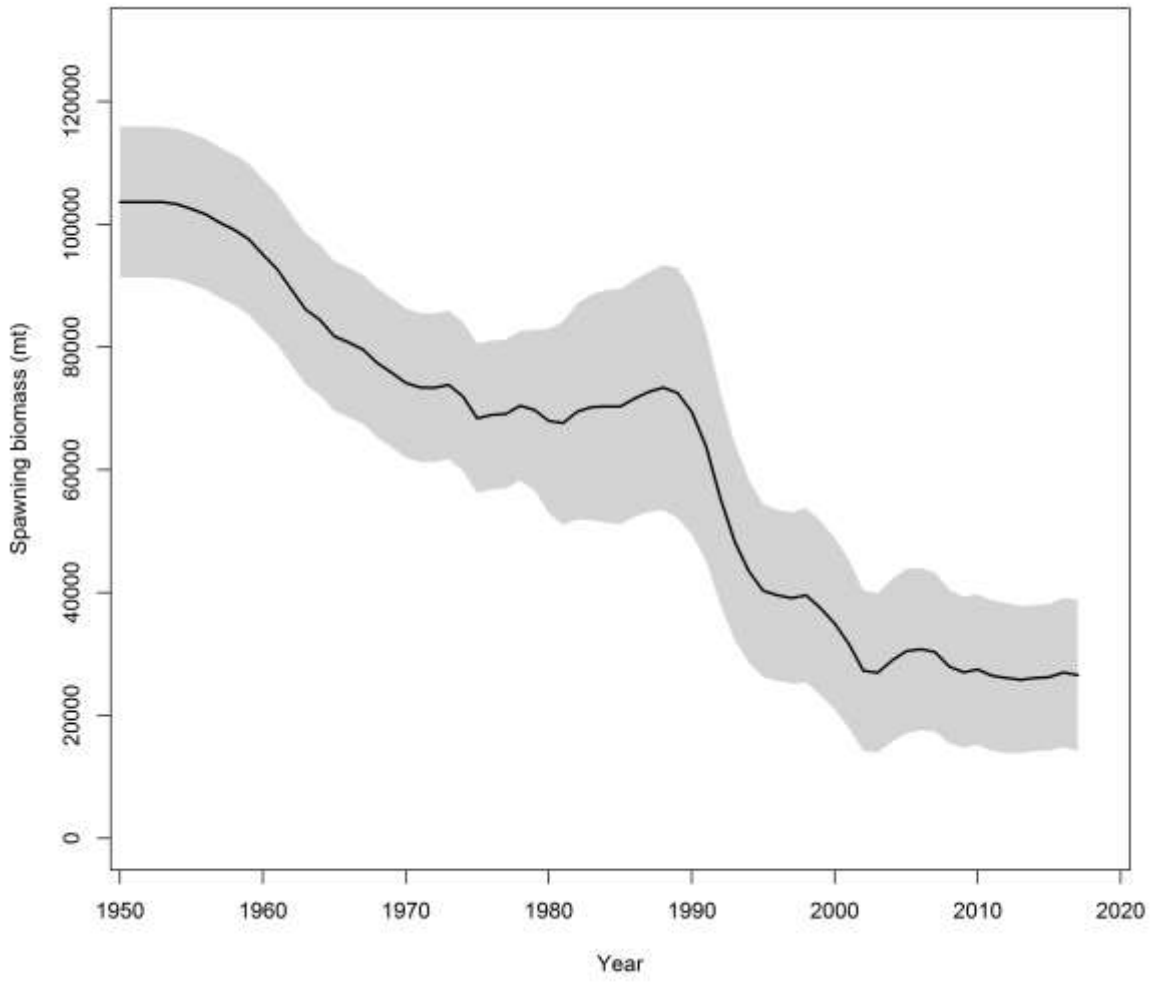

Figure 45. Spawning biomass trajectory and 95% confidence interval for the single region reference model for the assessment period.

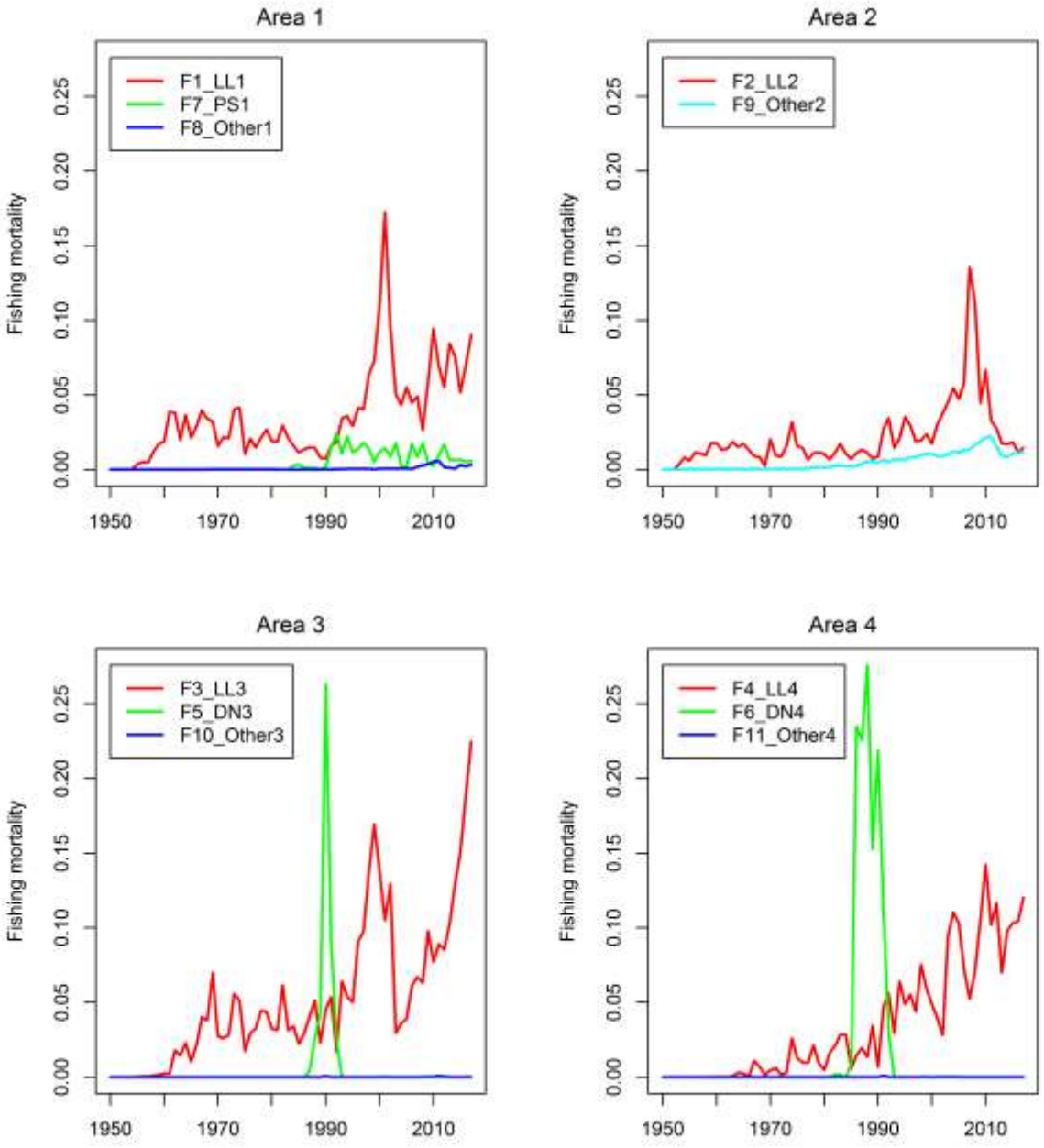

Figure 46. Trends in annual fishing mortality by fleet plotted by the area of operation of the fishery (single region reference model).

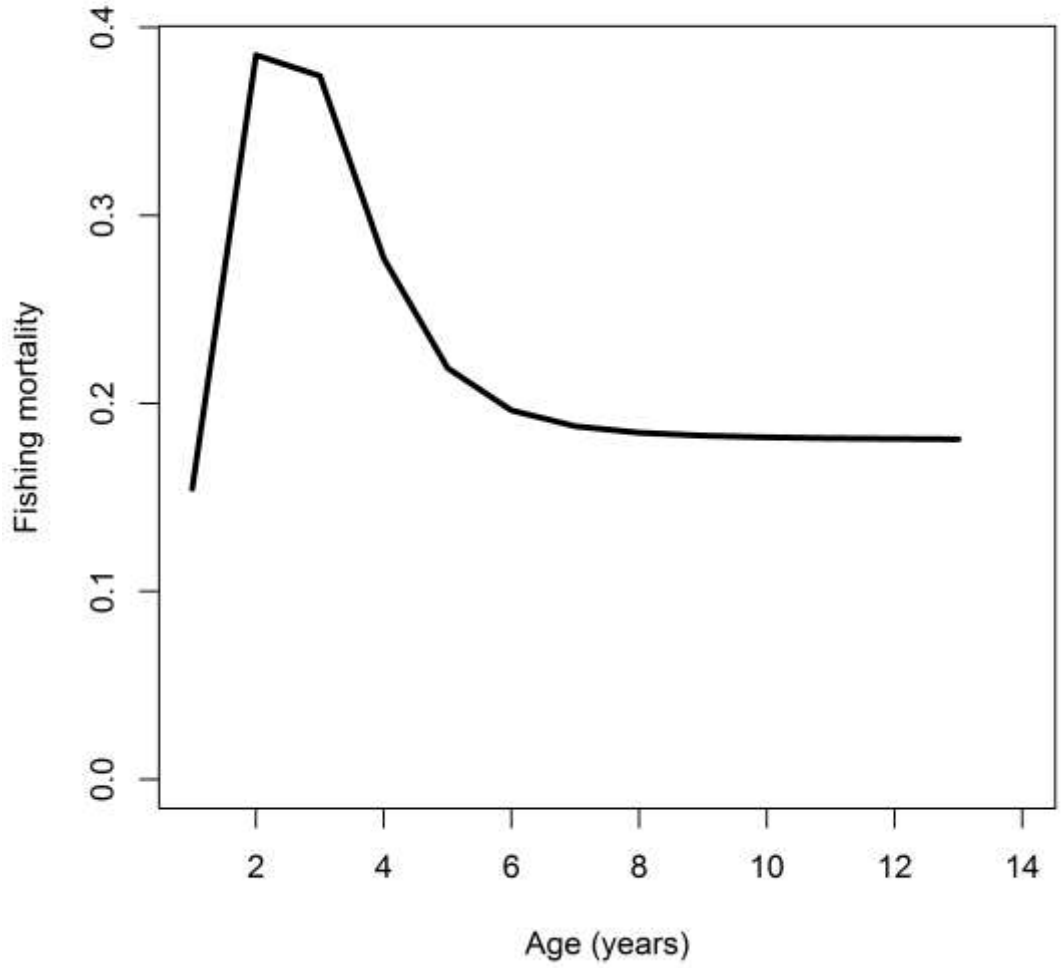

Figure 47. Composite fishing mortality by age class for the period used for the calculation of MSY based reference points (2017).

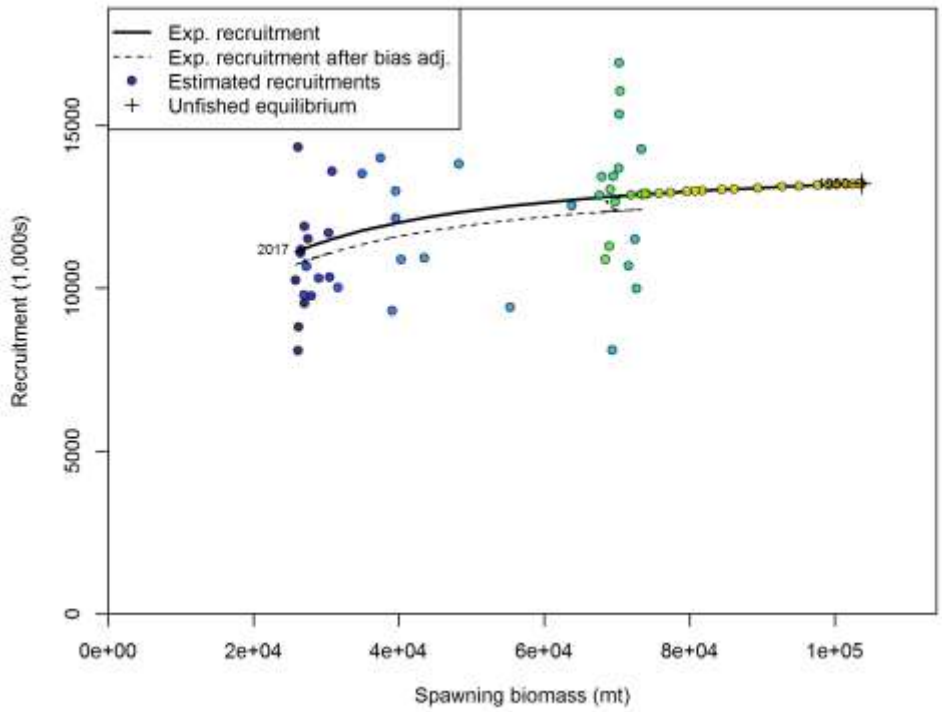

Figure 48. Relationship between equilibrium recruitment and equilibrium spawning biomass for the single region reference model with steepness of the SRR is fixed at 0.80 (black line). Point colors indicate year, with warmer colors indicating earlier years and cooler colors in showing later years.

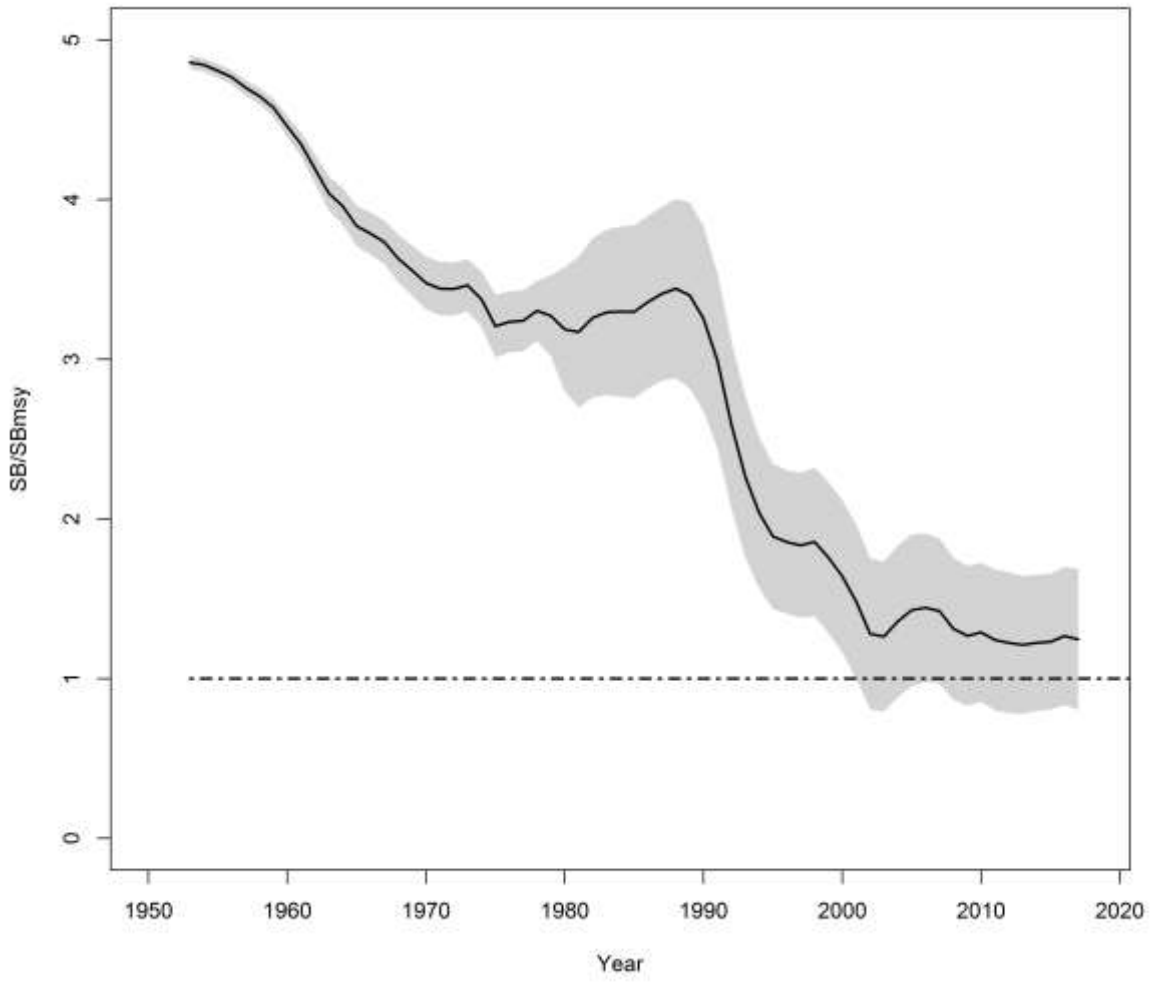

Figure 49. Annual spawning biomass relative to SB_{MSY} for the model period. The shaded area represents the 95% confidence interval. The horizontal dashed line represents the SB_{MSY} level.

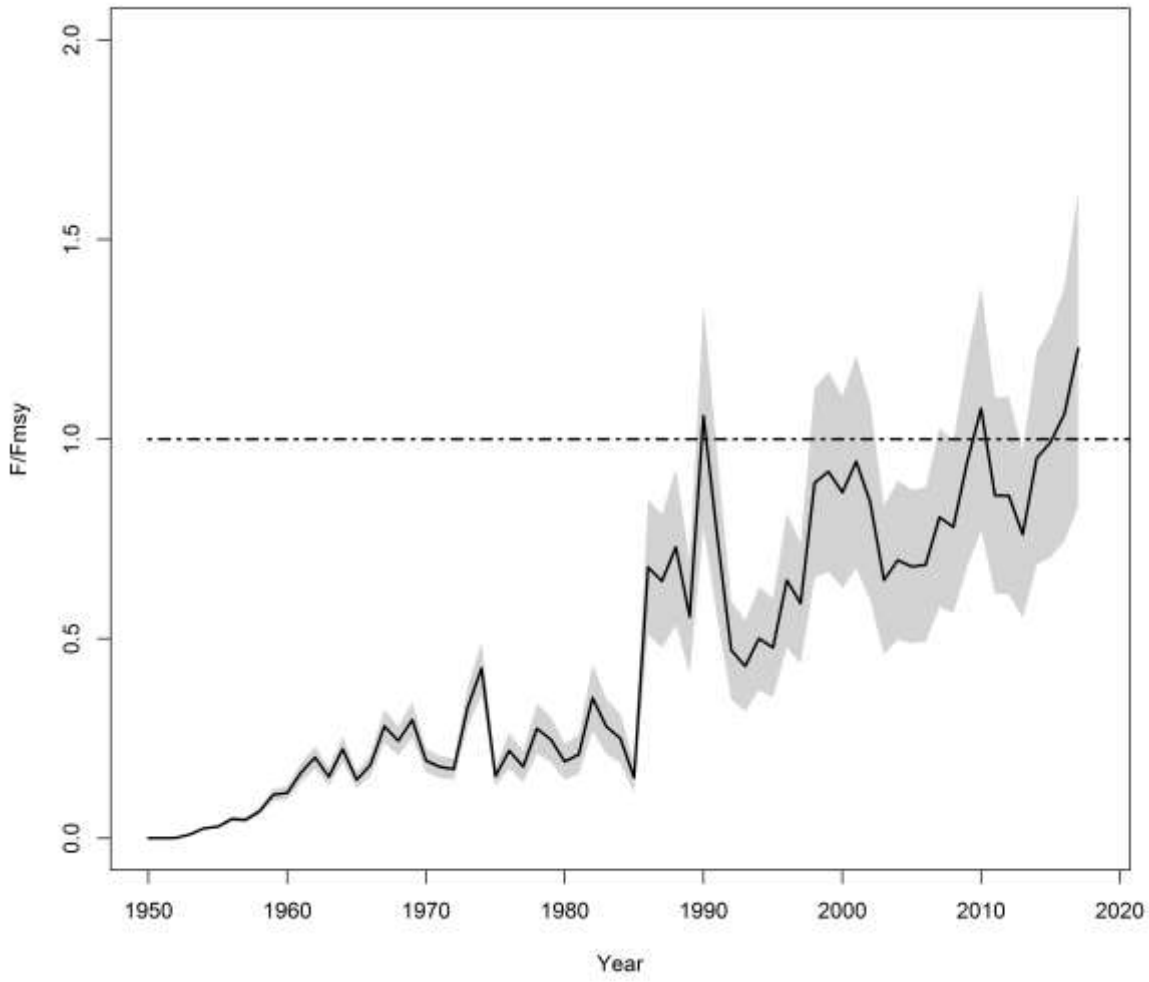

Figure 50. Annual fishing mortality relative to F_{MSY} for the model period. The shaded area represents the 95% confidence interval. The horizontal dashed line represents the F_{MSY} level.

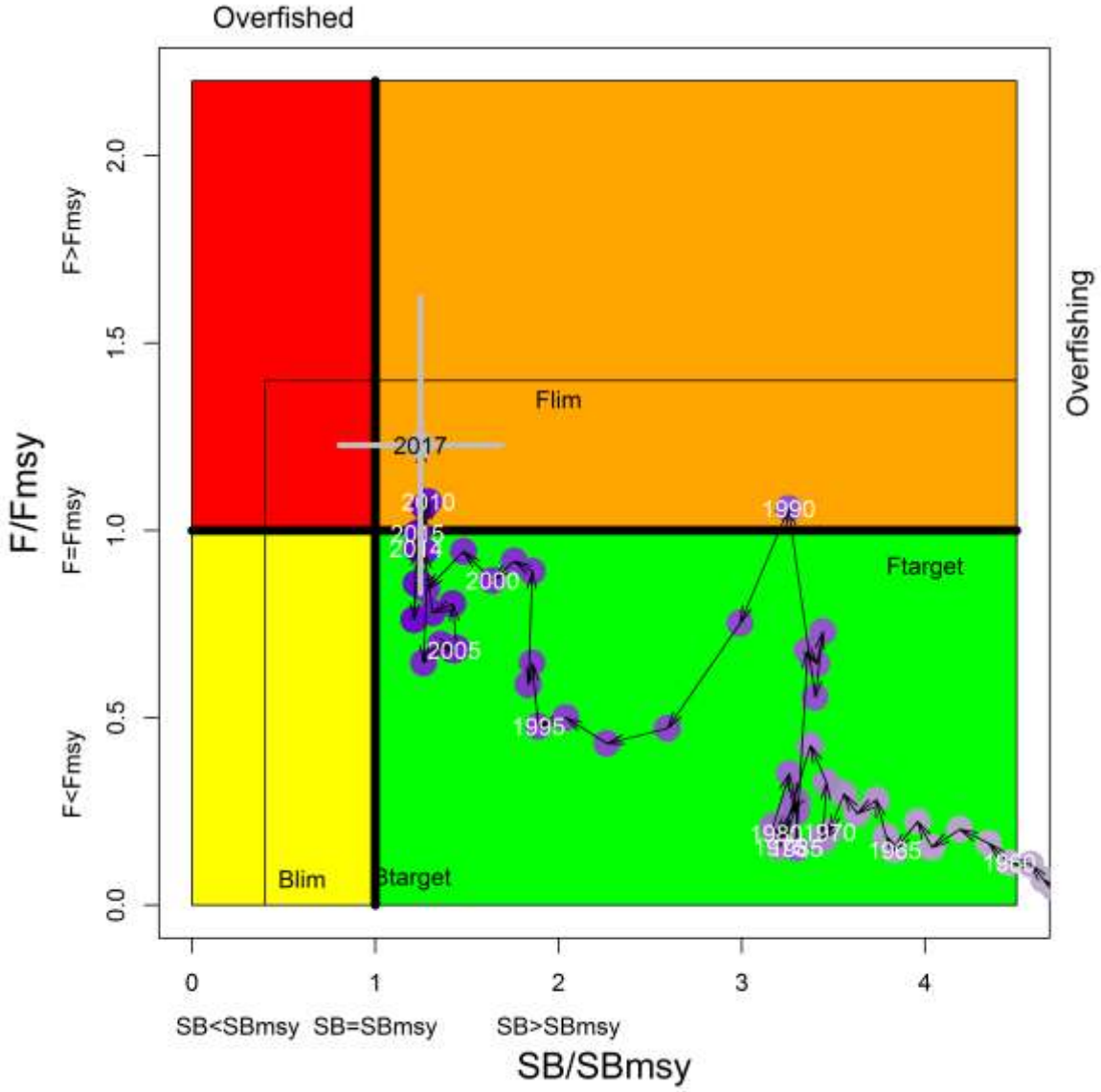

Figure 51. Annual stock status, relative to SB_{MSY} (x-axis) and F_{MSY} (y-axis) reference points for the *CPUE_SouthWest* reference model. The grey lines represent the 95% confidence interval associated with the 2017 stock status.

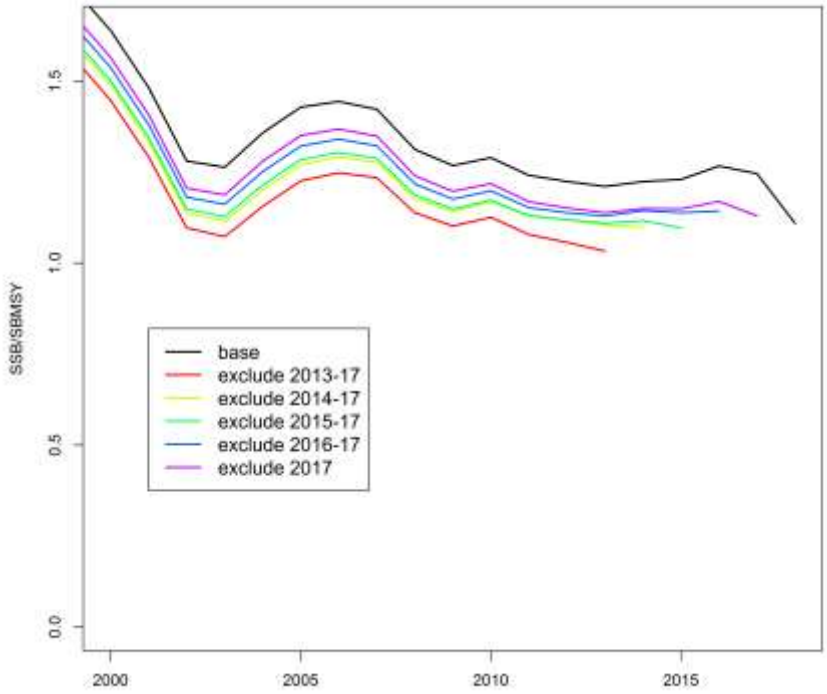

Figure 52. Successive estimates of recent stock status, relative to SB_{MSY} , from a retrospective analysis of the *CPUE_SouthWest* reference model.

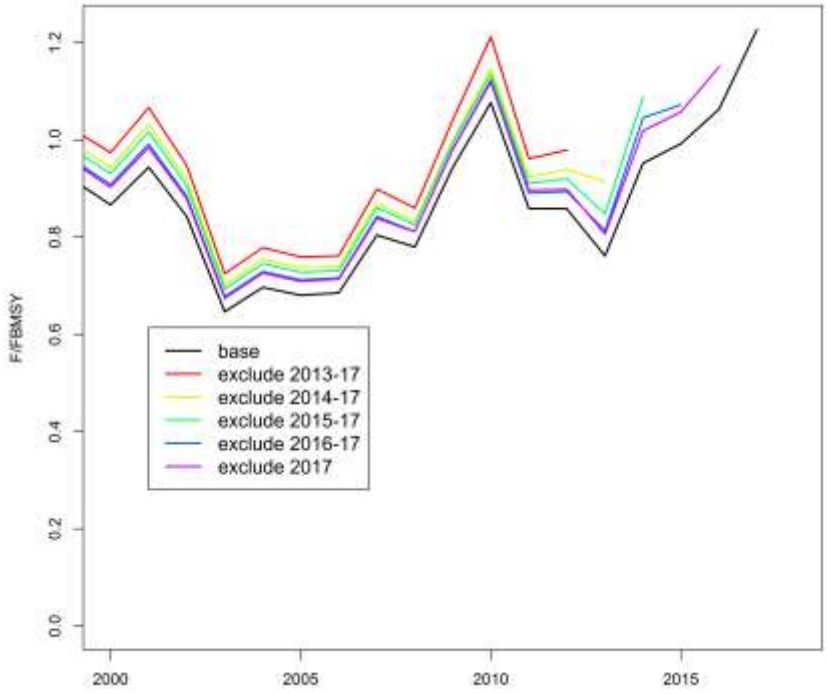

Figure 53. Successive estimates of recent stock status, relative to F_{MSY} , from a retrospective analysis of the *CPUE_SouthWest* reference model.

APPENDIX 1. RESULTS FROM THE PRELIMINARY PHASE OF THE STOCK ASSESSMENT MODELLING

Table A1. Main structural assumptions of the albacore tuna spatial models investigated in the preliminary modelling phase.

Index	Regional structure	CPUE indices	Selectivity	Catchability	Regional recruitment	Movement
R1_CPUE_All	Single	LL1-4	LL1=LL2; LL3=LL4	Independent	NA	NA
R1_CPUE_North	Single	LL1-2	LL1=LL2; LL3=LL4	Independent	NA	NA
R1_CPUE_South	Single	LL3-4	LL1=LL2; LL3=LL4	Independent	NA	NA
R2_CPUE_All	Two	LL1-4 (rescaled)	LL1=LL2; LL3=LL4	LL1=LL2	Regional proportion Regional devs	E to W; W to E
R2_CPUE_North	Two	LL1-2 (rescaled)	LL1=LL2; LL3=LL4	LL1=LL2	Regional proportion Regional devs	E to W; W to E
R2_CPUE_South	Two	LL3-4 (rescaled)	LL1=LL2; LL3=LL4	LL3=LL4	Regional proportion Regional devs	E to W; W to E
R4_Select_All	Four	LL1-4	LL1-4 shared	LL1-4 shared	Regional proportion Regional devs	1<>2 1<>3 2<>4 3< >4
West	Single	LL1,LL3	Independent	Independent	NA	NA
East	Single	LL2,LL4	Independent	Independent	NA	NA

Table A2. Estimates of management quantities for the set of stock assessment models that investigate spatial structure.

Model	SB_0	SB_{MSY}	SB_{MSY}/SB_0	SB_{2017}	SB_{2017}/SB_0	SB_{2017}/SB_{MSY}	F_{2017}/F_{MSY}	MSY
R1_CPUE_All	1,574,360	332,872	0.211	1,376,330	0.874	4.135	0.046	332,872
R1_CPUE_North	188,508	39,976	0.212	103,515	0.549	2.589	0.590	39,976
R1_CPUE_South	245,949	52,274	0.213	147,761	0.601	2.827	0.366	52,274
R2_CPUE_All	9,906,650	2,190,090	0.221	9,198,650	0.929	4.200	0.006	2,190,090
R2_CPUE_North	291,565	64,843	0.222	199,723	0.685	3.080	0.282	64,843
R2_CPUE_South	364,843	79,084	0.217	257,378	0.705	3.254	0.203	79,084
R4_Select_All	158,904	37,163	0.234	76,541	0.482	2.060	0.570	37,163
West	289,778	61,305	0.212	202,855	0.700	3.309	0.220	61,305
East	33,059,200	6,999,950	0.212	33,066,900	1.000	4.724	0.001	6,999,950

Table A3. CPUE likelihoods for the set of stock assessment models that investigate spatial structure. CPUE indices included in the overall likelihood are highlighted.

Model	Total	CPUE index				
		LL1	LL2	LL3	LL4	DN
R1_CPUE_All	-406.2	**-96.3**	**-116.3**	**-110.2**	**-78.8**	**-4.6**
R1_CPUE_North	-235.4	**-108.9**	**-120.9**	-61.1	-56.2	**-5.6**
R1_CPUE_South	-198.8	-85.4	-95.4	**-115.4**	**-78.8**	**-4.6**
R2_CPUE_All	-476.7	**-109.1**	**-131.4**	**-135.4**	**-96.4**	**-4.4**
R2_CPUE_North	-282.4	**-134.1**	**-143.9**	-58.9	-49.4	**-4.4**
R2_CPUE_South	-245.4	-77.5	-110.7	**-137.4**	**-103.1**	**-4.9**
R4_Select_All	-518.7	**-131.5**	**-161.5**	**-123.3**	**-97.8**	**-4.6**
West	-244.4	**-108.3**		**-129.2**		**-6.9**
East	-241.2		**-133.8**		**-103.3**	**-4.1**

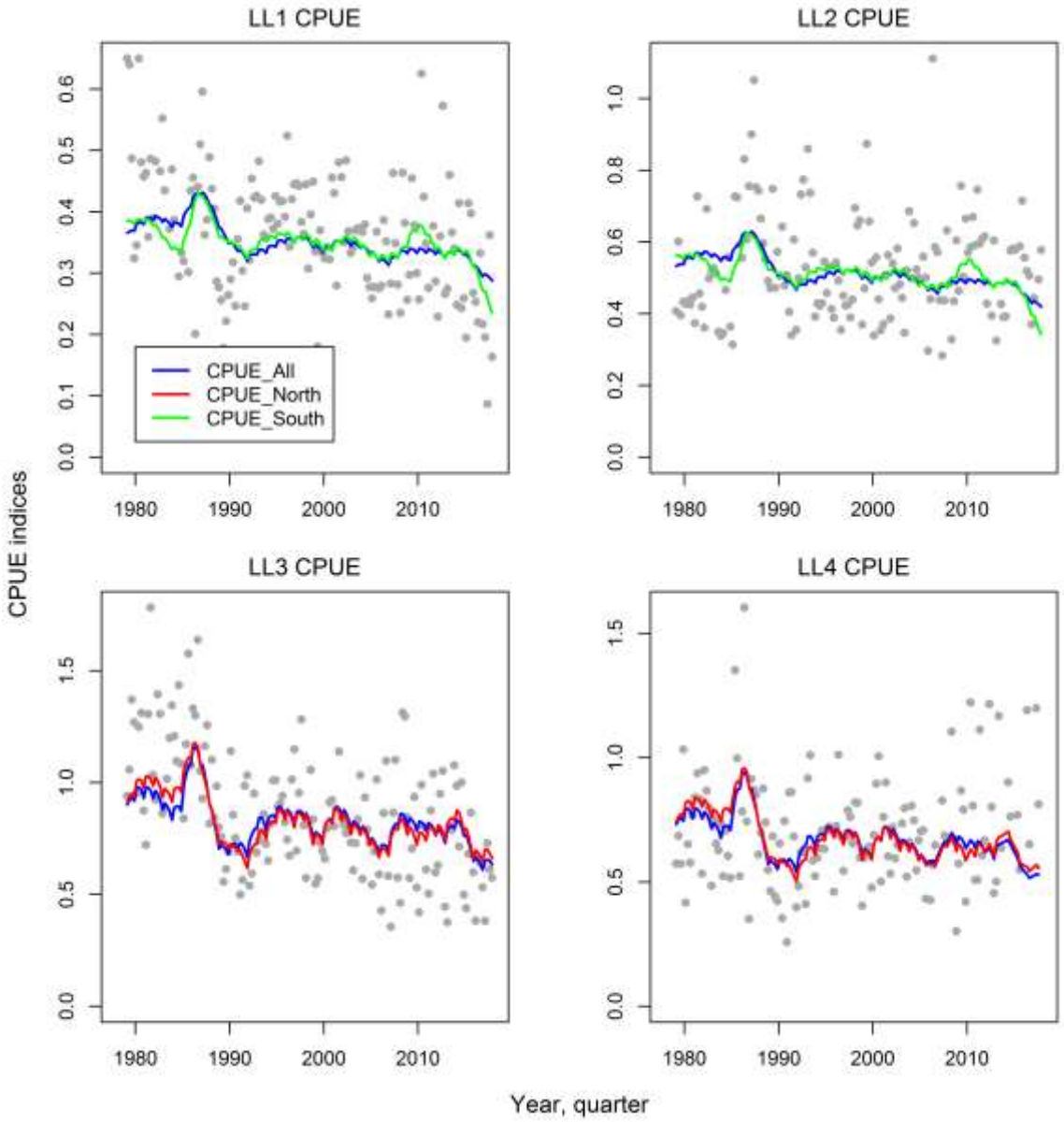

Figure A1. Fit to the longline CPUE indices for the One Region model options (R1) with different sets of CPUE indices included.

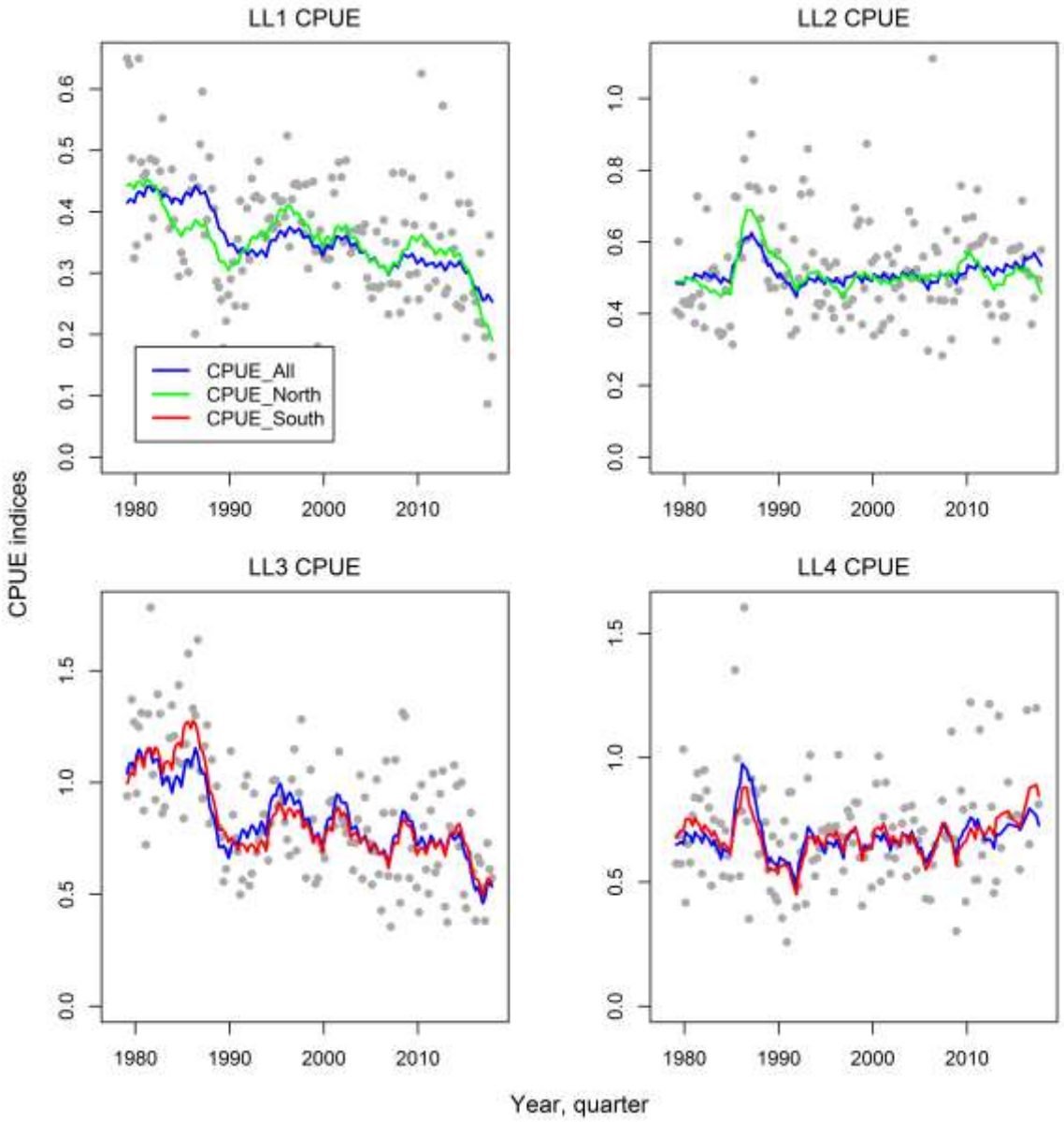

Figure A2. Fit to the longline CPUE indices for the Two Region model options (R2) with different sets of CPUE indices included.

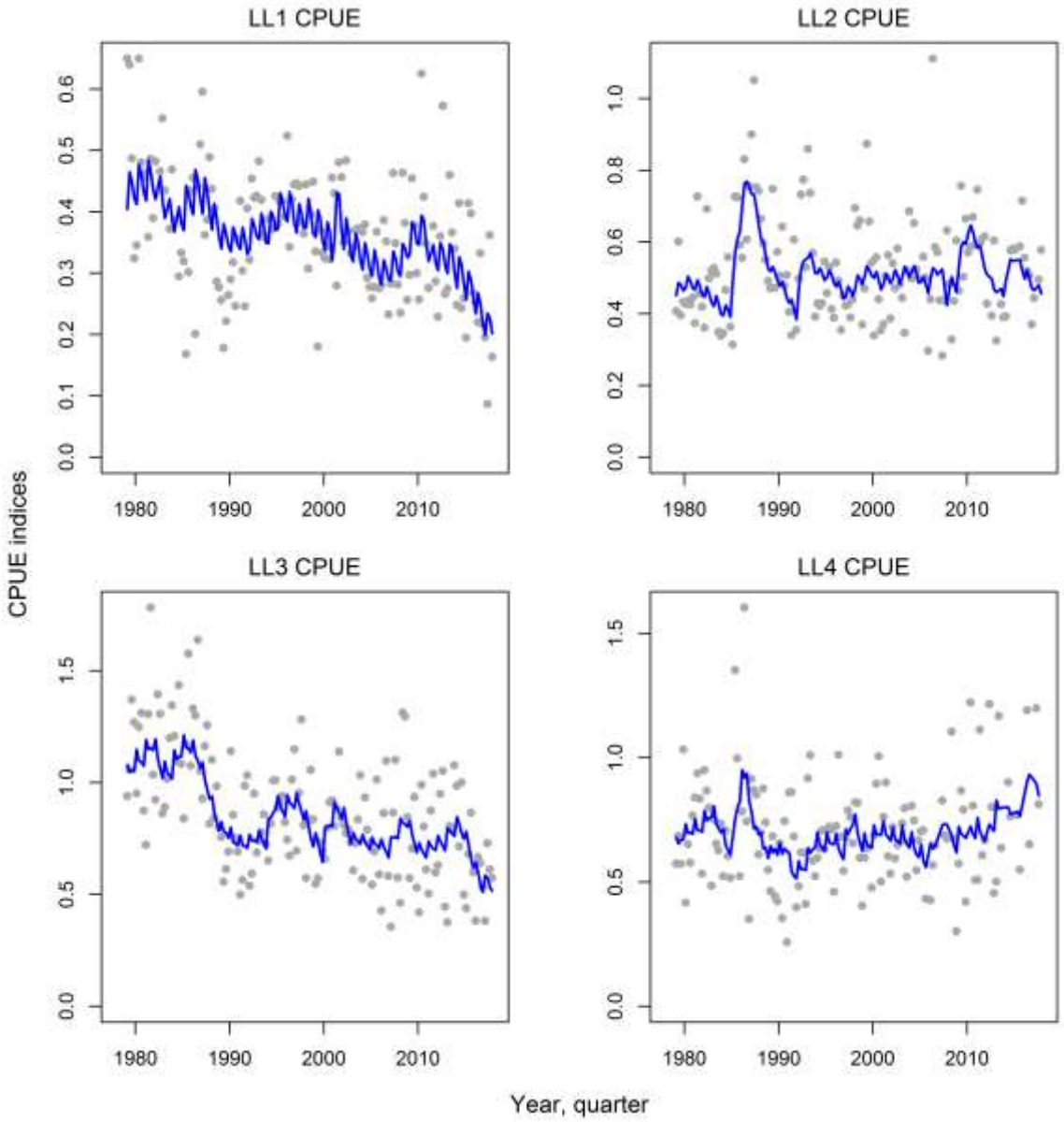

Figure A3. Fit to the longline CPUE indices for the Four Region model option *R4_Select_All* (all CPUE indices included).

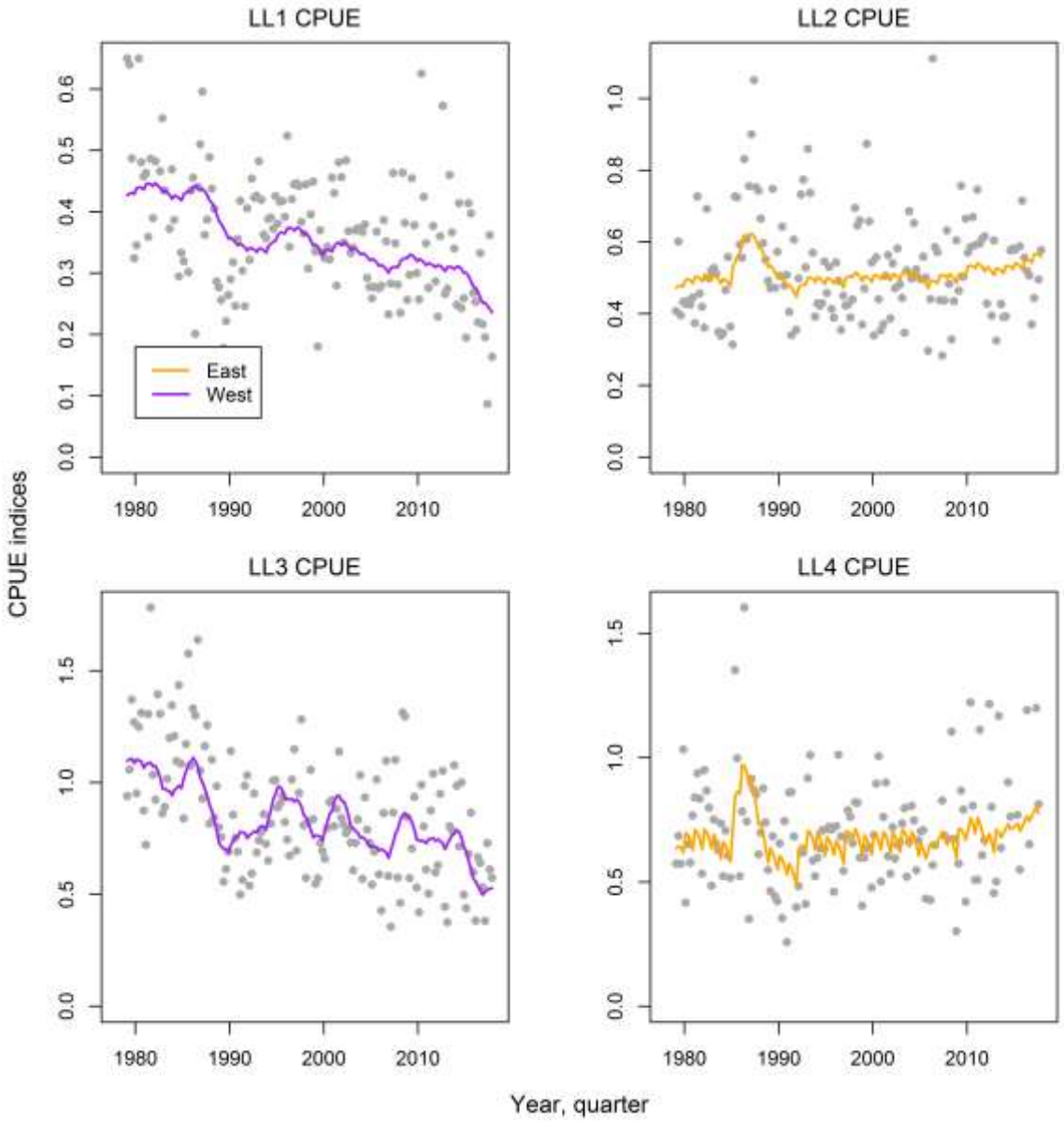

Figure A4. Fit to the longline CPUE indices for the separate *West* Region model (left) and *East* Region model (right).

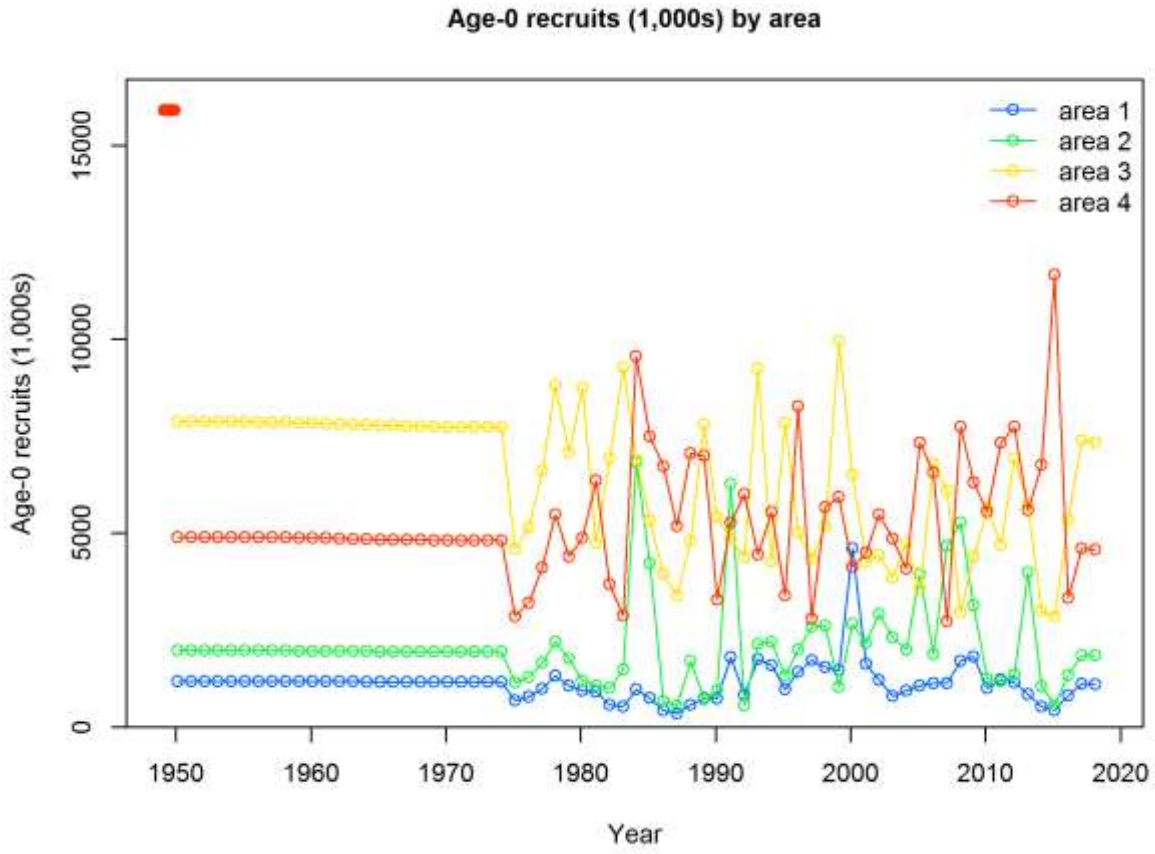

Figure A5. Distribution of annual recruitments amongst regions of the four region *R4_Select_All* model (area 1 = northwest, area 2 = northeast, area 3 = southwest, area 4 = southeast).

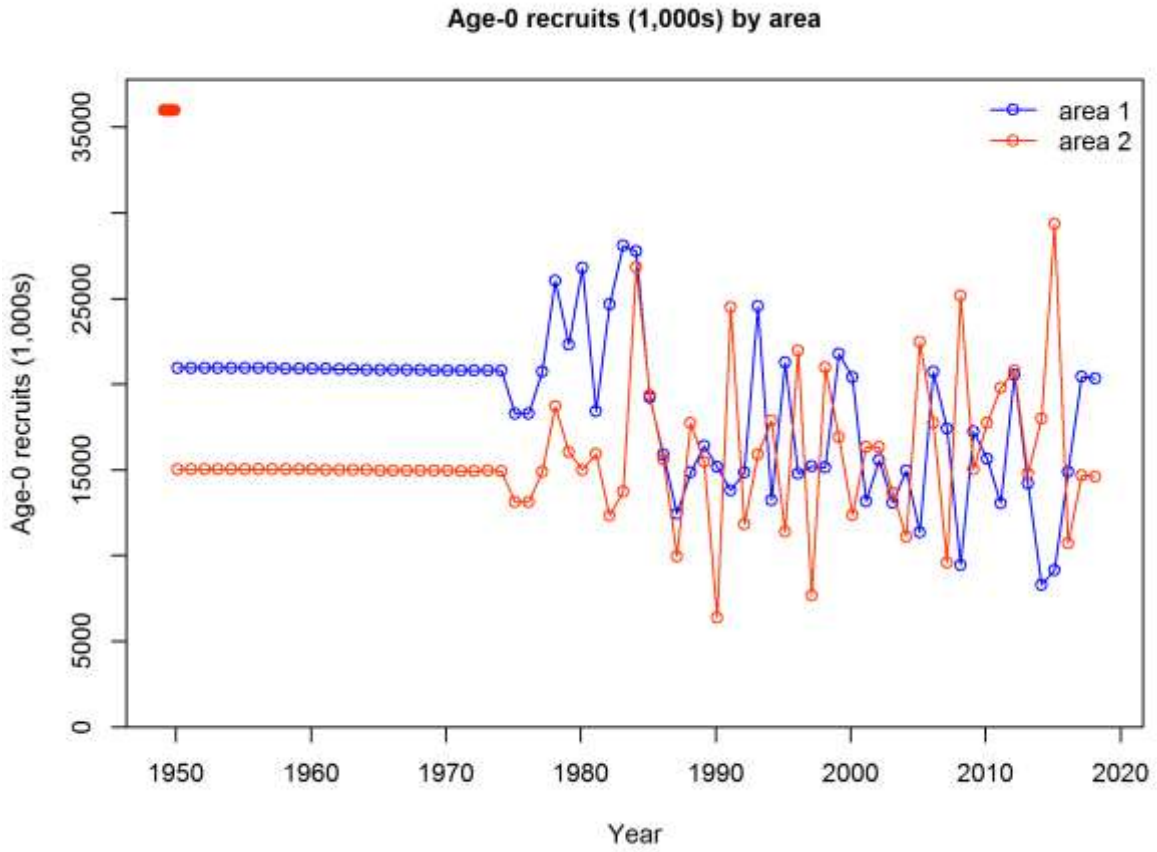

Figure A6. Distribution of annual recruitments amongst regions of the two region *R2_CPUE_South* model (area 1 = West, area 2 = East).